

Physics of Quantum Information

Alexander Shnirman and Ingo Kamleitner

Institute TKM, Karlsruhe Institute of Technology, Karlsruhe, Germany

(Dated: March 2, 2012)

Contents

I. General Information	6
II. Elements of classical computing	6
A. Turing machine	6
B. Circuit model	7
C. Computational complexity	8
D. Energy cost of irreversibility, Landauer's argument	9
III. Short history of quantum computing	9
IV. Basic concepts of quantum computing	10
A. A qubit	10
B. A register	11
C. Gates	11
1. One-bit gates	12
2. Two-bit gates	12
3. Universal set of quantum gates	13
D. Idea of quantum parallelism	13
V. Simplest quantum algorithms	14
A. Deutsch algorithm	14
B. Quantum Fourier transform	15
C. Role of entanglement	16
VI. One-bit manipulations	17
A. Switching on the Hamiltonian for an interval of time	17
B. Rabi Oscillations	17
C. Simplest two-bit gates: iSWAP and $\sqrt{\text{iSWAP}}$	19
VII. Adiabatic manipulations	20
A. Adiabatic "theorem"	20
B. Transformation to the adiabatic (instantaneous) basis	21
C. Geometric Phase	22

1. Example: Spin 1/2	23
D. Geometric interpretation	25
E. Non-Abelian Berry Phase (Holonomy)	25
F. Non-adiabatic corrections: Transitions	26
1. Super-adiabatic bases	26
2. Perturbation theory	27
3. Landau-Zener transition: perturbative solution	28
4. Landau-Zener transition: quasi-classical solution in the adiabatic basis	30
5. Landau-Zener transition: quasi-classical solution in the diabatic basis	31
6. Landau-Zener transition: exact solution	32
VIII. Open quantum systems	33
A. Density operator	34
B. Time evolution super operator	36
C. Microscopic derivations of master equations	38
1. Relation to the correlation function	44
2. Lamb shift for a two-level system	45
D. Golden Rule calculation of the energy relaxation time T_1 in a two-level system	46
E. Fluctuation Dissipation Theorem (FDT)	47
F. Longitudinal coupling, T_2^*	48
1. Classical derivation	48
2. Quantum derivation	49
G. $1/f$ noise, Echo	49
IX. Quantum measurement	51
1. Quantum Nondemolition Measurement (QND)	53
2. A free particle as a measuring device	54
3. A tunnel junction as a meter (will be continued as exercise)	54
4. Exercise	57
X. Josephson qubits	58
A. Elements of BCS theory (only main results shown in the lecture without derivations)	58

1. BCS Hamiltonian	58
2. Variational procedure	59
3. Excitations	62
4. Mean field	63
5. Order parameter, phase	64
6. Flux quantization	65
B. Josephson effect	66
C. Macroscopic quantum phenomena	68
1. Resistively shunted Josephson junction (RSJ) circuit	68
2. Particle in a washboard potential	69
3. Quantization	71
4. Josephson energy dominated regime	72
5. Charging energy dominated regime	72
6. Caldeira-Leggett model	73
D. Various qubits	75
1. Charge qubit	75
2. Flux qubit	78
3. Phase qubit	78
XI. Optical Qubits and Cavity QED	78
A. Photons as Qubits	78
B. Quantum Cryptography	79
C. Cavity QED	82
1. Coupling of photons with Cavity QED	86
XII. Ion Traps QC	88
A. System	88
B. Quantum computation	90
C. Limitations	92
XIII. Liquid state NMR QC	92
A. System	93
B. Time evolution	94

C. Magnetization Readout	95
D. Initial state and “labeling”	96
XIV. Elements of quantum error correction	98
A. Classical error correction	98
B. Quantum error correction	99
XV. Topological ideas	103
A. Error correction: stabilizers formalism	103
1. Stabilizers of the Shor code	104
B. Toric code	104
C. Majorana bound states	105
References	106

I. GENERAL INFORMATION

Literature:

- 1) Michael A. Nielsen and Isaac L. Chuang, "Quantum Computation and Quantum Information"
- 2) Goong Chen et al., "Quantum Computing Devices: Principles, Designs, and Analysis"
- 3) H.-P. Breuer and F. Petruccione, "The theory of open quantum systems"

II. ELEMENTS OF CLASSICAL COMPUTING

Computing - performing an algorithm. Important question by David Hilbert: "Does an algorithm exist, which could be used, in principle, to solve all the problems in mathematics". Hilbert believed the answer would be "yes". It turned out to be "no". Works by Alonzo Church and Alan Turing in the 1930s were devoted to proving this. They laid the foundations of computer science. As a result one can identify a class of "computable problems". Turing invented a simple model - Turing machine. It turned out to be very powerful.

Church-Turing thesis: The class of functions computable by a Turing machine corresponds exactly to the class of functions which we would naturally regard as being computable by an algorithm. Simply said: what can be computed in principle can be computed by a Turing machine. The thesis has not been proven but no evidence against the thesis appeared since its formulation more than 60 years ago.

A. Turing machine

Infinite tape with cells. In each cell an element of Alphabet can be written and erased. Example of an Alphabet: $\{0, 1, B\}$ (B is for blank). Turing "Head" moves along the tape and can have $N + 2$ internal states $q_s, q_h, q_1, \dots, q_N$. Here q_i is the initial or starting state, and q_h is the final or the halting state. The machine works according to instructions. Each instruction has the form

$$(q_i, A_i \rightarrow q_j, A_j, \textit{Right or Left}) \tag{1}$$

Here q_i is the current internal state of the Head and A_i is the current content of the cell on which the Head "stands". There must be apparently an instruction for each combination

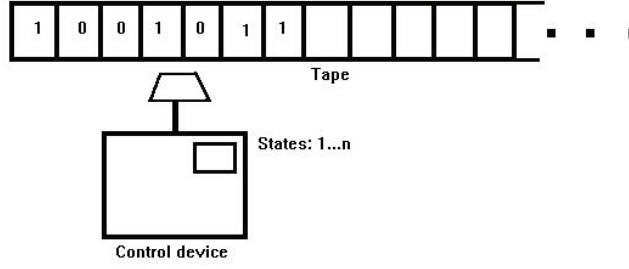


FIG. 1: Turing machine.

(q, A) (alternatively, if an instruction is not found the machine stops and the Head goes to q_h). Finally, the Head moves right or left according to the instruction.

B. Circuit model

Although "everything" can be computed using a Turing machine, the circuit model is much more convenient and much closer to the modern computers. It also allows an easy transition to quantum computing. The circuit model consists of gates and wires. Gates: NOT, AND, OR, NAND, XOR etc. Examples: NOT: $0 \rightarrow 1, 1 \rightarrow 0$. AND: $(0,0) \rightarrow 0, (0,1) \rightarrow 0, (1,0) \rightarrow 0, (1,1) \rightarrow 1$ or $(x,y) \rightarrow x \wedge y = x \cdot y$. XOR: $(x,y) \rightarrow x \oplus y = (x + y)[\text{mod } 2]$.

Consider an example: first we introduce the half-adder circuit (Fig. 2) and the full-adder one (Fig. 3). Finally in Fig. 4 the addition circuit for 3-digit binary numbers (x_3, x_2, x_1)

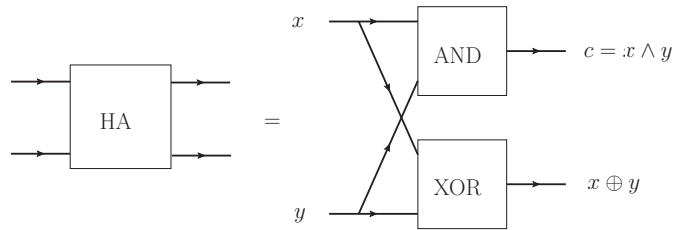


FIG. 2: Half-adder. Adds two binary numbers x and y . If both are 1, then 1 is put into the "carry" bit c , which will be used in the next step (for the next digit).

and (y_3, y_2, y_1) is shown.

Important concept: universal set of gates. These is the set of gates which allows to perform all possible algorithms.

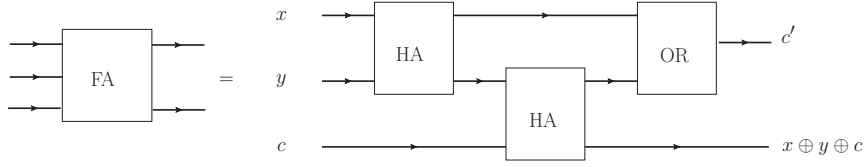


FIG. 3: Full-adder. Adds two binary numbers x and y and takes into account the "carry" bit c from the previous digit. Produces a new "carry" bit c' .

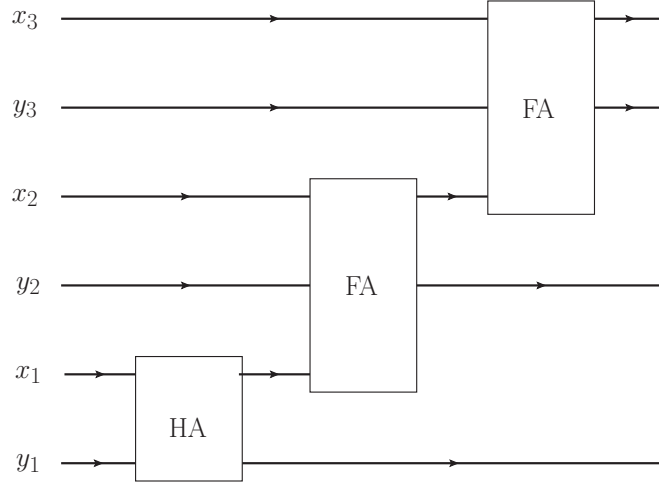


FIG. 4: Addition circuit for two 3-digits numbers.

C. Computational complexity

From all problems we consider only decision problems, i.e., such that the answer is "yes" or "no". Resources: time, space (memory), energy. Nowadays the most important seems to be time.

We want to know the time needed to solve a problem as a function of the input size. The later is measured in number of bits needed to encode the input. That is if number M is the input, its "size" is $n \approx \log_2 M$.

There are many complexity classes. The most important for us are:

P - solvable in polynomial time, i.e., the solution time scales as $O(p(n))$. One should just take the highest power in the polynomial. That is, if the computation takes $2n^4 + 2n^3 + n$ steps, one says it is $O(n^4)$.

NP - checkable in polynomial time. The best known example is factoring problem. As a decision problem it is formulated like this: does M have a divisor smaller than $M_1 < M$

but bigger than 1? It is not known if one can factor a number in polynomial time. The simplest protocol is definitely exponential in time. Indeed trying to divide M by all possible numbers (up to $\approx \sqrt{M}$) needs at least $\sqrt{M} \sim 2^{[(1/2) \log_2 M]} \sim e^{n/2}$ steps, where $n \sim \ln M$ is the input size. However if one knows a divisor m (this is called a *witness*) it takes only polynomial time to confirm that m is a divisor.

Big question - is **NP** equal to **P**? The answer is not known. There are many problems for which a polynomial algorithm is not known but it is also not proven that it does not exist.

NPC - NP complete - the "hardest" **NP** problems. One needs a concept of reduction here. Reduction is when we can solve problem B by first reducing it to problem A. Example: we can square a number if we know how to multiply numbers. A complete problem in a class is one to which all other problems in a class can be reduced. The existence of complete problems in a class is not guaranteed. Cook-Levin theorem: CSAT problem is complete in **NP**. CSAT (circuit satisfiability) problem is formulated as follows: given a circuit of AND, OR, and NOT gates is there an input which would give an output 1.

D. Energy cost of irreversibility, Landauer's argument

Gates like AND are irreversible. One bit of information is lost. R. Landauer has argued in 1961 that erasing one bit increases the entropy by $k_B \ln 2$ and, thus, the heat $k_B T \ln 2$ must be generated. Nowadays computers dissipate much more energy ($500 k_B T \ln 2$) per operation. The idea of Landauer was to make gates reversible and thus minimize the heating. Classical gates can be reversible in principle, but in practice the irreversible are used. As we will see below, in quantum computing the gates must be reversible.

III. SHORT HISTORY OF QUANTUM COMPUTING

Important ideas:

1) Around 1982 Richard Feynmann suggested to simulate physical systems using a computer built on principles of quantum mechanics. This was motivated by the inherent difficulty of simulating the many-body wave functions (especially those of fermions - sign problem) on classical computers.

2) Around 1985 David Deutsch tried to prove a stronger version of Church-Turing thesis

(that everything computable can be computed on Turing machine) using laws of physics. For that again a computer was needed which would be able to simulate any physical system. Since physical systems are quantum, a quantum computer was needed. Deutsch asked if quantum computers might be more efficient than classical ones and found simple examples of this.

3) The real breakthrough came in 1994 when Peter Shor found a polynomial factoring algorithm for a quantum computer. Factoring problem is in **NP** and all known classical algorithms are exponential. This discovery has initiated huge efforts worldwide to build a quantum computer. Partly this is so because factoring is the central element of the RSA security protocol.

4) In 1995 Lov Grover found another application for quantum computers - data base searching. The improvement is only logarithmical, but still this is good.

5) Starting from the 70s individual (microscopic and mesoscopic) systems were quantum mechanically manipulated. In quantum optics, NMR, mesoscopic solid state circuits few degrees of freedom were singled out and manipulated.

IV. BASIC CONCEPTS OF QUANTUM COMPUTING

Quantum computers are understood today to be able to solve exactly the same class of problems as the Turing machine can. *Some* of the problems are solved more efficiently (faster) on quantum computers. Example: Shor algorithm for factoring. Thus, mostly the **NP** problems are considered, for which no classical polynomial algorithm is known (but it is not proven that it does not exist either).

A. A qubit

Qubit is a quantum 2-level system. We will call these levels $|0\rangle$ and $|1\rangle$. A general pure state is given by $\alpha|0\rangle + \beta|1\rangle$ with the normalization condition $|\alpha|^2 + |\beta|^2 = 1$. Out of four real numbers contained in the complex α and β only two characterize the state. One is taken away by the normalization. Another by the fact that a pure state can be multiplied by an arbitrary phase. This is how a Bloch sphere description appears

$$|\psi\rangle = \cos \frac{\theta}{2} |0\rangle + e^{i\varphi} \sin \frac{\theta}{2} |1\rangle . \quad (2)$$

The Pauli matrices

$$\sigma_x = \begin{pmatrix} 0 & 1 \\ 1 & 0 \end{pmatrix} \quad \sigma_y = \begin{pmatrix} 0 & -i \\ i & 0 \end{pmatrix} \quad \sigma_z = \begin{pmatrix} 1 & 0 \\ 0 & -1 \end{pmatrix} \quad (3)$$

act on $|0\rangle = \begin{pmatrix} 1 \\ 0 \end{pmatrix}$ and $|1\rangle = \begin{pmatrix} 0 \\ 1 \end{pmatrix}$

We obtain $\langle\psi|\sigma_z|\psi\rangle = \cos^2\frac{\theta}{2} - \sin^2\frac{\theta}{2} = \cos\theta$. Further $\langle\psi|\sigma_x|\psi\rangle = \sin\theta\cos\varphi$ and $\langle\psi|\sigma_y|\psi\rangle = \sin\theta\sin\varphi$. Thus we see that $\langle\vec{\sigma}\rangle$ points on the sphere into the direction θ, φ .

If a qubit is in a mixed state, its density matrix can be written as

$$\rho = \frac{1}{2} (\sigma_0 + x\sigma_x + y\sigma_y + z\sigma_z) , \quad (4)$$

where $x^2 + y^2 + z^2 \leq 1$. If $x^2 + y^2 + z^2 = 1$ we have $\rho^2 = \rho$ and the state is pure. The vector x, y, z is then on the Bloch sphere. For a mixed state the Bloch vector is shorter than 1.

B. A register

A register is a string of N qubits. There are 2^N binary numbers one can encode. These are now quantum states of the form $|x\rangle = |01000101\dots\rangle$. They form an orthonormal basis. Thus we can denote the basis with $|x\rangle$, where $x = 0, 1, 2, 3, \dots, 2^N - 1$. A classical register could also be in one of the 2^N states. What is new in a quantum register is that it can be in an arbitrary superposition of states:

$$|\psi\rangle = \sum_{x=0}^{2^N-1} c_x |x\rangle . \quad (5)$$

Thus, a state of the register "encodes" 2^N complex numbers (probably $2^N - 1$ because of normalization and the general phase). This is a huge amount of information and this is why quantum computers should be efficient. Yet, all this information is not really accessible. Performing a measurement of the state of the register we lose immediately most of this information. Thus, quantum algorithms should be "smart" in order not to lose this huge amount before the useful information has been extracted.

C. Gates

All gates in quantum computers are reversible. Only at the end of computation a non-reversible measurement is performed. In more complicated algorithms and models measure-

ments are performed also during the computation, but we will not consider this now.

Thus, gates are unitary transformations of the states of a register. We start with single-bit gates.

1. One-bit gates

An analog of NOT gate is the quantum gate X defined by $X|0\rangle = |1\rangle$ and $X|1\rangle = |0\rangle$. This is actually nothing but the σ_x matrix

$$X = \begin{pmatrix} 0 & 1 \\ 1 & 0 \end{pmatrix}. \quad (6)$$

Analogously one defines $Y = \sigma_y$ and $Z = \sigma_z$ gates. Clearly Z gate is just a particular case of a phase gate $e^{i\varphi\sigma_z/2}$ for $\varphi = \pi$. Indeed $e^{i\pi\sigma_z/2} = i\sigma_z$. Analogously $e^{i\pi\sigma_x/2} = i\sigma_x$. This means that gates can be achieved by applying a Hamiltonian for a certain time.

Hadamard gate is defined by

$$H|0\rangle = \frac{|0\rangle + |1\rangle}{\sqrt{2}}, \quad H|1\rangle = \frac{|0\rangle - |1\rangle}{\sqrt{2}}. \quad (7)$$

or

$$H = \frac{1}{\sqrt{2}} \begin{pmatrix} 1 & 1 \\ 1 & -1 \end{pmatrix}. \quad (8)$$

or

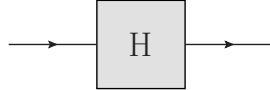


FIG. 5: Circuit symbol for Hadamard gate.

2. Two-bit gates

One of the most used two-bit gates is the CNOT or controlled NOT gate. In the matrix form it is given by

$$CNOT = \begin{pmatrix} 1 & 0 & 0 & 0 \\ 0 & 1 & 0 & 0 \\ 0 & 0 & 0 & 1 \\ 0 & 0 & 1 & 0 \end{pmatrix}, \quad (9)$$

where the 2-bit basis is ordered as follows $|00\rangle, |01\rangle, |10\rangle, |11\rangle$. The first bit is called control bit while the second is the target bit. If the control bit is in the state $|1\rangle$ the target bit is flipped, otherwise nothing is done. The circuit diagram is shown in Fig. 6.

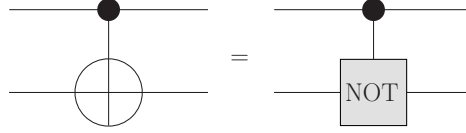


FIG. 6: Circuit diagram for CNOT gate. The solid vertex stands for the control bit.

Analogously one can define control- U gate, where U is any one-bit unitary gate. The matrix representation of this gate reads

$$CU = \begin{pmatrix} 1 & 0 & 0 & 0 \\ 0 & 1 & 0 & 0 \\ 0 & 0 & & U \\ 0 & 0 & & \end{pmatrix}. \quad (10)$$

The circuit diagram is shown in Fig. 7.

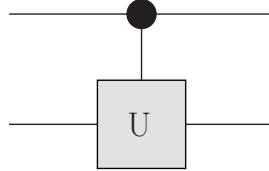


FIG. 7: Circuit diagram for CU gate. The solid vertex stands for the control bit.

3. Universal set of quantum gates

A universal set is the set of gates which are sufficient to construct an arbitrary unitary operation U on N bits, i.e., $U \in U(N)$. It turns out that arbitrary one-bit gates plus CNOT (or any other nontrivial two-bit gates) constitute an universal set.

D. Idea of quantum parallelism

Assume we have two registers $|r_1\rangle |r_2\rangle$.

Assume we can program an algorithm U_f which calculates a function $f(x) \in [0, 1, \dots, 2^N - 1]$. That is

$$U_f |x\rangle |0\rangle = |x\rangle |f(x)\rangle . \quad (11)$$

To define U_f fully we can assume

$$U_f |x\rangle |y\rangle = |x\rangle |y \oplus f(x)\rangle , \quad (12)$$

where \oplus means addition *mod*(2^N). This operator is definitely unitary.

Lets start with the state $|0\rangle |0\rangle$. Apply H gates on all the qubits of the register 1.

$$H_1 H_2 \dots H_N |000\dots\rangle = \frac{1}{2^{N/2}} (|0\rangle + |1\rangle)(|0\rangle + |1\rangle)(|0\rangle + |1\rangle) \dots = \frac{1}{2^{N/2}} \sum_{x=0}^{2^N-1} |x\rangle . \quad (13)$$

Thus the two registers are now in the state $\frac{1}{2^{N/2}} \sum_{x=0}^{2^N-1} |x\rangle |0\rangle$.

Now apply U_f

$$U_f \frac{1}{2^{N/2}} \sum_{x=0}^{2^N-1} |x\rangle |0\rangle = \frac{1}{2^{N/2}} \sum_{x=0}^{2^N-1} |x\rangle |f(x)\rangle . \quad (14)$$

Thus, in one run of our computer we have calculated $f(x)$ for all outputs!!! However it is difficult to use this result. A simple projection on one concrete value of x would destroy all the other results. The few known quantum algorithms manage to use the parallelism before the information is lost.

V. SIMPLEST QUANTUM ALGORITHMS

A. Deutsch algorithm

We have a 2-bit function $U_f |x\rangle |y\rangle = |x\rangle |y \oplus f(x)\rangle$. Perform an algorithm shown in Fig. 8

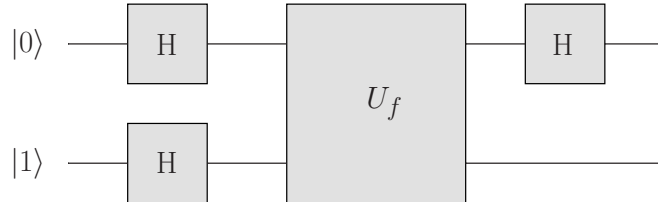


FIG. 8: Circuit diagram of Deutsch algorithm.

1)

$$|\psi_1\rangle = H \otimes H |0\rangle |1\rangle = \frac{1}{2}(|0\rangle + |1\rangle)(|0\rangle - |1\rangle)$$

2)

$$|\psi_2\rangle = U_f |\psi_1\rangle = \frac{1}{2} [|0\rangle (|f(0)\rangle - |1 \oplus f(0)\rangle) + |1\rangle (|f(1)\rangle - |1 \oplus f(1)\rangle)]$$

$$|\psi_2\rangle = \frac{1}{2} [(-1)^{f(0)} |0\rangle + (-1)^{f(1)} |1\rangle] (|0\rangle - |1\rangle)$$

3)

$$|\psi_3\rangle = H \otimes 1 |\psi_2\rangle = \frac{1}{\sqrt{2}} \begin{cases} \pm |0\rangle (|0\rangle - |1\rangle) & \text{if } f(0) = f(1) \\ \pm |1\rangle (|0\rangle - |1\rangle) & \text{if } f(0) \neq f(1) \end{cases}$$

Measuring the first qubit we can determine if $f(0) = f(1)$ or $f(0) \neq f(1)$. Note that U_f was applied only once. Classically we would have to calculate $f(x)$ twice in order to get the same information.

A generalization to functions of arguments consisting of many qubits is called Deutsch-Jozsa algorithm.

B. Quantum Fourier transform

A discrete Fourier transform a set of N complex numbers x_0, x_1, \dots, x_{N-1} into another set y_0, y_1, \dots, y_{N-1} according

$$y_k = \frac{1}{\sqrt{N}} \sum_{j=0}^{N-1} e^{2\pi i j k / N} x_j . \quad (15)$$

This can be presented as unitary transformation U_F . Indeed, assume we have a unitary transformation on a register of n qubits defined as follows

$$U_F |j\rangle = \frac{1}{\sqrt{2^n}} \sum_{k=0}^{2^n-1} e^{2\pi i j k / 2^n} |k\rangle . \quad (16)$$

Then

$$U_F \sum_{j=0}^{2^N-1} x_j |j\rangle = \frac{1}{\sqrt{2^N}} \sum_{k=0}^{2^n-1} \sum_{j=0}^{2^N-1} x_j e^{2\pi i j k / 2^n} |k\rangle = \sum_{k=0}^{2^n-1} y_k |k\rangle . \quad (17)$$

Quantum computer can implement U_F efficiently. Introduce a phase shift gate

$$R_k = \begin{pmatrix} 1 & 0 \\ 0 & e^{2\pi i / 2^k} \end{pmatrix} . \quad (18)$$

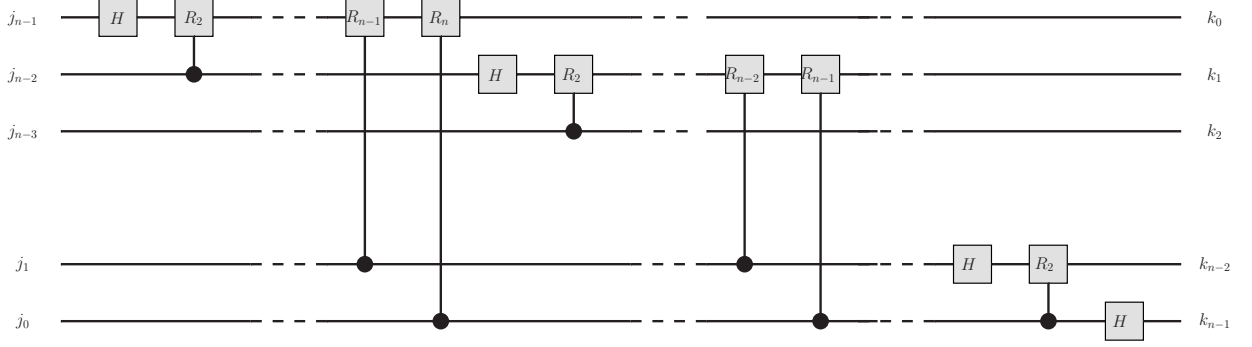


FIG. 9: Quantum Fourier Transform. The input number is given by $j = \sum_{m=0}^{n-1} j_m 2^m$.

The quantum Fourier transform is shown in Fig. 9. To understand this circuit we rewrite (16) as

$$U_F |j_{n-1}, \dots, j_0\rangle = \frac{1}{\sqrt{2^n}} \sum_{k_0, \dots, k_{n-1}=0,1} \exp \left[2\pi i \sum_{m=0}^{n-1} \sum_{l=0}^{n-1} \frac{j_m k_l}{2^{n-m-l}} \right] |k_{n-1}, \dots, k_0\rangle . \quad (19)$$

We see that the number of gates needed for QFT is given by $n + (n-1) + (n-2) + \dots + 1 = n(n+1)/2$. The classical Fast Fourier Transform (FFT) needs $O(n \cdot 2^n)$ gates. Thus the quantum algorithm is much more efficient. As said above this efficiency is not so simple to use.

C. Role of entanglement

Two qubits are called entangled if their state cannot be presented as a product state: $|\psi_{\text{prod}}\rangle = (\alpha_1 |0\rangle + \beta_1 |1\rangle)(\alpha_2 |0\rangle + \beta_2 |1\rangle)$. For example the following state is entangled $(1/\sqrt{2})(|00\rangle + |11\rangle)$.

Consider a product state of all n qubits of a register.

$$|\psi_{\text{prod}}\rangle = \prod_{m=0}^{n-1} (\alpha_m |0_m\rangle + \beta_m |1_m\rangle) . \quad (20)$$

This state is parametrized by $2n$ real numbers (Bloch angles). Clearly a general state of the register $\sum_{x=0}^{2^n-1} c_x |x\rangle$ is parametrized by many more numbers ($2n-2$ complex numbers). Thus the entanglement is behind the huge quantum capacity of the register.

VI. ONE-BIT MANIPULATIONS

A. Switching on the Hamiltonian for an interval of time

The simplest (in theory) way to perform a single-bit gate is to switch a Hamiltonian for a finite interval of time Δt . That is $H(t) = g(t) V$, where $g(t < 0) = g(t > \Delta t) = 0$. The gate operator is then given by

$$U = e^{-i \frac{\theta}{2} V}, \quad (21)$$

where $\hbar\theta = 2 \int dt g(t)$. For example if we chose $V = \sigma_z$ we obtain

$$U = e^{-i \frac{\theta}{2} \sigma_z} = \cos \frac{\theta}{2} - i \sin \frac{\theta}{2} \sigma_z \quad (22)$$

Thus, choosing $\theta = \pi$ we obtain $U = i\sigma_z$. Since the total phase is not important we have $U = iZ \sim Z$. Analogously we can obtain gates X and Y .

Let us now choose $\theta = \pi/2$ and $V = \sigma_y$. We then obtain

$$U = \frac{1}{\sqrt{2}}(1 - i\sigma_y) = \frac{1}{\sqrt{2}} \begin{pmatrix} 1 & -1 \\ 1 & 1 \end{pmatrix}. \quad (23)$$

To obtain the Hadamard gate we have now to apply $X = \sigma_x$:

$$\sigma_x \cdot \frac{1}{\sqrt{2}}(1 - i\sigma_y) = \frac{1}{\sqrt{2}}(\sigma_x + \sigma_z) = H. \quad (24)$$

B. Rabi Oscillations

We consider a spin (qubit) in a constant magnetic field B_z and an oscillating field along x axis:

$$H = -\frac{1}{2}B_z \sigma_z - \Omega_R \cos \omega t \sigma_x. \quad (25)$$

We use $\sigma_x = \sigma_+ + \sigma_-$ and obtain

$$H = -\frac{1}{2}B_z \sigma_z - \frac{1}{2}\Omega_R(e^{i\omega t} + e^{-i\omega t})(\sigma_+ + \sigma_-). \quad (26)$$

We introduce the rotating frame. That is we introduce new wave functions like $|\tilde{\psi}\rangle = R(t)|\psi\rangle$. The Schrödinger equation for $|\tilde{\psi}\rangle$ reads

$$i\partial_t |\tilde{\psi}\rangle = i\dot{R}|\psi\rangle + RH|\psi\rangle = i\dot{R}R^{-1}|\tilde{\psi}\rangle + RHR^{-1}|\tilde{\psi}\rangle. \quad (27)$$

Thus the rotating frame Hamiltonian reads

$$\tilde{H} = i\dot{R}R^\dagger + RHR^\dagger . \quad (28)$$

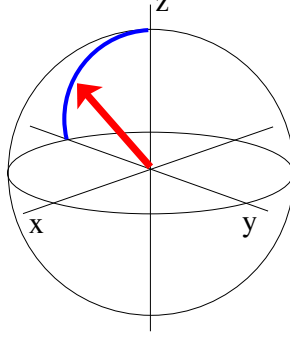


FIG. 10: Rabi oscillations in the rotating frame.

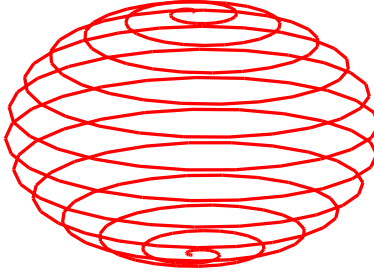


FIG. 11: Rabi oscillations in the lab frame.

We chose a concrete $R = \exp(-i\omega \frac{\sigma_z}{2} t)$. Then

$$\tilde{H} = -\frac{1}{2}(B_z - \omega) \sigma_z - \frac{1}{2}\Omega_R(e^{i\omega t} + e^{-i\omega t})(\sigma_+e^{-i\omega t} + \sigma_-e^{i\omega t}) . \quad (29)$$

$$\tilde{H} = -\frac{1}{2}(B_z - \omega) \sigma_z - \frac{1}{2}\Omega_R\sigma_x - \frac{1}{2}\Omega_R(\sigma_+e^{-2i\omega t} + \sigma_-e^{2i\omega t}) . \quad (30)$$

The rotating wave approximation (RWA) gives

$$\tilde{H} = -\frac{1}{2}(B_z - \omega) \sigma_z - \frac{1}{2}\Omega_R\sigma_x . \quad (31)$$

The simplest situation is at resonance $\omega = B_z$. Then we have an effective magnetic field Ω_R in the x direction and the spin precesses around the x axis exactly as in the case of Hamiltonian switching, but in the rotating frame (see Fig. 10 and Fig. 11). Note that the

Rabi frequency Ω_R can be time-dependent. Then, the situation is exactly as in the previous subsection and the angle of rotation θ is given by $\theta/2 = \int dt \Omega_R(t)$. This is called the "integral theorem". A nice thing is that the rotation angle is only sensitive to the integral of Ω_R , thus higher fidelity of manipulations.

Consider now a phase shifted driving:

$$H = -\frac{1}{2}B_z \sigma_z - \Omega_R \sin \omega t \sigma_x . \quad (32)$$

This gives

$$H = -\frac{1}{2}B_z \sigma_z - \frac{1}{2i}\Omega_R(e^{i\omega t} - e^{-i\omega t})(\sigma_+ + \sigma_-) . \quad (33)$$

Further, in the rotating frame

$$\tilde{H} = -\frac{1}{2}(B_z - \omega) \sigma_z - \frac{1}{2i}\Omega_R(e^{i\omega t} - e^{-i\omega t})(\sigma_+ e^{-i\omega t} + \sigma_- e^{i\omega t}) . \quad (34)$$

$$\tilde{H} = -\frac{1}{2}(B_z - \omega) \sigma_z - \frac{1}{2}\Omega_R \sigma_y - \frac{1}{2i}\Omega_R(\sigma_+ e^{-2i\omega t} - \sigma_- e^{2i\omega t}) . \quad (35)$$

The rotating wave approximation (RWA) gives

$$\tilde{H} = -\frac{1}{2}(B_z - \omega) \sigma_z - \frac{1}{2}\Omega_R \sigma_y . \quad (36)$$

Thus by choosing a different driving phase one can induce rotations around the y -axis in the rotating frame. Usually both phases are used so that arbitrary manipulations can be performed.

C. Simplest two-bit gates: iSWAP and $\sqrt{\text{iSWAP}}$

We consider the following Hamiltonian:

$$H = \frac{J}{4} (\sigma_x^{(1)} \sigma_x^{(2)} + \sigma_y^{(1)} \sigma_y^{(2)}) = \frac{J}{2} (\sigma_+^{(1)} \sigma_-^{(2)} + \sigma_-^{(1)} \sigma_+^{(2)}) , \quad (37)$$

where $\sigma_{\pm} \equiv (\sigma_x \pm i\sigma_y)/2$. We have $\sigma_+ |1\rangle = |0\rangle$ and $\sigma_- |0\rangle = |1\rangle$. (This is somewhat counterintuitive, because in spin physics we would call $|0\rangle = |\uparrow\rangle$ and $|1\rangle = |\downarrow\rangle$.)

In the basis $|00\rangle, |01\rangle, |10\rangle, |11\rangle$ this Hamiltonian reads

$$H = \frac{J}{2} \begin{pmatrix} 0 & 0 & 0 & 0 \\ 0 & 0 & 1 & 0 \\ 0 & 1 & 0 & 0 \\ 0 & 0 & 0 & 0 \end{pmatrix} . \quad (38)$$

It is clear that the operator e^{-iHt} works as $\hat{1}$ in the subspace $|00\rangle, |11\rangle$ and as $e^{-i\frac{J}{2}\sigma_x t}$ in the subspace $|01\rangle, |10\rangle$. Thus we obtain

$$e^{-iHt} = \begin{pmatrix} 1 & 0 & 0 & 0 \\ 0 & \cos \theta & i \sin \theta & 0 \\ 0 & i \sin \theta & \cos \theta & 0 \\ 0 & 0 & 0 & 1 \end{pmatrix}, \quad (39)$$

where $\theta = -Jt/2$. Choosing $\theta = \pi/2$ we obtain iSWAP gate. If we disregard the multiplier i this is a usual classical *SWAP* gate which swaps the two states of two qubits. However, choosing $\theta = \pi/4$ we obtain the purely quantum $\sqrt{\text{iSWAP}}$ gate. Clearly, this gate entangles the two qubits.

VII. ADIABATIC MANIPULATIONS

A. Adiabatic "theorem"

We consider the Hamiltonian $H = H_0 + V(t)$. Assume that the perturbation once switched on remains forever (see Fig. 12).

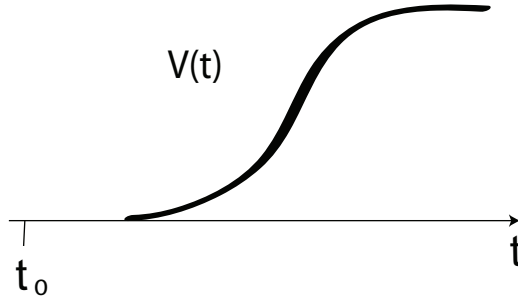


FIG. 12: Perturbation $V(t)$ that does not disappear.

The evolution operator in the interaction representation reads

$$U_I(t, t_0) = T \exp \left(-\frac{i}{\hbar} \int_{t_0}^t dt' V_I(t') \right). \quad (40)$$

Assume the initial state is the eigenstate $|n\rangle$ of H_0 . We obtain

$$|\Psi_I(t)\rangle = U_I(t, t_0) |n\rangle \approx \left(1 - \frac{i}{\hbar} \int_{t_0}^t dt' V_I(t') \right) |n\rangle, \quad (41)$$

(Recall, $|m\rangle$ are the eigenstates of H_0). The amplitude $a_{n \rightarrow m}$ in the expansion of the wave function $|\Psi_I(t)\rangle$ is given by

$$a_{n \rightarrow m} = -\frac{i}{\hbar} \int_{t_0}^t dt' V_{mn}(t') e^{i\omega_{mn}t'} . \quad (42)$$

We integrate by parts:

$$a_{n \rightarrow m} = -\frac{V_{mn}(t')}{\hbar\omega_{mn}} e^{i\omega_{mn}t'} \Big|_{t_0}^t + \frac{1}{\hbar} \int_{t_0}^t dt' \left(\frac{\partial V_{mn}(t')}{\partial t'} \right) \frac{e^{i\omega_{mn}t'}}{\omega_{mn}} . \quad (43)$$

At t_0 there was no perturbation, $V(t_0) = 0$, thus

$$a_{n \rightarrow m} = -\frac{V_{mn}(t)}{\hbar\omega_{mn}} e^{i\omega_{mn}t} + \frac{1}{\hbar} \int_{t_0}^t dt' \left(\frac{\partial V_{mn}(t')}{\partial t'} \right) \frac{e^{i\omega_{mn}t'}}{\omega_{mn}} . \quad (44)$$

Let us try to understand the meaning of the first term of (44). Recall the time-independent perturbation theory for Hamiltonian $H = H_0 + V$. The corrected (up to the first order) eigenstate $|\tilde{n}\rangle$ is given by

$$|\tilde{n}\rangle \approx |n\rangle - \sum_{m \neq n} \frac{V_{mn}}{E_m - E_n} |m\rangle \quad (45)$$

It is clear that the first term of (44) and the first order corrections in (45) have something to do with each other (are the same). To compare we have to form in both cases the time-dependent Schrödinger wave function. From (44) we obtain the interaction representation wave function $|\Psi_I\rangle = |n\rangle + \sum_{m \neq n} a_{n \rightarrow m}(t) |m\rangle$, which leads in the Schrödinger picture to

$$|\Psi(t)\rangle = |n\rangle e^{-iE_n t/\hbar} - \sum_{m \neq n} \frac{V_{mn}}{E_m - E_n} |m\rangle e^{-iE_n t/\hbar} \quad (46)$$

The same we get from (45) (upon neglecting corrections to the energy E_n).

Thus, the first term of (44) corresponds to the state "adjusting" itself to the new Hamiltonian, i.e., remaining the eigenstate of the corrected Hamiltonian $H = H_0 + V$. The "real" transitions can only be related to the second term of (44).

Idea of adiabatic approximation: if $\partial V_{mn}(t)/\partial t$ is small, than no real transition will happen, and, the state will remain the eigenstate of a slowly changing Hamiltonian.

B. Transformation to the adiabatic (instantaneous) basis

New idea: follow the eigenstates of the changing Hamiltonian $H(t)$. It is convenient to introduce a vector of parameters $\vec{\chi}$ upon which the Hamiltonian depends and which change

in time. $H(t) = H(\vec{\chi}(t))$. We no longer consider a situation when only a small perturbation is time-dependent. Diagonalize the Hamiltonian for each $\vec{\chi}$. Introduce instantaneous eigenstates $|n(\vec{\chi})\rangle$, such that $H(\vec{\chi}) |n(\vec{\chi})\rangle = E_n(\vec{\chi}) |n(\vec{\chi})\rangle$. Since $H(\vec{\chi})$ changes continuously, it is reasonable to assume that $|n(\vec{\chi})\rangle$ do so as well. Introduce a unitary transformation

$$R(t, t_0) \equiv \sum_n |n(\vec{\chi}(t_0))\rangle \langle n(\vec{\chi}(t))| = \sum_n |n_0\rangle \langle n(\vec{\chi}(t))| . \quad (47)$$

For brevity $|n_0\rangle \equiv |n(\vec{\chi}(t_0))\rangle$. Idea: if $|\Psi(t)\rangle \propto |n(\vec{\chi}(t))\rangle$, i.e., follows adiabatically, the new wave function: $|\Phi(t)\rangle = R(t, t_0) |\Psi(t)\rangle \propto |n_0\rangle$ does not change at all. Let's find the Hamiltonian governing time evolution of $|\Phi(t)\rangle$:

$$i\hbar \dot{|\Phi\rangle} = i\hbar R \dot{|\Psi\rangle} + i\hbar \dot{R} |\Psi\rangle = RH(t) |\Psi\rangle + i\hbar \dot{R} |\Psi\rangle = [RHR^{-1} + i\hbar \dot{R}R^{-1}] |\Phi\rangle \quad (48)$$

Thus the new Hamiltonian is given by

$$\tilde{H} = RHR^{-1} + i\hbar \dot{R}R^{-1} \quad (49)$$

The first term is diagonal. Indeed

$$\begin{aligned} R(t, t_0) H(t) R(t_0, t) &= \sum_{nm} |n_0\rangle \langle n(\vec{\chi}(t))| H(\vec{\chi}(t)) |m(\vec{\chi}(t))\rangle \langle m_0| \\ &= \sum_n E_n(\vec{\chi}(t)) |n_0\rangle \langle n_0| . \end{aligned} \quad (50)$$

Thus transitions can happen only due to the second term which is proportional to the time derivative of R , i.e., it is small for slowly changing Hamiltonian.

C. Geometric Phase

The operator $i\hbar \dot{R}R^{-1}$ may have diagonal and off-diagonal elements. The latter will be responsible for transitions and will be discussed later. Here we discuss the role of the diagonal elements, e.g.,

$$V_{nn}(t) = \langle n_0 | i\hbar \dot{R}R^{-1} | n_0 \rangle = i\hbar \langle \dot{n}(\vec{\chi}(t)) | n(\vec{\chi}(t)) \rangle = i\hbar \dot{\vec{\chi}} \langle \vec{\nabla} n(\vec{\chi}) | n(\vec{\chi}) \rangle . \quad (51)$$

This (real) quantity serves as an addition to energy $E_n(\vec{\chi})$, i.e., $\delta E_n = V_n n$. Thus, state $|n_0\rangle$ acquires an additional phase

$$\delta \Phi_n = - \int dt \delta E_n = -i \int dt \langle \dot{n}(\vec{\chi}(t)) | n(\vec{\chi}(t)) \rangle . \quad (52)$$

This phase is well defined only for closed path, i.e., when the Hamiltonian returns to itself. Indeed the choice of the basis $|n(\vec{\chi})\rangle$ is arbitrary up to a phase. Instead of $|n(\vec{\chi})\rangle$ we could have chosen $e^{-i\Lambda_n(\vec{\chi})} |n(\vec{\chi})\rangle$. Instead of (51) we would then obtain

$$V_{nn}(t) = i\hbar \langle \dot{n}(\vec{\chi}(t)) | n(\vec{\chi}(t)) \rangle + \hbar \dot{\Lambda}_n(\vec{\chi}(t)) . \quad (53)$$

Thus the extra phase is, in general, not gauge invariant. For closed path we must choose the basis $|n(\vec{\chi})\rangle$ so that it returns to itself. That is $|n(\vec{\chi})\rangle$ depends only on the parameters $\vec{\chi}$ and not on the path along which $\vec{\chi}$ has been arrived. This means $\Lambda_n(t_0) = \Lambda_n(t_0 + T)$, where T is the traverse time of the closed contour. In this case the integral of $\dot{\Lambda}_n$ vanishes and we are left with

$$\Phi_{Berry,n} \equiv \delta\Phi_n = -i \int dt \langle \dot{n}(\vec{\chi}(t)) | n(\vec{\chi}(t)) \rangle = -i \int d\vec{\chi} \langle \vec{\nabla} n | n \rangle \quad (54)$$

This is Berry's phase. It is a geometric phase since it depends only on the path in the parameter space and not on velocity along the path. Physical meaning (thus far) only for superpositions of different eigenstates.

1. Example: Spin 1/2

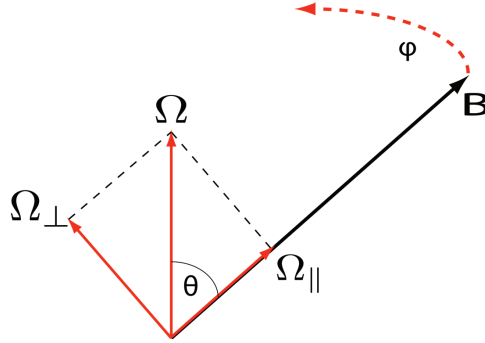


FIG. 13: Time-dependent magnetic field.

We consider a spin-1/2 in a time-dependent magnetic field $\vec{B}(t)$: $\dot{\vec{b}} = \vec{\Omega} \times \vec{b}$, where $\vec{b} \equiv \vec{B}/|\vec{B}|$ and $\vec{\Omega}$ is the angular velocity. The instantaneous position of \vec{B} is determined by the angles $\theta(t)$ and $\varphi(t)$. The Hamiltonian reads

$$H(t) = -\frac{1}{2} \vec{B}(t) \cdot \vec{\sigma} \quad (55)$$

We transform to the rotating frame with $|\Phi(t)\rangle = R(t) |\Psi(t)\rangle$ such that \vec{b} is the z -axis in the rotating frame. Here $|\Psi\rangle$ is the wave function in the laboratory frame while $|\Phi(t)\rangle$ is the wave function in the rotating frame. It is easy to find R^{-1} since it transforms a spin along the z -axis (in the rotating frame) into a spin along \vec{B} (in the lab frame), i.e., into the time dependent eigenstate $|n(\vec{B}(t))\rangle = |\uparrow(\vec{B}(t))\rangle$. Namely $R^{-1} |\uparrow_z\rangle = |\uparrow(\vec{B}(t))\rangle$. Thus

$$R^{-1}(t) = e^{-\frac{i\varphi(t)}{2} \sigma_z} e^{-\frac{i\theta(t)}{2} \sigma_y} . \quad (56)$$

This gives

$$RHR^{-1} = -\frac{1}{2} |\vec{B}| \sigma_z \quad (57)$$

and

$$i\dot{R}R^{-1} = -\frac{\dot{\theta}}{2} \sigma_y - \frac{\dot{\varphi}}{2} e^{i\frac{\theta}{2} \sigma_y} \sigma_z e^{-i\frac{\theta}{2} \sigma_y} = -\frac{\dot{\theta}}{2} \sigma_y - \frac{\dot{\varphi}}{2} (\cos \theta \sigma_z - \sin \theta \sigma_x) . \quad (58)$$

We can write

$$i\dot{R}R^{-1} = -\frac{1}{2} \vec{\Omega} \cdot \vec{\sigma} , \quad (59)$$

where $\vec{\Omega} = (-\dot{\varphi} \sin \theta, \dot{\theta}, \dot{\varphi} \cos \theta)$ is the angular velocity vector expressed in the rotating frame.

We obtain

$$[i\dot{R}R^{-1}]_{diag} = -\frac{\dot{\varphi}}{2} \cos \theta \sigma_z \quad (60)$$

For the Berry phase this would give

$$\Phi_{\uparrow/\downarrow, Berry} = \pm \frac{1}{2} \int \dot{\varphi} \cos \theta dt = \pm \frac{1}{2} \int \Omega_{\parallel} dt , \quad (61)$$

where Ω_{\parallel} is the projection of the angular velocity on the direction of \vec{B} (see Fig. 13). This is however a wrong answer. What we forgot to check is whether the basis vectors return to themselves after a full rotation $\theta(t_0 + T) = \theta(t_0)$, $\varphi(t_0 + T) = \varphi(t_0) + 2\pi$. The operator that transforms the eigenvector at $t = t_0$ to the eigenvector at $t = t_0 + T$ is given by

$$R^{-1}(t_0 + T)R(t_0) = e^{-i\frac{\varphi+2\pi}{2} \sigma_z} e^{-\frac{i\theta}{2} \sigma_y} e^{\frac{i\theta}{2} \sigma_y} e^{i\frac{\varphi}{2} \sigma_z} = e^{-i\pi \sigma_z} . \quad (62)$$

Thus the states $|\uparrow / \downarrow\rangle$ get an extra phase $\mp\pi$. The correct, gauge invariant Berry's phase reads

$$\Phi_{\uparrow/\downarrow, Berry} = \pm \frac{1}{2} \int \dot{\varphi} (\cos \theta - 1) dt = \pm \frac{1}{2} \int d\varphi (\cos \theta - 1) . \quad (63)$$

It is given by the solid angle (see Fig. 14).

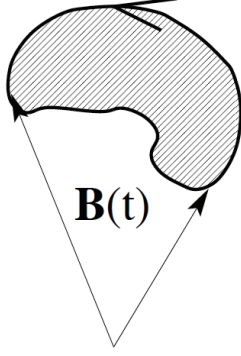


FIG. 14: Solid angle.

D. Geometric interpretation

Once again we have a Hamiltonian, which depends on time via a vector of parameters $\vec{\chi}(t)$, i.e., $H(t) = H(\vec{\chi}(t))$. The Berry's phase of the eigenvector $|\Psi_n\rangle$ is given by

$$\Phi_{n,Berry} = i \int_{t_0}^t \langle \Psi_n | \partial_t \Psi_n \rangle dt' = i \int_{t_0}^t \langle \Psi_n | \vec{\nabla}_{\vec{\chi}} \Psi_n \rangle \dot{\vec{\chi}} dt' = i \int_{t_0}^t \langle \Psi_n | \vec{\nabla}_{\vec{\chi}} \Psi_n \rangle d\vec{\chi} . \quad (64)$$

We introduce a "vector potential" in the parameter space

$$\vec{A}_n(\vec{\chi}) \equiv \langle \Psi_n | i \vec{\nabla}_{\vec{\chi}} | \Psi_n \rangle , \quad (65)$$

which gives

$$\Phi_{n,Berry} = \oint_C \vec{A}_n(\vec{\chi}) d\vec{\chi} . \quad (66)$$

Further

$$\Phi_{n,Berry} = \int (\vec{\nabla}_{\vec{\chi}} \times \vec{A}_n) \cdot d\vec{S} = \int \vec{B}_n \cdot d\vec{S} . \quad (67)$$

Thus the Berry's phase is given by the flux of an effective "magnetic field" $\vec{B}_n \equiv \vec{\nabla}_{\vec{\chi}} \times \vec{A}_n$. Clearly, one needs at least two-dimensional parameter space to be able to traverse a contour with a flux through it (see Fig. 15).

E. Non-Abelian Berry Phase (Holonomy)

Imagine we have a degenerate subspace of N instantaneous eigenvectors. The rotating frame Hamiltonian $\tilde{H} = RHR^{-1} + i\hbar \dot{R}R^{-1}$, restricted to this subspace has the form

$$H_{s,kl} = \text{const} + \langle k | i\hbar \dot{R}R^{-1} | l \rangle . \quad (68)$$

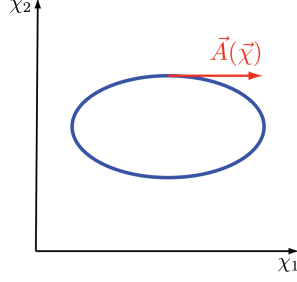


FIG. 15: Contour in the parameter space.

This matrix is not necessarily diagonal. Thus nontrivial evolution can happen in the subspace. We generalize the vector potential to a matrix

$$\vec{A}_{kl}(\vec{\chi}) \equiv \langle \Psi_k | i \vec{\nabla}_{\vec{\chi}} | \Psi_l \rangle , \quad (69)$$

The evolution operator in the subspace is a path ordered exponent

$$U_s = P e^{i \oint_C \vec{A}_{kl}(\vec{\chi}) d\vec{\chi}} . \quad (70)$$

Thus it is no longer "only" a phase.

F. Non-adiabatic corrections: Transitions

1. Super-adiabatic bases

The Hamiltonian (49) in the adiabatic basis reads $\tilde{H} = R H R^\dagger + i \dot{R} R^\dagger$. Lets call it $H_1 = \tilde{H}$. If the case is adiabatic, i.e., $R(t)$ is slow, the new Hamiltonian $H_1(t)$ is also slow. We can again find its instantaneous eigen-basis $|n_1(t)\rangle$, such that $H_1(t) |n_1(t)\rangle = E_1(t) |n_1(t)\rangle$. We introduce the transformation $R_1 = \sum_n |n(t)\rangle \langle n_1(t)|$. Transforming to the superadiabatic basis $|n_1\rangle$ we obtain the Hamiltonian

$$H_2 = R_1 H_1 R_1^{-1} + i \dot{R}_1 R_1^{-1} . \quad (71)$$

These iterations can be continued as suggested by Berry [1]. It seems that the rotation R_1 and further rotations R_2, R_3, \dots are closer and closer to $\hat{1}$. Indeed, since we have an adiabatic case, \dot{R} is small. Then, $i \dot{R} R^{-1}$ is also small and, since its the only term that is non-diagonal in H_1 , the diagonalization R_1 must be a very small rotation. Thus, $|n_1\rangle$ is a better approximation to the state of the system assuming it started in the eigenstate $|n\rangle$.

Berry showed that this logic works for a certain number of iterations and one can improve the precision of adiabatic calculations. However at some point a problem arises: the series H, H_1, H_2, \dots stops converging. It turns out to be an asymptotic series.

Let's first understand what would happen if the superadiabatic iteration scheme would always converge. Then the adiabatic theorem would be exact. Indeed, if we started in a state $|n\rangle$, during the evolution with the time-dependent $H(t)$ we would be in the state $|n_\infty\rangle$ (since the superadiabatic iteration converge). After the Hamiltonian stops changing in time, we have $H = H_1 = H_2 = \dots$ and the system is again in the state $|n\rangle$. Thus real transitions never happen.

In reality transitions do happen. However, the slower is $H(t)$ the better works the superadiabatic scheme and the transitions appear only after very many iterations. The transition probability is thus very small. Below we investigate the transition probability.

2. Perturbation theory

We can treat the Hamiltonian (49) perturbatively. $\tilde{H}(t) = H_0(t) + V(t)$, where

$$H_0(t) = \sum_n E_n(\vec{\chi}(t)) |n_0\rangle \langle n_0| , \quad (72)$$

and

$$V(t) = i\hbar \dot{R} R^{-1} = i\hbar \sum_{n,m} |n_0\rangle \langle \dot{n}(\vec{\chi}(t)) | m(\vec{\chi}(t)) \rangle \langle m_0| . \quad (73)$$

H_0 is diagonal, but time dependent. Interaction representation is simple to generalize:

$$|\Phi(t)\rangle \equiv e^{-\frac{i}{\hbar} \int_{t_0}^t dt' H_0(t')} |\Phi_I(t)\rangle \quad (74)$$

and

$$i\hbar \frac{d}{dt} |\Phi_I\rangle = V_I(t) |\Phi_I\rangle , \quad (75)$$

where

$$V_I(t) \equiv e^{\frac{i}{\hbar} \int_{t_0}^t dt' H_0(t')/\hbar} V(t) e^{-\frac{i}{\hbar} \int_{t_0}^t dt' H_0(t')/\hbar} \quad (76)$$

($H_0(t)$ commutes with itself at different times).

For the transition probability (of the first order) this gives

$$\begin{aligned}
P_{n \rightarrow m} &\approx \frac{1}{\hbar^2} \left| i\hbar \int_{t_0}^t dt' \langle \dot{n}(\vec{\chi}(t')) | n(\vec{\chi}(t')) \rangle e^{-i \int_{t_0}^{t'} dt'' [E_n(\vec{\chi}(t'')) - E_m(\vec{\chi}(t''))]/\hbar} \right|^2 \\
&= \left| \int_{t_0}^t dt' \langle \dot{n}(\vec{\chi}(t')) | n(\vec{\chi}(t')) \rangle e^{-i \int_{t_0}^{t'} dt'' [E_n(\vec{\chi}(t'')) - E_m(\vec{\chi}(t''))]/\hbar} \right|^2 .
\end{aligned} \tag{77}$$

3. Landau-Zener transition: perturbative solution

$$H(t) = -\frac{1}{2} (\epsilon(t)\sigma_z + \Delta\sigma_x) \tag{78}$$

Parameter $\chi(t) = \epsilon(t) = \alpha t$.

The eigenstates (dependent on χ)

$$\begin{aligned}
|0(\chi = \epsilon)\rangle &= \cos(\eta/2) |\uparrow\rangle + \sin(\eta/2) |\downarrow\rangle \\
|1(\chi = \epsilon)\rangle &= -\sin(\eta/2) |\uparrow\rangle + \cos(\eta/2) |\downarrow\rangle ,
\end{aligned} \tag{79}$$

where $\tan \eta \equiv \Delta/\epsilon$. We find also the eigenenergies (dependent on $\chi = \epsilon$) $E_{0/1} = \mp(1/2)\sqrt{\epsilon^2 + \Delta^2}$.

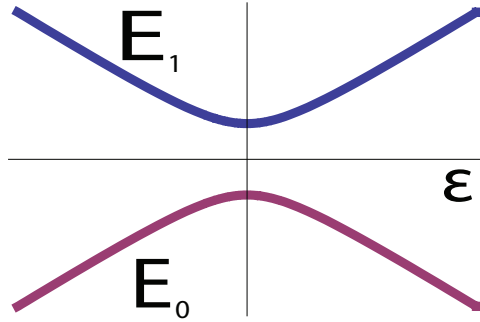


FIG. 16: Energy levels $E_0(\epsilon)$ and $E_1(\epsilon)$.

We obtain $\langle \dot{1} | 0 \rangle = -(1/2)\dot{\eta}$. From $\cot \eta = (\alpha t/\Delta)$ we obtain $\dot{\eta} = -\sin^2 \eta (\alpha/\Delta) = -\frac{\Delta\alpha}{\Delta^2 + \alpha^2 t^2}$. In the adiabatic basis the Schrödinger equation for the wave function $|\psi\rangle = a(t)|0(\epsilon)\rangle + b(t)|1(\epsilon)\rangle$ reads

$$i\hbar \frac{d}{dt} \begin{pmatrix} a \\ b \end{pmatrix} = -\frac{1}{2} \begin{pmatrix} \sqrt{\Delta^2 + \epsilon(t)^2} & -2i\hbar \langle \dot{0} | 1 \rangle \\ -2i\hbar \langle \dot{1} | 0 \rangle & -\sqrt{\Delta^2 + \epsilon(t)^2} \end{pmatrix} \begin{pmatrix} a \\ b \end{pmatrix} . \tag{80}$$

We obtain

$$i\hbar \frac{d}{dt} \begin{pmatrix} a \\ b \end{pmatrix} = -\frac{1}{2} \begin{pmatrix} \sqrt{\Delta^2 + \alpha^2 t^2} & \frac{i\hbar\Delta\alpha}{\Delta^2 + \alpha^2 t^2} \\ -\frac{i\hbar\Delta\alpha}{\Delta^2 + \alpha^2 t^2} & -\sqrt{\Delta^2 + \alpha^2 t^2} \end{pmatrix} \begin{pmatrix} a \\ b \end{pmatrix}. \quad (81)$$

There is a pair of special points in the complex t -plane $t = \pm t_0 = \pm i\Delta/\alpha$.

Assume that at $t \rightarrow -\infty$ the system was in the state $|0(\chi = \epsilon = -\infty)\rangle$. What is the probability that at $t \rightarrow \infty$ a transition will happen to the state $|1(\chi = \epsilon = \infty)\rangle$? From Eq. (77) we obtain

$$P_{0 \rightarrow 1} \approx \left| \int_{-\infty}^{\infty} dt' \langle 1|0 \rangle e^{(i/\hbar) \int_0^{t'} dt'' \sqrt{\Delta^2 + \alpha^2 t''^2}} \right|^2. \quad (82)$$

(The lower limit of integration in the exponent was changed to 0, this just adds a constant phase which does not change the probability).

For the transition probability this gives

$$P_{0 \rightarrow 1} \approx \left| \frac{1}{2} \int_{-\infty}^{\infty} dt' \frac{\Delta\alpha}{\Delta^2 + \alpha^2 t'^2} e^{(i/\hbar) \int_0^{t'} dt'' \sqrt{\Delta^2 + \alpha^2 t''^2}} \right|^2. \quad (83)$$

Introducing a new (dimensionless) time $\tau \equiv \alpha t/\Delta$ we obtain

$$P_{0 \rightarrow 1} \approx \left| \frac{1}{2} \int_{-\infty}^{\infty} d\tau' \frac{1}{1 + \tau'^2} e^{i\gamma \int_0^{\tau'} d\tau'' \sqrt{1 + \tau''^2}} \right|^2, \quad (84)$$

where $\gamma \equiv \Delta^2/(\hbar\alpha)$. We see that the result depends only on γ .

Smart people (M. Berry) have calculated this integral and got

$$P_{0 \rightarrow 1} \approx \left| (\pi/3) e^{-\frac{\pi\gamma}{4}} \right|^2 = (\pi^2/9) e^{-\frac{\pi\gamma}{2}}. \quad (85)$$

Problem: the result is non-analytic in α which characterizes the slowness of the change of the Hamiltonian. Thus the logic of our perturbative expansion does not work. The result is actually exponentially small for small enough α and not only small because it is proportional to α . It cannot be excluded that higher order contributions will give also exponentially small results.

4. Landau-Zener transition: quasi-classical solution in the adiabatic basis

Once again the Schrödinger equation in the adiabatic basis reads

$$i\hbar \frac{d}{dt} \begin{pmatrix} a \\ b \end{pmatrix} = -\frac{1}{2} \begin{pmatrix} \sqrt{\Delta^2 + \alpha^2 t^2} & \frac{i\hbar\Delta\alpha}{\Delta^2 + \alpha^2 t^2} \\ -\frac{i\hbar\Delta\alpha}{\Delta^2 + \alpha^2 t^2} & -\sqrt{\Delta^2 + \alpha^2 t^2} \end{pmatrix} \begin{pmatrix} a \\ b \end{pmatrix}. \quad (86)$$

We observe that the Hamiltonian has two special points in the complex plain: $t = \pm t_0 = \pm \frac{i\Delta}{\alpha}$ (Fig. 17). For $t \rightarrow -\infty$ the system is in the state $|0\rangle = |\downarrow\rangle$. The asymptotic solution at $t \rightarrow -\infty$ reads

$$a \approx \exp \left\{ \frac{i}{2\hbar} \int_0^t d\tau \sqrt{\Delta^2 + \alpha^2 \tau^2} \right\}. \quad (87)$$

and $b \approx 0$. Instead of solving the Schrödinger equation (86) on the real t -axis we "go

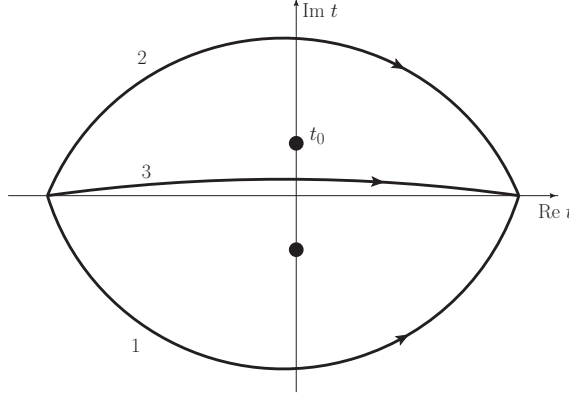


FIG. 17: Three contours.

around" in the complex plane. Let us investigate how the asymptotic Eq. (87) behaves if we go along the contours 1, 2, 3 of Fig. 17. Since in (86) $\sqrt{\Delta^2 + \alpha^2 \tau^2}$ is assumed positive, for $\tau \rightarrow -\infty$ we obtain $\sqrt{\Delta^2 + \alpha^2 \tau^2} \approx -\alpha\tau$ and $a \approx e^{-\frac{i\alpha\tau^2}{4}}$. Along contour 3 (along the real axis) $\sqrt{\Delta^2 + \alpha^2 \tau^2}$ remains positive. Thus, for $\tau \rightarrow +\infty$ we have $\sqrt{\Delta^2 + \alpha^2 \tau^2} \approx \alpha\tau$. Thus, along the real axis we obtain $a \approx e^{\frac{i\alpha\tau^2}{4}}$ for $\tau \rightarrow +\infty$. This exponent corresponds to state $|0\rangle = |\uparrow\rangle$. Thus contour 3 corresponds to the adiabatic evolution. On the other hand, along contours 1 and 2 the solution $a \approx e^{-\frac{i\alpha\tau^2}{4}}$ remains the same at $\tau \rightarrow -\infty$ and at $\tau \rightarrow +\infty$. At $\tau \rightarrow +\infty$ this corresponds to the state $|1\rangle = |\uparrow\rangle$. These contours describe the Landau-Zener transition. However we should have gotten the non-zero b . Let's leave this task and go further to the calculation in the diabatic basis.

5. *Landau-Zener transition: quasi-classical solution in the diabatic basis*

In the diabatic basis $|\uparrow / \downarrow\rangle$ the Schrödinger equation reads

$$i\hbar \frac{d}{dt} \begin{pmatrix} A \\ B \end{pmatrix} = -\frac{1}{2} \begin{pmatrix} \alpha t & \Delta \\ \Delta & -\alpha t \end{pmatrix} \begin{pmatrix} A \\ B \end{pmatrix}. \quad (88)$$

For $t \rightarrow -\infty$ the system is in the state $|\downarrow\rangle$, i.e. $|A(-\infty)| = 0$ and $|B(-\infty)| = 1$.

We obtain ($\hbar = 1$)

$$\begin{aligned} \left(i \frac{d}{dt} + \frac{1}{2}\alpha t\right) A &= -\frac{\Delta}{2} B \\ \left(i \frac{d}{dt} - \frac{1}{2}\alpha t\right) B &= -\frac{\Delta}{2} A. \end{aligned} \quad (89)$$

This gives

$$\left(i \frac{d}{dt} + \frac{1}{2}\alpha t\right) \left(i \frac{d}{dt} - \frac{1}{2}\alpha t\right) B = \frac{\Delta^2}{4} B. \quad (90)$$

Further

$$\left(-\frac{d^2}{dt^2} - \frac{\alpha^2 t^2}{4} - \frac{i\alpha}{2}\right) B = \frac{\Delta^2}{4} B. \quad (91)$$

We attempt a semiclassical solution $A = e^{iS}$ and obtain

$$\dot{S}^2 - i\ddot{S} = \frac{\alpha^2 t^2 + \Delta^2}{4} + \frac{i\alpha}{2}. \quad (92)$$

We again "go around" the point $t = 0$ along a contour such that everywhere $\alpha^2 |t|^2 \gg \Delta^2$.

Then we can perform an expansion in $\Delta/(\alpha t)$. We write $S = S_0 + S_1$ and obtain $S_0 = -\frac{\alpha t^2}{4}$.

For S_1 we obtain

$$2\dot{S}_0\dot{S}_1 + \dot{S}_1^2 - i\ddot{S}_1 = \frac{\Delta^2}{4}. \quad (93)$$

Leaving only the first term in the RHS we obtain

$$\dot{S}_1 = -\frac{\Delta^2}{4\alpha t} = -\frac{\gamma}{4t}. \quad (94)$$

This gives

$$S_1 = -\frac{\gamma}{4} \ln t + \text{const.} \quad (95)$$

(the constant should be chosen so that S_1 is real for $t \rightarrow -\infty$). Upon the traversal of the contour (in the upper half-plane) the function S_1 acquires an imaginary part

$$\text{Im}[S_1] = \frac{\pi\gamma}{4}. \quad (96)$$

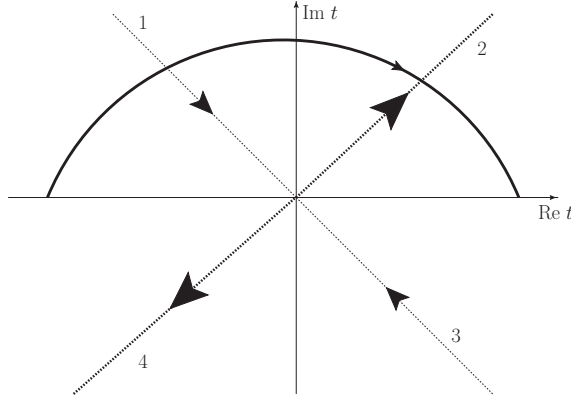


FIG. 18: Stokes lines. In complex analysis a Stokes line, named after Sir George Gabriel Stokes, is a line in the complex plane which 'turns on' different kinds of behaviour when one 'passes over' this line. Somewhat confusingly, this definition is sometimes used for anti-Stokes lines.

The question is whether we choose a contour in the lower or in the upper half-plane. The asymptotic solution for $t \rightarrow -\infty$ reads $e^{iS_0} = e^{-\frac{i\alpha t^2}{2}}$. In Fig. 18 the so called Stokes lines are shown on which $e^{-\frac{i\alpha t^2}{2}}$ is real. On Stokes lines 1 and 3 the function $e^{-\frac{i\alpha t^2}{2}}$ is exponentially small (decreases with increasing $|t|$). On Stokes lines 2 and 4 the function $e^{-\frac{i\alpha t^2}{2}}$ is exponentially large (increases with increasing $|t|$). We start from the negative real axis on which $B \approx e^{-\frac{i\alpha t^2}{2}}$. If we would continue in the lower half-plane this solution would first become exponentially large at line 4. There another solution $e^{\frac{i\alpha t^2}{2}}$ would be exponentially small. This another solution would become large on line 3 where the original solution is small and we should "drop". On the other hand, if we continue in the upper half-plane the solution $e^{-\frac{i\alpha t^2}{2}}$ first becomes small at line 1. However we do not have there the big solution $e^{\frac{i\alpha t^2}{2}}$ since it was not there on the real negative axis. This we continue with the solution $e^{-\frac{i\alpha t^2}{2}}$ all the way to the positive real axis.

The transition probability, thus, reads

$$P_{0 \rightarrow 1} = \frac{|B(+\infty)|^2}{|B(-\infty)|^2} = e^{-2\text{Im}[S_1]} = e^{-\frac{\pi\gamma}{2}}. \quad (97)$$

6. Landau-Zener transition: exact solution

The exact result is known (Landau 1932, Zener 1932, Stückelberg 1932, Majorana 1932). It reads: $P_{0 \rightarrow 1} = e^{-\frac{\pi\gamma}{2}}$ for arbitrary γ .

VIII. OPEN QUANTUM SYSTEMS

In the undergraduate course it is mostly assumed that the quantum system of interest is completely isolated from its surroundings. The state of the system is described by a vector $|\psi(t)\rangle$, and its time evolution is given by the unitary operator e^{-iHt} where H is the Hamiltonian of the system. If the system is controlled coherently, e.g. by a laser field, or by an external magnetic field, it is strictly speaking not a closed system any more, because of its interaction with the external field. However, in many cases this interaction can be accounted for by a modification of the Hamiltonian (which might now be time-dependent), and we can still treat the system like a closed system. In such cases, we say the system interacts with a “classical” field.

However, there are many situations in which this is not the case. As a simple example consider qubit A as the system of interest, which interacts with another qubit B which is initially in the state $|0\rangle$. We use the interaction Hamiltonian Eq. (38) and choose $t = -\pi/J$ to obtain an iSWAP gate, which essentially swaps the states of the two states. The evolution of qubit A is:

$$\begin{aligned} |\psi(0)\rangle = |0\rangle &\rightarrow |\psi(t)\rangle = |0\rangle \\ |\psi(0)\rangle = |1\rangle &\rightarrow |\psi(t)\rangle = |0\rangle \end{aligned} \tag{98}$$

No unitary evolution operator acting on the Hilbert space \mathcal{H}_A of qubit A results in such a transformation!!! Of course, this transformation can be described by a unitary operator in the larger Hilbert space $\mathcal{H}_A \otimes \mathcal{H}_B$.

In real experiments, the system of interest often interacts with an environment E (e.g. a bath in its thermal equilibrium) with infinitely degrees of freedom. It is a hopeless task to find the total evolution operator in $\mathcal{H}_A \otimes \mathcal{H}_E$, and often the state and / or the Hamiltonian of E is not known. We have to find other methods, and that is the aim of the theory of open quantum systems. We follow in part the book of Breuer and Petruccione (see literature list).

An environment generally has the following effects on a quantum systems

- **Decoherence:** Superpositions of macroscopically distinct states are strongly suppressed.
- **Dephasing:** Off-diagonals of the density matrix in the basis of the energy eigenstates

get reduced. This can have two causes: Phase averaging if the energy is not known exactly (sometimes reversible by spin echo), and decoherence (non-reversible)

- **Dissipation:** Exchange of energy between system and environment. This changes the populations of the density matrix and eventually leads to the equilibrium state $\rho_S(t \rightarrow \infty) = \frac{1}{Z} e^{-H/k_B T}$ at the temperature of the environment.

A. Density operator

We can formulate quantum mechanics using either state vectors $|\psi\rangle$, or state operators ρ (usually referred to as density operator). The table I shows a brief comparison:

	State vector	Density operator
State	$ \psi\rangle$	$\rho = \psi\rangle\langle\psi $
Time evolution	$\frac{d}{dt} \psi\rangle = -iH \psi\rangle$	$\frac{d}{dt} \rho = -i[H, \rho]$
Expectation value of O	$\langle\psi O \psi\rangle$	$\text{Tr}(\rho O)$
Probability of measuring m	$ \langle m \psi \rangle ^2$	$\langle m \rho m \rangle$

TABLE I: State vectors and density operators for pure states

The density operator formalism has two big advantages:

- **Statistical mixtures:** We do not know the state with certainty, but we know that with probability p_j we are in the state $|\psi_j\rangle$. In the state vector formalism, we have to evolve all states $|\psi_j\rangle$, calculate each expectation value $\langle O \rangle_j = \langle\psi_j| O |\psi_j\rangle$ and take the average $\langle O \rangle = \sum_j \langle O \rangle_j$ (same for probabilities). In the density operator formalism we just use $\rho = \sum_j p_j |\psi_j\rangle\langle\psi_j|$, and continue as with a pure state.
- **Subsystems:** If the state vector of a composite system AB is $|\psi_{AB}\rangle$, we can generally not assign a state vector to the subsystems A and B (\rightarrow entanglement). However, we can always describe the subsystems by a density operator which is obtained by the partial trace of the density operator of the composite system, e.g. $\rho_A = \text{Tr}_B \rho_{AB}$.

The first property is very useful in statistical mechanics, while the second is very valuable for open quantum systems, where the system S of interest is part of a much larger composite system SE .

A density operator has the following properties:

- $\text{Tr}(\rho)=1$ (\rightarrow sum of all probabilities)
- $\text{Tr}(\rho^2) \leq 1$, “=” if and only if the system is in a pure state.
- $\rho^\dagger = \rho$
- $\rho \geq 0$: Eigenvalues between zero and one (\rightarrow probabilities)

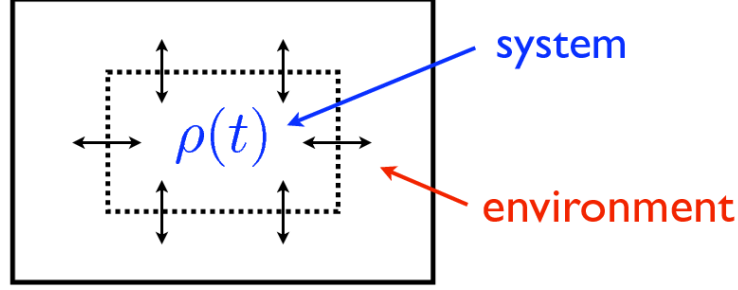
Different physical situations can lead to the same density matrix. Consider the Bell states $|\phi^\pm\rangle = (|00\rangle \pm |11\rangle)/\sqrt{2}$. Both result in reduced density operators $\rho_A = \rho_B = \mathbb{1}/2$, as do the other two Bell states, or an equal mixture of all pure states (this describes the situation in which we have no information about the state). This imposes the question whether the density operator formalism is sufficient to describe all physical situations. The answer is a definite yes if one is interested in the prediction of probabilities of measurement outcomes only, as is usually the case in any physical theory. More precisely, it can be shown that no measurement on system A can distinguish between two physical situations which are described by the same density operator ρ_A .

Just like an operator defines a linear transformation in Hilbert space, a linear transformation in operator space (called Liouville space) is called a super operator. We denote these with calligraphic fonts. For a super operator \mathcal{M} to define a valid transformation of a density operator, it has to preserve the above properties. Therefore \mathcal{M} has to be trace preserving and positive. The latter means that $\mathcal{M}\rho \geq 0$ if $\rho \geq 0$. Actually, to demand positivity is not sufficient, also $\mathcal{M} \otimes \mathbb{1}$ has to be positive for the identity operator in any dimension. This is called completely positive, and reflects the fact that transforming the system with \mathcal{M} and doing nothing to another system on the moon still results in a positive density operator.

Every trace preserving, completely positive transformation (called a quantum map) can be written with Kraus operators K_j

$$\mathcal{M}\rho = \sum_j K_j \rho K_j^\dagger, \quad \text{with } \sum_j K_j^\dagger K_j = \mathbb{1}. \quad (99)$$

This representation theorem for quantum operations is due to Kraus. A unitary transformation is a special case of a quantum map. An example for a non-unitary transformation is Eq. (98), which is achieved with $K_0 = |0\rangle\langle 0|$ and $K_1 = |0\rangle\langle 1|$.



$$\begin{array}{ccc}
 \rho_{SE}(0) & \xrightarrow[\text{Schrödinger Gl.}]{\text{unitär}} & \rho_{SE}(t) = U_{SE}(t)\rho_{SE}(0)U_{SE}^\dagger(t) \\
 \downarrow \text{Tr}_E & & \downarrow \text{Tr}_E \\
 \rho_S(0) & \xrightarrow[\text{master Gleichung}]{\text{nicht unitär}} & \rho_S(t) = \mathcal{V}(t)\rho_S(0)
 \end{array}$$

FIG. 19: Environment plus system approach to open system dynamics.

A super operator is uniquely specified by its action on all $|j\rangle\langle k|$, where $\{|j\rangle\}$ forms a complete set in Hilbert space ($\{|j\rangle\langle k|\}$ forms a complete set in Liouville space). Note that unlike in the specification of a unitary operation, also the action on off-diagonals has to be given.

B. Time evolution super operator

The remainder of this section is about the time evolution of the density operator of a quantum system S which is coupled to an environment E . The total system $S + E$ will be considered as a closed system (see Fig. 19) and evolves according to the von Neumann equation $\frac{d}{dt}\rho = -i[H, \rho]$. Therefore, the system S evolution is given by the exact master equation

$$\frac{d}{dt}\rho_S = -i\text{Tr}_E[H_{SE}, \rho_{SE}]. \quad (100)$$

This equation by itself is quite useless because its solution involves solving the infinitely large total system $S + E$. However, Eq. (100) will later serve as a starting point for approximations to derive a master equation which involves only the reduced density operator ρ_S , and we

will go this path in the following subsection.

The formally define the time evolution super operator

$$\rho_S(t) = \mathcal{V}_S(t)\rho_S(0), \quad (101)$$

which, of course, has to be trace preserving and completely positive[11], but might not be invertible. Along the lines of the diagram in Fig. 19 we can easily see that $\mathcal{V}_S(t)$ has a Kraus operator representation if we use $\rho_{SE}(0) = \rho_S(0) \otimes \rho_E(0)$ and $\rho_E = \sum_{\alpha} \lambda_{\alpha} |\varphi_{\alpha}\rangle\langle\varphi_{\alpha}|$

$$\begin{aligned} \mathcal{V}_S(t)\rho_S(0) &= \text{Tr}_E [U_{SE}(t)\rho_S(0) \otimes \rho_E(0)U_{SE}^{\dagger}(t)] \\ &= \sum_{\alpha\beta} \langle\varphi_{\beta}|U_{SE}(t)|\varphi_{\alpha}\rangle \sqrt{\lambda_{\alpha}}\rho_S(0)\sqrt{\lambda_{\alpha}}\langle\varphi_{\alpha}|U_{SE}(t)|\varphi_{\beta}\rangle \\ &= \sum_{\alpha\beta} K_{\alpha\beta}\rho_S(0)K_{\alpha\beta}^{\dagger}. \end{aligned} \quad (102)$$

Note that $W_{\alpha\beta}$ are operators in the \mathcal{H}_S . This equation shows that the dynamics which are obtained by the coupling to an environment are trace preserving and completely positive. But for further calculations, it is not very useful because we do not know $U_{SE}(t)$.

Instead we pursue another path. If we assume that

$$\mathcal{V}_S(t_1 + t_2) = \mathcal{V}_S(t_1)\mathcal{V}_S(t_2), \quad (103)$$

then the set $\mathcal{V}_S(t)$ forms a semi group and therefore has a generator

$$\mathcal{V}_S(t) = \exp(\mathcal{L}t). \quad (104)$$

This immediately yield a first-order differential equation for the reduced density matrix

$$\frac{d}{dt}\rho_S(t) = \mathcal{L}\rho_S(t) \quad (105)$$

where \mathcal{L} is called the Liouville super operator or Liouvillian. For a closed system, the Liouvillian is given by the commutator with the Hamiltonian, i.e. $\mathcal{L}\rho_S = -i[H_S, \rho_S]$. A master equation of the form Eq. (105) is called a Markovian master equation, i.e. the evolution at time t only depends on the state of the system at this time.

A general master equation is not Markovian and can not be brought into the form Eq. (105). The reason is that the system S continuously changes the state of the environment. As a result, the system at time t interacts with an environmental state which

depends on the systems state at all times $0 < t' < t$ and the assumption Eq. (102) is not justified. The most general master equation can be written as

$$\frac{d}{dt}\rho_S(t) = \int_0^t dt' \mathcal{K}(t-t')\rho_S(t'), \quad (106)$$

where $\mathcal{K}(t-t')$ is called the memory kernel. If the memory time is short, we can approximate $\mathcal{K}(t-t') \approx \delta(t-t')\mathcal{L}$ to get a Markovian master equation.

Lindblad [2] as well as Gorini, Kossakowski, and Sudarshan [3] showed that the most general form of a Markovian master equation which preserves the trace and positivity is

$$\frac{d}{dt}\rho_S = -i[H, \rho_S] + \sum_{k=1}^{N^2-1} \gamma_k \left(L_k \rho_S L_k^\dagger - \frac{1}{2} L_k^\dagger L_k \rho_S - \frac{1}{2} L_k^\dagger L_k \right). \quad (107)$$

This master equation is said to be in Lindblad form. The Hamiltonian H is generally not H_S but might also include coherent corrections due to the environment like the Lamb shift. The incoherent evolution is represented by at most $N^2 - 1$ Lindblad operators L_k where N is the dimension of the Hilbert space \mathcal{H}_S . The γ_k are the rates for the *quantum jumps* $\rho_S \rightarrow L_k \rho_S L_k^\dagger$ and can be absorbed into the Lindblad operators.

C. Microscopic derivations of master equations

In this subsection we derive a Markovian master equation for ρ_S from the underlying physics of $S + E$. In doing so, we will perform a number of approximation which we will discuss at the end. The Hamiltonian of $S + E$ is

$$H_{SE} = H_S + H_E + H_I, \quad (108)$$

where $H_I = \sum_j A_j \otimes B_j$ is the interaction Hamiltonian and A acts on \mathcal{H}_S and B on \mathcal{H}_E . As before, we will assume that initially the system and the environment are not correlated, i.e. $\rho_{SE}(0) = \rho_S(0) \otimes \rho_E$, and also that the environment is at equilibrium at temperature T such that $e^{iH_E t} \rho_E e^{-iH_E t} = \rho_E$. We proceed by going into the interaction picture by transforming the von Neumann equation with $e^{i(H_S+H_E)t}$ to find

$$\frac{d}{dt}\rho_{SE}(t) = -i[H_I(t), \rho_{SE}(t)] \quad (109)$$

$$\rho_{SE}(t) = \rho_{SE}(0) - i \int_0^t ds [H_I(s), \rho_{SE}(s)], \quad (110)$$

where $H_I(t) = A(t) \otimes B(t) = e^{iH_S t} A e^{-iH_S t} \otimes e^{iH_E t} B e^{-iH_E t}$ (for simplicity we do not use the most general interaction Hamiltonian). We now substitute the integral version Eq. (110) into Eq. (109), then take the trace over E :

$$\frac{d}{dt}\rho_S(t) = -i\text{Tr}_E[H_I(t), \rho_{SE}(0)] - \text{Tr}_E \left\{ \int_0^t ds [H_I(t), [H_I(s), \rho_{SE}(s)]] \right\} \quad (111)$$

Our first assumption is that

$$\text{Tr}_E[H_I(t), \rho_{SE}(0)] = 0 \quad (112)$$

which will be mathematically motivated later. Physically it means that the dynamics at time t should not depend on the state $\rho_S(0)$ at time $t = 0$.

$$\frac{d}{dt}\rho_S(t) = - \int_0^t ds \text{Tr}_E[H_I(t), [H_I(s), \rho_{SE}(s)]] \quad (113)$$

This is still not a closed equation for ρ_S because ρ_{SE} still appears on the right hand side. We substitute the Born approximation

$$\rho_{SE}(s) = \rho_S(s) \otimes \rho_E \quad (114)$$

which states that the environment does not get disturbed by the system, and get a closed equation for ρ_S :

$$\frac{d}{dt}\rho_S(t) = - \int_0^t ds \text{Tr}_E[H_I(t), [H_I(t-s), \rho_S(t-s) \otimes \rho_E]] \quad (115)$$

We also substituted s by $t-s$. This equation is not Markovian because ρ_S is not only needed at time t , but at all times between zero and t . We therefore perform the Markov approximation

$$\rho_S(t-s) = \rho_S(t) \quad (116)$$

which is valid if the integrand vanishes for large s .

$$\frac{d}{dt}\rho_S(t) = - \int_0^t ds \text{Tr}_E[H_I(t), [H_I(t-s), \rho_S(t) \otimes \rho_E]]. \quad (117)$$

This so called Redfield equation still does not describe a semi group because the generator explicitly depends on time t through the integration range. But because the integrand is assumed to vanish for large s , we can extend the integration to infinity to arrive at the Markovian master equation

$$\frac{d}{dt}\rho_S(t) = - \int_0^\infty ds \text{Tr}_E[H_I(t), [H_I(t-s), \rho_S(t) \otimes \rho_E]]. \quad (118)$$

By substituting $H_I(t) = A(t) \otimes B(t)$ and some simple algebra we finally find

$$\frac{d}{dt}\rho_S(t) = \int_0^\infty ds \Gamma(s) \left[A(t-s)\rho_S(t)A(t)^\dagger - A^\dagger(t)A(t-s)\rho_S(t) \right] + \text{h.c.}, \quad (119)$$

where h.c. stands for hermitian conjugate and where we defined the bath correlation function

$$\Gamma(s) = \text{Tr}_E[B(s)B\rho_E]. \quad (120)$$

It is interesting to see that no details of the environment are needed, only the bath correlation function is important.

Let us review the approximations we have done so far:

- **Eq. (112):** This requires $\text{Tr}_E[B(t)\rho_E] = 0$. Imagine that this trace is not zero, then it is still a constant c because ρ_E is stationary. We can write $H_I = A \otimes (B - c\mathbb{1}) + cA$. If we absorb cA into the system Hamiltonian then the new H_I fulfills Eq. (112). Therefore this is not an approximation but can always be fulfilled exactly.
- **Born appr.:** This means that the coupling H_I is weak and the environment is large such that the system can not change the state of the environment. Typically the system can excite the environment, but as long as the excitation decays rapidly the system will still see the environment in a thermal equilibrium (time average of ρ_E).
- **Markov appr.:** The integrand vanishes if the bath correlation function vanishes. When the bath correlation function vanishes on a time τ_B , then this approximation is satisfied if H_I does not change the state appreciably during τ_B .
- $t \rightarrow \infty$: The extension of the integrand requires a fast decay of $\Gamma(s)$.

Everything therefore depends on a fast decay of the bath correlation function. For this to be valid we have to know that E has many degrees α of freedom and the system couples to many of them $B = \sum_\alpha b_\alpha$, and therefore $\langle B(s)B \rangle = \sum_\alpha \langle b_\alpha(s)b_\alpha \rangle$. Each $\langle b_\alpha(s)b_\alpha \rangle$ has its specific time behavior, often oscillating with some transition frequency of the degree α . The average of all these oscillations typically is zero unless at time $s = 0$ because for each degree of freedom $\langle b_\alpha^2 \rangle > 0$. To ensure that there is no beating one need an infinite number of degrees of freedom. See also Fig. 20.

The master equation Eq. (119) can not be written in Lindblad form. Therefore it can result in negative probabilities, which we will discuss later. We will now cast the ME into

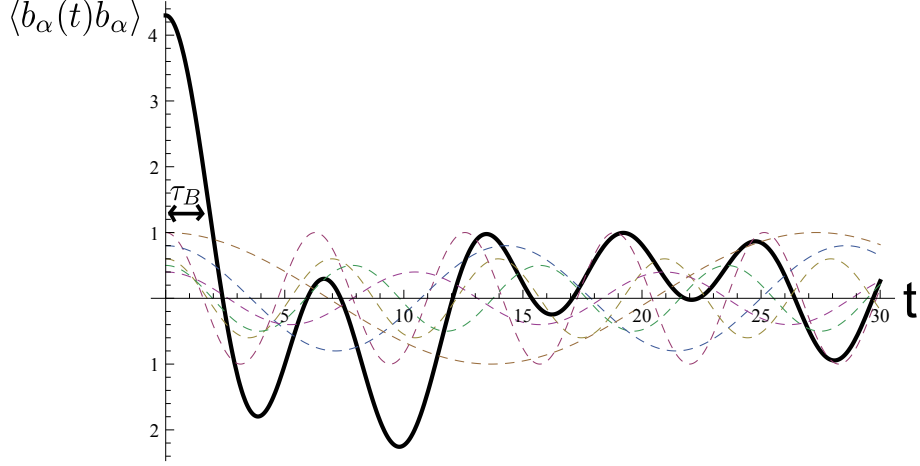


FIG. 20: The sum of the oscillations has a pronounced initial peak, and decays over a time τ_B . The more frequencies, the better the decay. If the number of frequencies is finite, the bath correlation will reoccur at some time. Therefore, the bath needs to have an infinite number of degrees of freedom for our approximations to be valid.

Lindblad form by performing the so called secular approximation. For simplicity we consider only a two-level system, but the generalization is straight forward.

We first decompose A into *eigen operators* of the Hamiltonian

$$\begin{aligned}
 A &= \sum_{jk=e,g} \langle j|A|k\rangle |j\rangle\langle k| = A_0 + A_1 + A_{-1} \\
 A_0 &= \langle g|A|g\rangle |g\rangle\langle g| + \langle e|A|e\rangle |e\rangle\langle e| \\
 A_1 &= \langle e|A|g\rangle |e\rangle\langle g| \\
 A_{-1} &= \langle g|A|e\rangle |g\rangle\langle e|.
 \end{aligned} \tag{121}$$

This has that advantage the A_j can be transformed into the interaction picture by multiplication with a phase factor

$$A_j(t) = e^{-i\omega_j t} A_j \tag{122}$$

with

$$\begin{aligned}
 \omega_{-1} &= E_e - E_g \\
 \omega_0 &= 0 \\
 \omega_1 &= E_g - E_e.
 \end{aligned} \tag{123}$$

From Eq. (119) we obtain

$$\begin{aligned}\frac{d}{dt}\rho_S(t) &= \sum_{jk=-1}^1 \int_0^\infty ds \Gamma(s) e^{-i\omega_j(t-s)} e^{i\omega_k t} \left[A_j \rho_S(t) A_k^\dagger - A_k^\dagger A_j \rho_S(t) \right] + \text{h.c.}, \\ &= \sum_{jk=-1}^1 \tilde{\Gamma}(\omega_j) e^{i(\omega_k - \omega_j)t} \left[A_j \rho_S(t) A_k^\dagger - A_k^\dagger A_j \rho_S(t) \right] + \text{h.c.},\end{aligned}\quad (124)$$

where we have defined the Laplace transform of the bath correlation functions

$$\tilde{\Gamma}(\omega) = \int_0^\infty ds \Gamma(s) e^{i\omega s} \quad (125)$$

If the interaction to the environment is small compared to $(\omega_k - \omega_j)$, then we can use the RWA, which in this context is called the secular approximation, and only keep terms with $\omega_k = \omega_j$ (see Exercise 1):

$$\frac{d}{dt}\rho_S(t) = \sum_{j=-1}^1 \tilde{\Gamma}(\omega_j) \left[A_j \rho_S(t) A_j^\dagger - A_j^\dagger A_j \rho_S(t) \right] + \text{h.c.} \quad (126)$$

If $\tilde{\Gamma}(\omega_j)$ were positive, then this equation would be in Lindblad form. We now separate the imaginary part from the real part

$$\tilde{\Gamma}(\omega) = \frac{1}{2}\gamma(\omega) + i \text{Im}\tilde{\Gamma}(\omega) \quad (127)$$

and by substituting into Eq. (126) we see that the $A_j \rho_S(t) A_j^\dagger$ cancels in the imaginary contribution. We find

$$\frac{d}{dt}\rho_S(t) = -i[H_{\text{LS}}, \rho_S] + \sum_{j=-1}^1 \gamma(\omega_j) \left[A_j \rho_S(t) A_j^\dagger - \frac{1}{2} A_j^\dagger A_j \rho_S(t) - \frac{1}{2} \rho_S(t) A_j^\dagger A_j \right], \quad (128)$$

where we defined the Lamb shift Hamiltonian

$$H_{\text{LS}} = \sum_{l=-1}^1 \text{Im}\tilde{\Gamma}(\omega_l) A_l^\dagger A_l. \quad (129)$$

We finally transform back into the Schrödinger picture

$$\frac{d}{dt}\rho_S(t) = -i[H_S + H_{\text{LS}}, \rho_S] + \sum_{j=-1}^1 \gamma(\omega_j) \left[A_j \rho_S(t) A_j^\dagger - \frac{1}{2} A_j^\dagger A_j \rho_S(t) - \frac{1}{2} \rho_S(t) A_j^\dagger A_j \right]. \quad (130)$$

This is our final master equation, which is in Lindblad form and therefore guarantees a positive density operator. The Lamb shift is an energy shift of the system induced by the environment, but it does not change the eigenstates of the system because $[H_{\text{LS}}, H_S] = 0$.

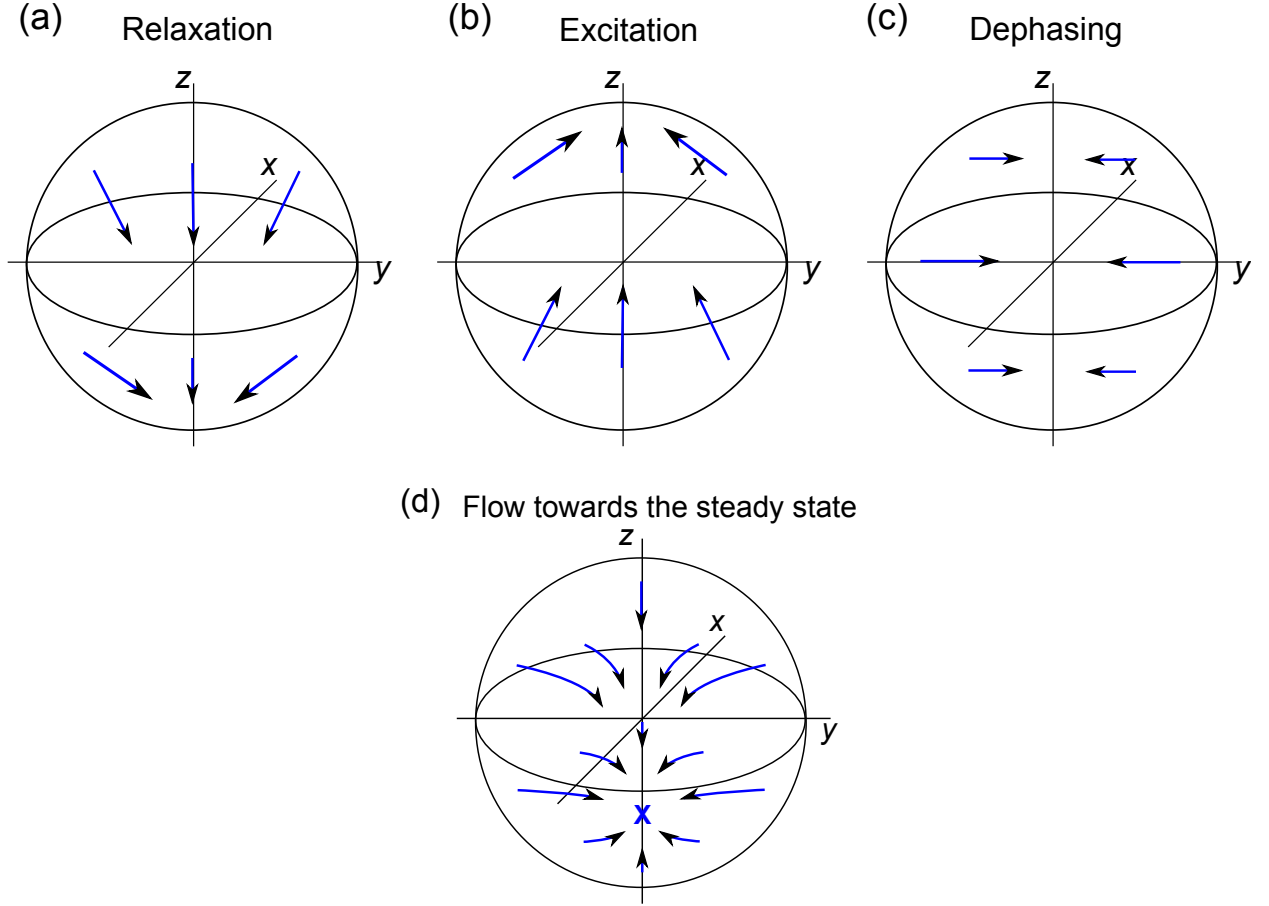


FIG. 21: The effect of the Lindblad terms on the qubit in the interaction picture. In the Schrödinger picture, there is an additional rotation around the z -axis.

The incoherent part of the evolution is due to the Lindblad term, which is often called dissipator.

The environment usually has all different frequencies. However, only the frequencies which are transition frequencies of the system can induce transitions, e.g. $\gamma(E_e - E_g)$ induces relaxations [see Fig. 21 (a)] and $\gamma(E_g - E_e)$ induces excitations [see Fig. 21 (b)]. The slow frequencies of the environment, i.e. $\gamma(0)$, can not change the population of the energy eigenstates, but reduces the off-diagonals (dephasing) [see Fig. 21 (c)].

The ME has a steady state [see Fig. 21 (d)] with

$$\rho_{eg}(t \rightarrow \infty) = 0 \quad (131)$$

$$\rho_z(t \rightarrow \infty) = -\frac{\gamma(E_e - E_g) - \gamma(E_g - E_e)}{\gamma(E_e - E_g) + \gamma(E_g - E_e)} \quad (132)$$

where $\rho_z = \rho_{ee} - \rho_{gg}$.

The time evolution is given by (see exercise 2)

$$\rho_{eg}(t) = \rho_{eg}(0)e^{i(E_g - E_e)t}e^{-t/T_2} \quad (133)$$

$$\rho_z(t) = \rho_z(\infty) + [\rho_z(0) - \rho_z(\infty)]e^{-t/T_1} \quad (134)$$

The relaxation time T_1 depends on $\gamma(\omega \neq 0)$ and on the off-diagonal matrix elements of A . For the dephasing time one can write

$$T_2^{-1} = T_1^{-1}/2 + (T_2^*)^{-1}, \quad (135)$$

where $(T_2^*)^{-1}$ is called the pure dephasing rate and depends on $\gamma(\omega = 0)$ and on the diagonal matrix elements of A . Eq. (135) shows that there can not be energy relaxation without dephasing, while it is possible to have pure dephasing without energy relaxation.

Quantum opticians almost only use such a ME of Lindblad form because of its simplicity and because all the approximations are very well satisfied in typical quantum optics applications. The predictions based on this ME can very accurately describe experiments. In solid state physics, people often don't like this equation because the weak coupling and the short bath correlation time τ_B are often not satisfied. However, for quantum computing devices we can only use systems which are very weakly coupled to any environment. Therefore, the description of a qubit on the basis of a Lindblad equation is well justified.

1. Relation to the correlation function

In the derivation of the Lindblad master equation we have defined a correlation function

$$\Gamma(t) = C(t) = \text{Tr}_E[B(t)B\rho_E], \quad (136)$$

where ρ_E denotes the density matrix of the environment (bath) in thermal equilibrium. The additional notation $C(t)$ is introduced for convenient and consistency with the literature, where a correlator is called C . Further we have defined the Laplace transform

$$\tilde{\Gamma}(\omega) = \int_0^\infty dt \Gamma(t)e^{i\omega t}. \quad (137)$$

The Laplace transform $\tilde{\Gamma}(\omega)$ gives both the dissipative rates $\gamma(\omega) = 2\text{Re}\tilde{\Gamma}(\omega)$ and the Lamb shift (renormalization) via $\text{Im}\tilde{\Gamma}(\omega)$. We now find the relation between these quantities and the Fourier transform of the correlation function

$$C(\nu) = \int_{-\infty}^\infty C(t)e^{i\nu t} dt. \quad (138)$$

Note, that $C(\nu)$ is real, since $C(-t) = C^*(t)$. The last equation holds because B is hermitian.

We obtain

$$\begin{aligned}\tilde{\Gamma}(\omega) &= \int_0^\infty dt C(t) e^{i\omega t - \delta t} = \int_0^\infty dt e^{i\omega t - \delta t} \int \frac{d\nu}{2\pi} C(\nu) e^{-i\nu t} \\ &= \int \frac{d\nu}{2\pi} C(\nu) \frac{1}{i\nu - i\omega + \delta} = i \int \frac{d\nu}{2\pi} C(\nu) \frac{1}{\omega - \nu + i\delta} .\end{aligned}\quad (139)$$

Thus we obtain

$$\text{Re } \tilde{\Gamma}(\omega) = \frac{1}{2} C(\omega) \quad , \quad \gamma(\omega) = C(\omega) . \quad (140)$$

$$\text{Im } \tilde{\Gamma}(\omega) = P.V. \int \frac{d\nu}{2\pi} C(\nu) \frac{1}{\omega - \nu} \quad (141)$$

2. Lamb shift for a two-level system

It is interesting to calculate the Lamb shift for a 2-level system. We have derived

$$H_{\text{LS}} = \sum_{l=-1}^1 \text{Im} \tilde{\Gamma}(\omega_j) A_j^\dagger A_j . \quad (142)$$

From (121) we see that

$$A_0 = a \hat{1} + b \sigma_z \quad , \quad A_1 = c \sigma_- \quad , \quad A_{-1} = c^* \sigma_+ . \quad (143)$$

(recall that $|g\rangle = |0\rangle = |\uparrow\rangle$). We should also take $a = 0$, since this part does not give a coupling between the qubit and the bath. We obtain

$$\begin{aligned}H_{\text{LS}} &= b^2 \text{Im} \tilde{\Gamma}(0) + |c|^2 \text{Im} \tilde{\Gamma}(\omega_1) \left(\frac{1}{2} + \frac{1}{2} \sigma_z \right) + |c|^2 \text{Im} \tilde{\Gamma}(-\omega_1) \left(\frac{1}{2} - \frac{1}{2} \sigma_z \right) \\ &= \text{const} - \frac{\sigma_z}{2} |c|^2 \left[\text{Im} \tilde{\Gamma}(-\omega_1) - \text{Im} \tilde{\Gamma}(\omega_1) \right] ,\end{aligned}\quad (144)$$

where $\omega_1 = E_g - E_e = -\Delta E$. This

$$H_{\text{LS}} = -\frac{1}{2} \delta \Delta E \sigma_z \quad (145)$$

with the renormalization of the energy difference given by

$$\delta \Delta E = |c|^2 P.V. \int \frac{d\nu}{2\pi} \left[\frac{C(\nu)}{(\Delta E - \nu)} - \frac{C(\nu)}{(-\Delta E - \nu)} \right] = |c|^2 P.V. \int \frac{d\nu}{2\pi} \left[\frac{C(\nu) + C(-\nu)}{\Delta E - \nu} \right] \quad (146)$$

Introducing the symmetrized correlator $S(\nu) \equiv \frac{1}{2}(C(\nu) + C(-\nu))$ we, finally, obtain

$$\delta \Delta E = |c|^2 P.V. \int \frac{d\nu}{2\pi} \frac{2S(\nu)}{(\Delta E - \nu)} = -|c|^2 P.V. \int \frac{d\nu}{2\pi} \frac{2\Delta E S(\nu)}{(\nu^2 - (\Delta E)^2)} . \quad (147)$$

D. Golden Rule calculation of the energy relaxation time T_1 in a two-level system

We now analyze the dissipative processes in two-level systems (qubits) in a more detailed fashion. The goal is to develop a deeper understanding. Let us first consider a purely transverse coupling between a qubit and a bath

$$H = -\frac{1}{2}\Delta E \sigma_z - \frac{1}{2}X \sigma_x + H_{\text{bath}} , \quad (148)$$

where X is a bath operator. To compare with the previous section we have $A = -(1/2)\sigma_x$ and $B = X$. We denote the ground and excited states of the free qubit by $|0\rangle$ and $|1\rangle$, respectively. In the weak-noise limit we consider X as a perturbation and apply Fermi's golden rule to obtain the relaxation rate, $\Gamma_{\downarrow} = \Gamma_{|1\rangle \rightarrow |0\rangle}$, and excitation rate, $\Gamma_{\uparrow} = \Gamma_{|0\rangle \rightarrow |1\rangle}$.

For the relaxation the initial state is actually given by $|1\rangle |i\rangle$, where $|i\rangle$ is some state of the environment. This state is not known, but we assume, that the environment is in thermal equilibrium. Thus the probability to have state $|i\rangle$ is given by $\rho_i = Z^{-1} e^{-\beta E_i} (H_{\text{bath}} |i\rangle = E_i |i\rangle)$. The final state is given by $|0\rangle |f\rangle$, where $|f\rangle$ is the state of the environment after the transition. To obtain the relaxation rate of the qubit we have to sum over all possible $|i\rangle$ states (with probabilities ρ_i) and over all $|f\rangle$. Thus, for Γ_{\downarrow} we obtain

$$\begin{aligned} \Gamma_{\downarrow} &= \frac{2\pi}{\hbar} \sum_{i,f} \rho_i \left| \langle i | \langle 1 | \frac{1}{2} X \sigma_x | 0 \rangle | f \rangle \right|^2 \delta(E_i + \Delta E - E_f) \\ &= \frac{2\pi}{\hbar} \frac{1}{4} \sum_{i,f} \rho_i \left| \langle i | X | f \rangle \right|^2 \delta(E_i + \Delta E - E_f) \\ &= \frac{2\pi}{\hbar} \frac{1}{4} \sum_{i,f} \rho_i \langle i | X | f \rangle \langle f | X | i \rangle \frac{1}{2\pi\hbar} \int dt e^{i\frac{t}{\hbar} (E_i + \Delta E - E_f)} \\ &= \frac{1}{4\hbar^2} \int dt \sum_i \rho_i \langle i | X(t) X | i \rangle e^{i\frac{t}{\hbar} \Delta E} \\ &= \frac{1}{4\hbar^2} C_X(\omega = \Delta E/\hbar) = \frac{1}{4\hbar^2} \langle X_{\omega=\Delta E/\hbar}^2 \rangle . \end{aligned} \quad (149)$$

Similarly, we obtain

$$\Gamma_{\uparrow} = \frac{1}{4\hbar^2} C_X(\omega = -\Delta E/\hbar) = \frac{1}{4\hbar^2} \langle X_{\omega=-\Delta E/\hbar}^2 \rangle . \quad (150)$$

How is this all related to the relaxation time of the diagonal elements of the density matrix (T_1)?. To understand this we write down the master equation for the probabilities $p_0 = \rho_{00}$ and $p_1 = \rho_{11}$:

$$\begin{aligned} \dot{p}_0 &= -\Gamma_{\uparrow} p_0 + \Gamma_{\downarrow} p_1 \\ \dot{p}_1 &= -\Gamma_{\downarrow} p_1 + \Gamma_{\uparrow} p_0 . \end{aligned} \quad (151)$$

We observe that the total probability $p_0 + p_1$ is conserved and should be equal 1. Then for p_0 we obtain

$$\dot{p}_0 = -(\Gamma_\uparrow + \Gamma_\downarrow)p_0 + \Gamma_\uparrow, \quad (152)$$

which gives

$$p_0(t) = \frac{\Gamma_\downarrow}{\Gamma_\uparrow + \Gamma_\downarrow} + \left(p_0(0) - \frac{\Gamma_\downarrow}{\Gamma_\uparrow + \Gamma_\downarrow} \right) e^{-(\Gamma_\uparrow + \Gamma_\downarrow)t}, \quad (153)$$

and $p_1(t) = 1 - p_0(t)$.

For the relaxation time we thus find

$$\frac{1}{T_1} = \Gamma_\downarrow + \Gamma_\uparrow = \frac{1}{2\hbar^2} S_X(\omega = \Delta E/\hbar), \quad (154)$$

and for the equilibrium magnetization

$$\langle \sigma_z \rangle_{t=\infty} = p_0(t=\infty) - p_1(t=\infty) = \frac{\Gamma_\downarrow - \Gamma_\uparrow}{\Gamma_\downarrow + \Gamma_\uparrow} = \frac{A_X(\omega = \Delta E/\hbar)}{S_X(\omega = \Delta E/\hbar)}, \quad (155)$$

where we have introduced the antisymmetrized correlator $A_X(\omega) \equiv \frac{1}{2}(C_X(\omega) - C_X(-\omega))$.

E. Fluctuation Dissipation Theorem (FDT)

Are $C(\omega)$ and $C(-\omega)$ related? In other words, what is the relation between the symmetrized correlator $S(\omega)$ and the antisymmetrized one $A(\omega)$? We use the spectral decomposition in the eigenbasis of the Hamiltonian of the environment $H_{\text{bath}} |n\rangle = E_n |n\rangle$:

$$\begin{aligned} C(t) &= \text{Tr}(\rho_E B(t)B) = \frac{1}{Z} \sum_n e^{-\beta E_n} \langle n| B(t)B |n\rangle \\ &= \frac{1}{Z} \sum_{n,m} e^{-\beta E_n} \langle n| B(t) |m\rangle \langle m| B |n\rangle = \frac{1}{Z} \sum_{n,m} e^{-\beta E_n} e^{i(E_n - E_m)t} |\langle m| B |n\rangle|^2. \end{aligned} \quad (156)$$

Thus

$$C(\omega) = \int dt C(t) e^{i\omega t} = \frac{1}{Z} \sum_{n,m} e^{-\beta E_n} |\langle m| B |n\rangle|^2 2\pi \delta(\omega - (E_m - E_n)). \quad (157)$$

For $C(-\omega)$ we obtain

$$\begin{aligned} C(-\omega) &= \frac{1}{Z} \sum_{n,m} e^{-\beta E_n} |\langle m| B |n\rangle|^2 2\pi \delta(-\omega - (E_m - E_n)) \\ &= \frac{1}{Z} \sum_{n,m} e^{-\beta E_n} |\langle m| B |n\rangle|^2 2\pi \delta(\omega - (E_n - E_m)) \\ &= \frac{1}{Z} \sum_{n,m} e^{-\beta E_m} |\langle m| B |n\rangle|^2 2\pi \delta(\omega - (E_m - E_n)) \\ &= \frac{1}{Z} \sum_{n,m} e^{-\beta(E_n + \omega)} |\langle m| B |n\rangle|^2 2\pi \delta(\omega - (E_m - E_n)) \\ &= e^{-\beta\omega} C(\omega). \end{aligned} \quad (158)$$

The relation $C(-\omega) = e^{-\beta\omega}C(\omega)$ is called the Fluctuation-Dissipation-Theorem (this time a real theorem). A simple algebra then gives $S(\omega) = \coth\left(\frac{\beta\omega}{2}\right) A(\omega)$. Thus we obtain the detailed balance relation

$$\frac{\Gamma_{\uparrow}}{\Gamma_{\downarrow}} = e^{-\beta\Delta E} . \quad (159)$$

We also observe that the probabilities $p_0(t = \infty) = \frac{1}{e^{-\beta\Delta E} + 1}$ and $p_1(t = \infty) = 1 - p_0(t = \infty)$ are the equilibrium ones. Finally,

$$\langle\sigma_z\rangle_{t=\infty} = \frac{A_X(\omega = \Delta E/\hbar)}{S_X(\omega = \Delta E/\hbar)} = \tanh \frac{\Delta E}{2k_B T} , \quad (160)$$

F. Longitudinal coupling, T_2^*

$$H = -\frac{1}{2}\Delta E \sigma_z - \frac{1}{2}X \sigma_z + H_{\text{bath}} , \quad (161)$$

1. Classical derivation

Treating X as a classical variable one obtains

$$\begin{aligned} \langle\sigma_+(t)\rangle &\propto \left\langle e^{-\frac{i}{\hbar} \int_0^t dt' X(t')} \right\rangle = e^{-\frac{1}{2\hbar^2} \int_0^t dt' \int_0^t dt'' \langle X(t')X(t'') \rangle} \\ &= \exp\left(-\frac{1}{2\hbar^2} \int \frac{d\omega}{2\pi} S_X(\omega) \frac{\sin^2(\omega t/2)}{(\omega/2)^2}\right) . \end{aligned} \quad (162)$$

If we make the usual Golden Rule substitution $\sin^2(\omega t/2)/(\omega/2)^2 \rightarrow 2\pi\delta(\omega) t$ in Eq. (162) we obtain

$$\ln P(t) = -\frac{1}{2\hbar^2} S_X(\omega = 0) t . \quad (163)$$

Thus we obtain

$$\frac{1}{T_2^*} = \frac{1}{2\hbar^2} S_X(\omega = 0) . \quad (164)$$

When both longitudinal and transverse coupling are present one obtains for the dephasing time

$$\frac{1}{T_2} = \frac{1}{2T_1} + \frac{1}{T_2^*} . \quad (165)$$

How about $1/f$ noise? Is $1/T_2^$ infinite?*

2. Quantum derivation

We calculate the time evolution of the off-diagonal element of the qubit's density matrix:

$$\langle \sigma_+(t) \rangle = e^{-\frac{i\Delta Et}{\hbar}} \text{Tr} \left[\sigma_+ S(t, 0) \rho_0 S^\dagger(t, 0) \right], \quad (166)$$

where

$$S(t, 0) \equiv T e^{\frac{i}{\hbar} \int_0^t \frac{X(t')}{2} \sigma_z dt'}. \quad (167)$$

Obviously, the evolution operators S and S^\dagger do not flip the spin, while the operator σ_+ in Eq. (166) imposes a selection rule such that the spin is in the state $|\downarrow\rangle$ on the forward Keldysh contour (i.e., in $S(t, 0)$) and in the state $|\uparrow\rangle$ on the backward contour (i.e., in $S^\dagger(t, 0)$). Thus, we obtain $\langle \sigma_+(t) \rangle = P(t) \exp(-i\Delta Et/\hbar) \langle \sigma_+(0) \rangle$, where

$$P(t) \equiv \left\langle \left[\tilde{T} \exp \left(-\frac{i}{\hbar} \int_0^t \frac{X(t')}{2} dt' \right) \right] \left[T \exp \left(-\frac{i}{\hbar} \int_0^t \frac{X(t')}{2} dt' \right) \right] \right\rangle. \quad (168)$$

The last expression can be represented as a single integral on the Keldysh contour C :

$$P(t) \equiv \langle T_C \exp \left(-\frac{i}{\hbar} \int_C \frac{X(t')}{2} dt' \right) \rangle. \quad (169)$$

Using the fact that the fluctuations of X are Gaussian, we arrive at

$$\ln P(t) = -\frac{1}{8\hbar^2} \int_C \int_C dt_1 dt_2 \langle T_C X(t_1) X(t_2) \rangle. \quad (170)$$

We rewrite the double integral as four integrals from 0 to t :

$$\begin{aligned} \ln P(t) &= -\frac{1}{8\hbar^2} \int_0^t \int_0^t dt_1 dt_2 \left\{ \langle T X(t_1) X(t_2) \rangle + \langle \tilde{T} X(t_1) X(t_2) \rangle + \langle X(t_1) X(t_2) \rangle + \langle X(t_2) X(t_1) \rangle \right\} \\ &= -\frac{1}{2\hbar^2} \int_0^t \int_0^t dt_1 dt_2 S_X(t_1 - t_2) = -\frac{1}{2\hbar^2} \int \frac{d\omega}{2\pi} S_X(\omega) \frac{\sin^2(\omega t/2)}{(\omega/2)^2}. \end{aligned} \quad (171)$$

G. $1/f$ noise, Echo

A more elaborate analysis is needed when the noise spectral density is singular at low frequencies. In this subsection we consider Gaussian noise. The random phase accumulated at time t :

$$\Delta\phi = \int_0^t dt' X(t') \quad (172)$$

is then Gaussian-distributed, and one can calculate the decay law of the free induction (Ramsey signal) as $f_{z,R}(t) = \langle \exp(i\Delta\phi) \rangle = \exp(-(1/2)\langle \Delta\phi^2 \rangle)$. This gives

$$f_{z,R}(t) = \exp \left[-\frac{t^2}{2} \int_{-\infty}^{+\infty} \frac{d\omega}{2\pi} S_X(\omega) \operatorname{sinc}^2 \frac{\omega t}{2} \right], \quad (173)$$

where $\operatorname{sinc} x \equiv \sin x/x$.

In an echo experiment, the phase acquired is the difference between the two free evolution periods:

$$\Delta\phi_E = -\Delta\phi_1 + \Delta\phi_2 = -\int_0^{t/2} dt' X(t') + \int_{t/2}^t dt' X(t'), \quad (174)$$

so that

$$f_{z,E}(t) = \exp \left[-\frac{t^2}{2} \int_{-\infty}^{+\infty} \frac{d\omega}{2\pi} S_X(\omega) \sin^2 \frac{\omega t}{4} \operatorname{sinc}^2 \frac{\omega t}{4} \right]. \quad (175)$$

1/f spectrum: Here and below in the analysis of noise with $1/f$ spectrum we assume that the $1/f$ law extends in a wide range of frequencies limited by an infrared cut-off ω_{ir} and an ultraviolet cut-off ω_c :

$$S_X(\omega) = 2\pi A/|\omega| = A/|f|, \quad \omega_{\text{ir}} < |\omega| < \omega_c. \quad (176)$$

The infra-red cutoff ω_{ir} is usually determined by the measurement protocol, as discussed further below. The decay rates typically depend only logarithmically on ω_{ir} , and the details of the behavior of the noise power below ω_{ir} are irrelevant to logarithmic accuracy.

The infra-red cutoff ω_{ir} may be set, and controlled, by the details of the experiment. For instance, when a measurement of dephasing, performed over a short time t , is averaged over many runs, the fluctuations with frequencies down to the inverse of the total signal acquisition time contribute to the phase randomization. Here we focus on the case $\omega_{\text{ir}} t \gtrsim 1$.

For $1/f$ noise, at times $t \ll 1/\omega_{\text{ir}}$, the free induction (Ramsey) decay is dominated by the frequencies $\omega < 1/t$, i.e., by the quasistatic contribution, and (173) reduces to:

$$f_{z,R}(t) = \exp \left[-t^2 A \left(\ln \frac{1}{\omega_{\text{ir}} t} + O(1) \right) \right]. \quad (177)$$

The infra-red cutoff ω_{ir} ensures the convergence of the integral.

For the echo decay we obtain

$$f_{z,E}(t) = \exp \left[-t^2 A \cdot \ln 2 \right]. \quad (178)$$

The echo method thus only increases the decay time by a logarithmic factor. This limited echo efficiency is due to the high frequency tail of the $1/f$ noise.

IX. QUANTUM MEASUREMENT

In standard quantum mechanics the measurement process is postulated as collapse of the wave function. If an observable A of a quantum system is measured, we need the eigenbasis of A : $A|n\rangle = A_n|n\rangle$. If the system before the measurement was in state $|\alpha\rangle = \sum c_n^\alpha |n\rangle$, i.e., the density matrix was given by $\rho_i = |\alpha\rangle\langle\alpha| = \sum_{n_1, n_2} c_{n_1}^\alpha c_{n_2}^{\alpha*} |n_1\rangle\langle n_2|$, then after the measurement we have a statistical mixture (mixed state) $\rho_f = \sum_n |c_n^\alpha|^2 |n\rangle\langle n|$, and the values A_n are obtained with probabilities $|c_n^\alpha|^2$. Note that the expectation value of A remains unchanged $\langle A \rangle = \text{Tr}(\rho_i A) = \text{Tr}(\rho_f A)$. If the initial state was a mixture $\rho_i = \sum_\alpha p_\alpha |\alpha\rangle\langle\alpha| = \sum_{\alpha, n_1, n_2} p_\alpha c_{n_1}^\alpha c_{n_2}^{\alpha*} |n_1\rangle\langle n_2|$ (we can always find a basis $|\alpha\rangle$ in which ρ_i is diagonal) after the measurement we obtain $\rho_f = \sum_{\alpha, n} p_\alpha |c_n^\alpha|^2 |n\rangle\langle n|$. That is the result A_n is observed with probability $\sum_\alpha p_\alpha |c_n^\alpha|^2$. We see that measurement is very similar to "pure" dephasing: the off-diagonal elements of the density matrix in the measurement basis $|n\rangle$ vanish, while the diagonal ones remain unchanged.

Measurement cannot be described by Schrödinger equation, as it corresponds to a non-unitary evolution. Among many (sometimes exotic) ways to understand what the measurement process is, we choose the most practical one advocated, first, by J. von Neumann [4]. This approach also has a very strong overlap with the theory of open quantum systems. Essentially, we will incorporate the measuring device into the environment of the measured system.

The idea is that the measurement device is another physical quantum system. The fact that A is being measured means that the measuring device couples to A . That is the Hamiltonian of the combined systems reads

$$H = H_S + H_M + g(t)A \otimes B, \quad (179)$$

where H_S governs the dynamics of the system, H_M - that of the meter, $g(t)$ is the switchable on and off coupling strength, and B is the observable of the meter which is coupled to the system's A . In a usual situation we would go to the interaction picture and calculate the dynamics of the combined system. For the measurement a different protocol is needed. When the system is not been measured there is no coupling, $g = 0$. Once a measurement has to be performed we switch $g(t)$ to be so large, that the interaction term $g(t)A \otimes B$ becomes much more important than the system's H_S , so that the later can be neglected.

Thus for the time of measurement

$$H \approx H_M + gA \otimes B . \quad (180)$$

Initially the system and the meter are not entangled, i.e., the state right before the measurement starts reads

$$|\psi_i\rangle = |\alpha\rangle |M\rangle = \sum_n c_n |n\rangle |M\rangle . \quad (181)$$

Here $|M\rangle$ is the initial state of the meter. The evolution operator of the combined systems then reads

$$U = e^{-i(\hat{1} \otimes H_M + gA \otimes B)t} = e^{-it \sum_n [|n\rangle \langle n| \otimes (H_M + gA_n B)]} . \quad (182)$$

Thus we obtain

$$|\psi_f\rangle = U |\psi_i\rangle = \sum_n c_n |n\rangle e^{-it(H_M + gA_n B)} |M\rangle = \sum_n c_n |n\rangle |M_n\rangle , \quad (183)$$

where

$$|M_n\rangle \equiv e^{-it(H_M + gA_n B)} |M\rangle . \quad (184)$$

We see that the system and the meter get entangled. The density matrix of the system is obtained tracing out the meter

$$\begin{aligned} \rho_S &= \text{Tr}_M[|\psi_f\rangle \langle \psi_f|] = \text{Tr}_M \left[\sum_{n_1, n_2} c_{n_1} c_{n_2}^* |M_{n_1}\rangle |n_1\rangle \langle n_2| \langle M_{n_2}| \right] \\ &= \sum_{n_1, n_2} c_{n_1} c_{n_2}^* \langle M_{n_2} | M_{n_1} \rangle |n_1\rangle \langle n_2| . \end{aligned} \quad (185)$$

In particular if all $|M_n\rangle$ are orthogonal to each other, i.e., $\langle M_{n_2} | M_{n_1} \rangle = \delta_{n_1, n_2}$, we obtain the density matrix postulated for the measurement collapse. This result is clear: a good measurement is performed if one can distinguish between the states of the meter corresponding to different A_n 's. Qualitatively it is clear from (184) that the states $|M_{n_1}\rangle$ and $|M_{n_2}\rangle$ will be the more different the larger is the difference $gt(A_{n_1} - A_{n_2})$. A strong measurement may be achieved by choosing a large enough combination gt . Thus, we see that the measurement happens not instantaneously, but a finite time is needed. During this time the states $|M_{n_1}\rangle$ and $|M_{n_2}\rangle$ become orthogonal and the density matrix of the system becomes diagonal in the basis $|n\rangle$. This time we can call measurement time but this is also the dephasing time. We will investigate the relation between the two later.

Since the meter is also a quantum system, a question arises how to distinguish the states $|M_{n_1}\rangle$ and $|M_{n_2}\rangle$, i.e., how to measure the meter. This could be done by another meter.

Thus we arrive at a chain of measuring devices, which measure each other's state in sequence. Where should one cut this chain off? A practical answer is the following: when the states of the last meter in the chain are easily distinguishable, i.e., are macroscopically different. Thus, the chain of meters can be also thought of as an amplifier. A small (microscopic) signal $A_{n_1} - A_{n_2}$ is being amplified to a stronger one. The theory of amplifiers is very interesting and rich, but it is beyond our course. Philosophically our practical answer is, however, unsatisfactory. We will not discuss here the (sometimes exotic) solutions like the one of many worlds or the one where the ultimate collapse happens in the brain of the human observer. All this is also beyond our course.

1. Quantum Nondemolition Measurement (QND)

Assume we cannot switch the coupling constant g between the measured system and the meter to be very strong. Then we are not allowed to neglect the system's Hamiltonian H_S . The time evolution is governed then by the full Hamiltonian (179). If the eigenbases of H_S and A do not coincide, i.e., $[H_S, A] \neq 0$, the initial state $|\alpha\rangle = \sum_n c_n |n\rangle$ ($|n\rangle$ is the eigenbasis of A) will evolve in such a way, that the probabilities $|c_n|^2$ will not be conserved. Thus no collapse-like measurement is possible. The only way to have it is to assure the commutativity $[H_S, A] = 0$. In this case the situation is very similar to the one described above, since $|n\rangle$ is the mutual eigenbasis of H_S and A_n . We obtain

$$U = e^{-i(H_S \otimes \hat{1} + \hat{1} \otimes H_M + gA \otimes B)t} = e^{-it \sum_n [|n\rangle\langle n| \otimes (E_n + H_M + gA_n B)]}, \quad (186)$$

where E_n are the eigenenergies, $H_S |n\rangle = E_n |n\rangle$. Thus we obtain

$$|\psi_f\rangle = U |\psi_i\rangle = \sum_n c_n e^{-iE_n t} |n\rangle e^{-i(H_M + gA_n B)} |M\rangle = \sum_n c_n e^{-iE_n t} |n\rangle |M_n\rangle. \quad (187)$$

Finally

$$\begin{aligned} \rho_S &= \text{Tr}_M[|\psi_f\rangle\langle\psi_f|] = \text{Tr}_M \left[\sum_{n_1, n_2} c_{n_1} c_{n_2}^* e^{-i(E_{n_1} - E_{n_2})t} |M_{n_1}\rangle |n_1\rangle \langle n_2| \langle M_{n_2}| \right] \\ &= \sum_{n_1, n_2} c_{n_1} c_{n_2}^* e^{-i(E_{n_1} - E_{n_2})t} \langle M_{n_2} | M_{n_1} \rangle |n_1\rangle \langle n_2|. \end{aligned} \quad (188)$$

In the strong measurement limit, $\langle M_{n_2} | M_{n_1} \rangle = \delta_{n_1, n_2}$, we get again a diagonal density matrix. This regime is called QND.

2. A free particle as a measuring device

This example is usually discussed in the literature, although, it makes little sense to have a single particle (a microscopic system) as a measuring device, unless it is measured then in sequence by another meter. Assume for simplicity a 1-D situation and an infinite mass of the particle. Then $H_M = \frac{p^2}{2m} = 0$. To be concrete we couple a qubit ($A = \sigma_z$) to the momentum of the particle p . We also assume a QND situation, i.e., $H_S = -\frac{1}{2}\Delta E \sigma_z$. The Hamiltonian of the combined system reads

$$H = -\frac{1}{2}\Delta E \sigma_z + g \sigma_z p . \quad (189)$$

Assume a particle is prepared ($|M\rangle$) as a wave packet of width Δx around $x = 0$. Then we obtain the final meter states

$$|M_{\uparrow/\downarrow}\rangle = e^{\mp i g t p} |M\rangle . \quad (190)$$

These are the wave packets shifted either to the left or to the right by gt . We arrive at a strong projective measurement if $gt \gg \Delta x$. If we would not assume an infinite mass, the wave packet would suffer from dispersion and the description would be somewhat more involved.

3. A tunnel junction as a meter (will be continued as exercise)

As a meter we choose a tunnel junction described by the Hamiltonian

$$H = H_L + H_R + H_T . \quad (191)$$

Here $H_L = \sum_k \epsilon_k L_k^\dagger L_k$ and $H_R = \sum_k \epsilon_k R_k^\dagger R_k$ describe the left and the right leads, which both are modeled as free electron gases kept at chemical potentials μ_L and μ_R respectively. The operators L_k and R_k are annihilations operators of electrons in the left and in the right lead respectively. The index k runs over all quantum numbers (momentum and spin). The equilibrium state of the leads is described by the occupation probabilities

$$n_L(k) = \langle L_k^\dagger L_k \rangle = n_F(\epsilon_k - \mu_L) = \frac{1}{e^{\beta(\epsilon_k - \mu_L)} + 1} , \quad (192)$$

and

$$n_R(k) = \langle R_k^\dagger R_k \rangle = n_F(\epsilon_k - \mu_R) = \frac{1}{e^{\beta(\epsilon_k - \mu_R)} + 1} . \quad (193)$$

The tunneling Hamiltonian is usually given by

$$H_T = \sum_{k_1, k_2} t \left[R_{k_1}^\dagger L_{k_2} + L_{k_2}^\dagger R_{k_1} \right] , \quad (194)$$

where t is the tunneling amplitude. For simplicity we assume that t is real (otherwise we would have t and t^* in front of the first and the second tunneling terms respectively) and independent of k_1 and k_2 .

As a warm-up let us calculate the current. The usual way is to introduce the current operator via $I \equiv \dot{N}_L = i[H, N_L]$ and to evaluate its expectation value perturbatively. Instead we will use the very popular nowadays method of Full Counting Statistics. Imagine that every transfer of an electron from left to right and from right to left is registered in a special counter. The counter is a physical system with the Hilbert space spanned by the states $|m\rangle$, where the number $m \in Z$, i.e., $m = 0, \pm 1, \pm 2, \dots$, denotes the number of electrons that have tunneled through the junction. In this Hilbert state one can introduce two ladder operators

$$e^{i\phi} = \sum_m |m+1\rangle \langle m| , \quad (195)$$

and its conjugated

$$e^{-i\phi} = \sum_m |m-1\rangle \langle m| . \quad (196)$$

The notation $e^{\pm i\phi}$ is related to the fact that the Hilbert state of the counter can be realized as a set of all 2π -periodic functions $|m\rangle = e^{im\phi}$. Then, clearly, $e^{i\phi}$ is the ladder operator. The counter is coupled to the tunnel junction by replacing the tunneling Hamiltonian by

$$H_T = \sum_{k_1, k_2} t \left[R_{k_1}^\dagger L_{k_2} e^{i\phi} + L_{k_2}^\dagger R_{k_1} e^{-i\phi} \right] . \quad (197)$$

We now want to write down the master equation for the reduced density matrix of the counter $\rho_c(m_1, m_2)$ after the electronic degrees of freedom have been traced out. The tunneling Hamiltonian has a form similar to the one we used in deriving the master equation

$$H_T = AX + A^\dagger X^\dagger , \quad (198)$$

where the system operator $A = e^{i\phi}$ (the system is now the counter) and the environment operator is

$$X = t \sum_{k_1, k_2} R_{k_1}^\dagger L_{k_2} . \quad (199)$$

The Markovian master equation we have derived earlier (here we use H_T as the interaction Hamiltonian between the counter and the environment) reads in the interaction representation

$$\begin{aligned}\frac{d}{dt}\rho_c(t) &= -\int_0^\infty d\tau \text{Tr}_E[H_T(t), [H_T(t-\tau), \rho_c(t) \otimes \rho_E]] \\ &= -\int_0^\infty d\tau \text{Tr}_E[AX(t) + A^\dagger X^\dagger(t), [AX(t-\tau) + A^\dagger X^\dagger(t-\tau), \rho_c(t) \otimes \rho_E]] .\end{aligned}\quad (200)$$

Note that A and A^\dagger are time independent because the counter's own Hamiltonian is equal to zero. Out of 16 combinations only 8 survive because the averages $\langle XX \rangle$ and $\langle X^\dagger X^\dagger \rangle$ vanish. We obtain

$$\begin{aligned}\frac{d}{dt}\rho_c(t) &= -\int_0^\infty d\tau \{AA^\dagger \rho_c \langle XX^\dagger(-\tau) \rangle + \rho_c A^\dagger A \langle X^\dagger(-\tau)X \rangle\} + h.c. \\ &\quad + \int_0^\infty d\tau \{A^\dagger \rho_c A \langle XX^\dagger(-\tau) \rangle + A \rho_c A^\dagger \langle X^\dagger(-\tau)X \rangle\} + h.c. .\end{aligned}\quad (201)$$

For the environment correlators we obtain

$$\begin{aligned}\langle XX^\dagger(-\tau) \rangle &= t^2 \sum_{k_1, k_2, p_1, p_2} \langle R_{k_1}^\dagger L_{k_2} L_{p_2}^\dagger(-\tau) R_{p_1}(-\tau) \rangle \\ &= t^2 \sum_{k_1, k_2, p_1, p_2} e^{i\tau(\epsilon_{p_1} - \epsilon_{p_2})} \langle R_{k_1}^\dagger L_{k_2} L_{p_2}^\dagger R_{p_1} \rangle \\ &= t^2 \sum_{k_1, k_2} e^{i\tau(\epsilon_{k_1} - \epsilon_{k_2})} n_F(\epsilon_{k_1} - \mu_R) [1 - n_F(\epsilon_{k_2} - \mu_L)]\end{aligned}\quad (202)$$

and

$$\begin{aligned}\langle X^\dagger(-\tau)X \rangle &= t^2 \sum_{k_1, k_2, p_1, p_2} \langle L_{p_2}^\dagger(-\tau) R_{p_1}(-\tau) R_{k_1}^\dagger L_{k_2} \rangle \\ &= t^2 \sum_{k_1, k_2, p_1, p_2} e^{i\tau(\epsilon_{p_1} - \epsilon_{p_2})} \langle L_{p_2}^\dagger R_{p_1} R_{k_1}^\dagger L_{k_2} \rangle \\ &= t^2 \sum_{k_1, k_2} e^{i\tau(\epsilon_{k_1} - \epsilon_{k_2})} n_F(\epsilon_{k_2} - \mu_L) [1 - n_F(\epsilon_{k_1} - \mu_R)]\end{aligned}\quad (203)$$

For the real parts of the Laplace transforms we obtain

$$\begin{aligned}\frac{\Gamma_{\leftarrow}}{2} &\equiv \text{Re} \int_0^\infty d\tau \langle XX^\dagger(-\tau) \rangle = \pi t^2 \sum_{k_1, k_2} \delta(\epsilon_{k_1} - \epsilon_{k_2}) n_F(\epsilon_{k_1} - \mu_R) [1 - n_F(\epsilon_{k_2} - \mu_L)] \\ &= \pi t^2 \nu^2 \int d\epsilon n_F(\epsilon - \mu_R) [1 - n_F(\epsilon - \mu_L)] ,\end{aligned}\quad (204)$$

where we have introduced the (constant) densities of states $\nu = \nu_L = \nu_R$. Analogously

$$\frac{\Gamma_{\rightarrow}}{2} \equiv \text{Re} \int_0^\infty d\tau \langle X^\dagger(-\tau)X \rangle = \pi t^2 \nu^2 \int d\epsilon n_F(\epsilon - \mu_L) [1 - n_F(\epsilon - \mu_R)] .\quad (205)$$

The combination $G_T \equiv (2\pi) \times 2\pi t^2 \nu^2$ is called the dimensionless tunneling conductance. At $T = 0$ and for $\mu_L > \mu_R$ we have $\hbar\Gamma_{\rightarrow} = \frac{G_T}{2\pi}(\mu_L - \mu_R)$, while $\Gamma_{\leftarrow} = 0$.

We obtain for the master equation taking into account that $A^\dagger A = A A^\dagger = 1$

$$\frac{d}{dt}\rho_c(t) = -(\Gamma_{\leftarrow} + \Gamma_{\rightarrow})\rho_c + \Gamma_{\leftarrow}A^\dagger\rho_c A + \Gamma_{\rightarrow}A\rho_c A^\dagger. \quad (206)$$

The density matrix $\rho_c(m_1, m_2)$ can in principle have non-diagonal elements. However, as can be seen from (206), if initially only diagonal elements were present, no off-diagonal elements would be generated. We assume this situation, which allows us to consider the charge that has tunneled classically and m becomes a classical "pointer". Namely we assume that at $t = 0$ the density matrix is given by $\rho_c(t = 0) = \delta_{m_1, m_2} \delta_{m_1, 0}$ (no charge has tunneled yet). Then, $p(m, t) \equiv \rho_c(m, m, t)$ is the probability that m charges have tunneled through. We obtain

$$\frac{d}{dt}p(m) = -(\Gamma_{\leftarrow} + \Gamma_{\rightarrow})p(m) + \Gamma_{\leftarrow}p(m+1) + \Gamma_{\rightarrow}p(m-1). \quad (207)$$

This equation is solved by a Fourier transform introducing the FCS generating function $\chi(\lambda) = \sum_m p(m)e^{-i\lambda m}$. We obtain

$$\begin{aligned} \frac{d}{dt}\chi(\lambda) &= -(\Gamma_{\leftarrow} + \Gamma_{\rightarrow})\chi(\lambda) + e^{i\lambda}\Gamma_{\leftarrow}\chi(\lambda) + e^{-i\lambda}\Gamma_{\rightarrow}\chi(\lambda) \\ &= [\Gamma_{\leftarrow}(e^{i\lambda} - 1) + \Gamma_{\rightarrow}(e^{-i\lambda} - 1)]\chi(\lambda). \end{aligned} \quad (208)$$

Taking into account the initial condition $\chi(\lambda, t = 0) = 1$ we obtain

$$\chi = e^{t[\Gamma_{\leftarrow}(e^{i\lambda}-1) + \Gamma_{\rightarrow}(e^{-i\lambda}-1)]}. \quad (209)$$

Having the generating function we can calculate, e.g., the total tunneled charge

$$\langle m \rangle = \sum_m mp(m) = i \frac{\partial}{\partial \lambda} \chi(\lambda, t) \Big|_{\lambda=0} = t(\Gamma_{\rightarrow} - \Gamma_{\leftarrow}). \quad (210)$$

The average current is clearly given by $\langle I \rangle = e\langle m \rangle/t = e(\Gamma_{\rightarrow} - \Gamma_{\leftarrow})$. As we have seen (at $T = 0$) we obtain $I = e\Gamma_{\rightarrow} = \frac{eG_T}{2\pi\hbar}(\mu_L - \mu_R) = \frac{e^2 G_T}{2\pi\hbar} V$. The tunnel conductance is given by $R_T^{-1} = G_T \frac{e^2}{h}$.

4. Exercise

We consider a qubit which is described by the Hamiltonian $H_S = -\frac{1}{2}\epsilon\sigma_z$, where the states $|0\rangle = |\uparrow\rangle$ and $|1\rangle = |\downarrow\rangle$ correspond to two positions of a charged particle. Imagine,

e.g., a double-well potential where a single electron is trapped. To describe the tunneling between the two minima we would have to include a term $-\frac{1}{2}\Delta\sigma_x$. We assume here no tunneling, $\Delta = 0$, in order to have a QND measurement. The tunneling amplitude of (194) is now replaced by $t \rightarrow t_0 + t_1\sigma_z$, with $|t_1| < |t_0|$. Now two different tunneling amplitudes correspond to states $|\uparrow\rangle$ and $|\downarrow\rangle$. The new tunneling Hamiltonian reads

$$H_T = \sum_{k_1, k_2} (t_0 + t_1\sigma_z) \left[R_{k_1}^\dagger L_{k_2} + L_{k_2}^\dagger R_{k_1} \right]. \quad (211)$$

The task is to find the reduced density matrix of the qubit and the counter after tracing out the microscopic degrees of freedom (electrons), $\rho(m_1, m_2, \sigma_1, \sigma_2)$.

X. JOSEPHSON QUBITS

A. Elements of BCS theory (only main results shown in the lecture without derivations)

Our purpose now is to get a bit of BCS theory in order to understand better the Josephson effect. The derivations are provided in the script but will not be shown in the lecture.

1. BCS Hamiltonian

Everything is done in the grand canonical ensemble. The grand canonical partition function

$$Z_\Omega = \sum_{n, N} e^{-\beta(E_{n, N} - \mu N)} \quad (212)$$

shows that at $T = 0$ one has to minimize $H_G = H - \mu N$ and at $T > 0$ one has to minimize $\Omega = \langle H \rangle - TS - \mu N$.

One considers attraction between electrons due to the longitudinal acoustic phonons. The Hamiltonian reads

$$H_G = \sum_{k, \sigma} (\epsilon_k - \mu) c_{k, \sigma}^\dagger c_{k, \sigma} - \frac{1}{2} \frac{g}{V} \sum_{k_1, \sigma_1, k_2, \sigma_2, q} c_{k_1+q, \sigma_1}^\dagger c_{k_2-q, \sigma_2}^\dagger c_{k_2, \sigma_2} c_{k_1, \sigma_1} \quad (213)$$

where the interaction term works only if the energy transfer $\epsilon_{k_1+q} - \epsilon_{k_1}$ is smaller than the Debye energy $\hbar\omega_D$.

Although the Hamiltonian conserves the number of particles, BCS (J. Bardeen, L. Cooper, and R. Schrieffer, 1957) constructed a trial wave function which is a superposition of different numbers of particles:

$$|BCS\rangle = \prod_k (u_k + v_k c_{k,\uparrow}^\dagger c_{-k,\downarrow}^\dagger) |0\rangle . \quad (214)$$

with the purpose to use u_k and v_k as variational parameters and minimize $\langle BCS | H_G | BCS \rangle$. For this purpose one can introduce a reduced BSC Hamiltonian. In this Hamiltonian only those terms are left that contribute to the average $\langle BCS | H_G | BCS \rangle$. The reduced Hamiltonian is the one in which $k_1 = -k_2$ and $\sigma_1 = -\sigma_2$:

$$H_{\text{BCS}} = \sum_{k,\sigma} (\epsilon_k - \mu) c_{k,\sigma}^\dagger c_{k,\sigma} - \frac{1}{2} \frac{g}{V} \sum_{k,q,\sigma} c_{k+q,\sigma}^\dagger c_{-k-q,-\sigma}^\dagger c_{-k,-\sigma} c_{k,\sigma} . \quad (215)$$

Renaming $k' = k + q$ we obtain

$$H_{\text{BCS}} = \sum_{k,\sigma} (\epsilon_k - \mu) c_{k,\sigma}^\dagger c_{k,\sigma} - \frac{1}{2} \frac{g}{V} \sum_{k,k',\sigma} c_{k',\sigma}^\dagger c_{-k',-\sigma}^\dagger c_{-k,-\sigma} c_{k,\sigma} , \quad (216)$$

or

$$H_{\text{BCS}} = \sum_{k,\sigma} (\epsilon_k - \mu) c_{k,\sigma}^\dagger c_{k,\sigma} - \frac{g}{V} \sum_{k,k'} c_{k',\uparrow}^\dagger c_{-k',\downarrow}^\dagger c_{-k,\downarrow} c_{k,\uparrow} , \quad (217)$$

Also the condition on k and k' gets simplified. We just demand that

$$\mu - \hbar\omega_D < \epsilon_k, \epsilon_{k'} < \mu + \hbar\omega_D . \quad (218)$$

2. Variational procedure

Normalization:

$$\begin{aligned} 1 &= \langle BCS | BCS \rangle = \langle 0 | \prod_{k_2} (u_{k_2}^* + v_{k_2}^* c_{-k_2,\downarrow} c_{k_2,\uparrow}) \prod_{k_1} (u_{k_1} + v_{k_1} c_{k_1,\uparrow}^\dagger c_{-k_1,\downarrow}^\dagger) |0\rangle \\ &= \prod_k (|u_k|^2 + |v_k|^2) . \end{aligned} \quad (219)$$

We further restrict ourselves to real u_k and v_k such that $u_k^2 + v_k^2 = 1$. Thus only one of them is independent. The following parametrization is helpful: $u_k = \cos \phi_k$, $v_k = \sin \phi_k$. We obtain

$$\begin{aligned} &\langle BCS | c_{k,\uparrow}^\dagger c_{k,\uparrow} | BCS \rangle \\ &= \langle 0 | \prod_{k_2} (u_{k_2} + v_{k_2} c_{-k_2,\downarrow} c_{k_2,\uparrow}) c_{k,\uparrow}^\dagger c_{k,\uparrow} \prod_{k_1} (u_{k_1} + v_{k_1} c_{k_1,\uparrow}^\dagger c_{-k_1,\downarrow}^\dagger) |0\rangle \\ &= v_k^2 \end{aligned} \quad (220)$$

$$\begin{aligned}
& \langle BCS | c_{k,\downarrow}^\dagger c_{k,\downarrow} | BCS \rangle \\
&= \langle 0 | \prod_{k_2} (u_{k_2} + v_{k_2} c_{-k_2,\downarrow} c_{k_2,\uparrow}) c_{k,\downarrow}^\dagger c_{k,\downarrow} \prod_{k_1} (u_{k_1} + v_{k_1} c_{k_1,\uparrow}^\dagger c_{-k_1,\downarrow}) | 0 \rangle \\
&= v_{-k}^2
\end{aligned} \tag{221}$$

$$\begin{aligned}
& \langle BCS | c_{k',\uparrow}^\dagger c_{-k',\downarrow}^\dagger c_{-k,\downarrow} c_{k,\uparrow} | BCS \rangle \\
&= \langle 0 | \prod_{k_2} (u_{k_2} + v_{k_2} c_{-k_2,\downarrow} c_{k_2,\uparrow}) c_{k',\uparrow}^\dagger c_{-k',\downarrow}^\dagger c_{-k,\downarrow} c_{k,\uparrow} \prod_{k_1} (u_{k_1} + v_{k_1} c_{k_1,\uparrow}^\dagger c_{-k_1,\downarrow}) | 0 \rangle \\
&= u_k v_k u_{k'} v_{k'}
\end{aligned} \tag{222}$$

This gives

$$\langle BCS | H_{\text{BCS}} | BCS \rangle = 2 \sum_k (\epsilon_k - \mu) v_k^2 - \frac{g}{V} \sum_{k,k'} u_k v_k u_{k'} v_{k'} \tag{223}$$

We vary with respect to ϕ_k

$$\frac{\partial}{\partial \phi_k} \langle BCS | H_{\text{BCS}} | BCS \rangle = 4(\epsilon_k - \mu) v_k u_k - 2 \frac{g}{V} (u_k^2 - v_k^2) \sum_{k'} u_{k'} v_{k'} = 0 . \tag{224}$$

We introduce $\Delta = \frac{g}{V} \sum_{k'} u_{k'} v_{k'}$ and obtain

$$2(\epsilon_k - \mu) v_k u_k = \Delta (u_k^2 - v_k^2) . \tag{225}$$

Trivial solution: $\Delta = 0$. E.g., the Fermi sea: $u_k = 0$ and $v_k = 1$ for $\epsilon_k < \mu$ and $u_k = 1$ and $v_k = 0$ for $\epsilon_k > \mu$.

We look for nontrivial solutions: $\Delta \neq 0$. Then from

$$(\epsilon_k - \mu) \sin 2\phi_k = \Delta \cos 2\phi_k \tag{226}$$

we obtain

$$\sin 2\phi_k = 2u_k v_k = \frac{\Delta}{\sqrt{\Delta^2 + (\epsilon_k - \mu)^2}} \tag{227}$$

$$\cos 2\phi_k = u_k^2 - v_k^2 = \frac{\epsilon_k - \mu}{\sqrt{\Delta^2 + (\epsilon_k - \mu)^2}} \tag{228}$$

Then from definition of $\Delta = \frac{g}{V} \sum_k u_k v_k$ we obtain the self-consistency equation

$$\Delta = \frac{g}{2V} \sum_k \frac{\Delta}{\sqrt{\Delta^2 + (\epsilon_k - \mu)^2}} \tag{229}$$

or

$$\begin{aligned}
1 &= \frac{g}{2V} \sum_k \frac{1}{\sqrt{\Delta^2 + (\epsilon_k - \mu)^2}} = \frac{g\nu_0}{2} \int_{-\hbar\omega_D}^{\hbar\omega_D} d\xi \frac{1}{\sqrt{\Delta^2 + \xi^2}} \\
&= g\nu_0 \int_0^{\hbar\omega_D/\Delta} dx \frac{1}{\sqrt{1+x^2}} = g\nu_0 \ln(\sqrt{1+x^2} + x) \Big|_0^{\hbar\omega_D/\Delta} \approx g\nu_0 \ln \frac{2\hbar\omega_D}{\Delta}
\end{aligned} \tag{230}$$

We have assumed $\Delta \ll \hbar\omega_D$. This gives

$$\Delta = 2\hbar\omega_D e^{-\frac{1}{\nu_0 g}} \tag{231}$$

We want to convince ourselves that the total energy of the new state is smaller than the energy of the trivial solution (fully filled Fermi sphere).

$$\begin{aligned}
E_{BCS} &= \langle BCS | H_{BCS} | BCS \rangle = 2 \sum_k (\epsilon_k - \mu) v_k^2 - \frac{g}{V} \sum_{k,k'} u_k v_k u_{k'} v_{k'} \\
&= 2 \sum_k (\epsilon_k - \mu) v_k^2 - \Delta \sum_k u_k v_k,
\end{aligned} \tag{232}$$

whereas

$$E_{Norm} = \langle Norm | H_{BCS} | Norm \rangle = 2 \sum_k (\epsilon_k - \mu) \theta(\mu - \epsilon_k). \tag{233}$$

We obtain

$$\Delta E = E_{BCS} - E_{Norm} = 2 \sum_k (\epsilon_k - \mu) (v_k^2 - \theta(\mu - \epsilon_k)) - \Delta \sum_k u_k v_k, \tag{234}$$

With $\xi_k = \epsilon_k - \mu$,

$$v_k^2 = \sin^2 \phi_k = \frac{1 - \cos 2\phi_k}{2} = \frac{1}{2} - \frac{\xi_k}{2\sqrt{\Delta^2 + \xi_k^2}} \tag{235}$$

and

$$u_k v_k = \frac{\Delta}{2\sqrt{\Delta^2 + \xi_k^2}} \tag{236}$$

we obtain

$$\Delta E = \sum_k \left(2\xi_k \left[\frac{1}{2} - \frac{\xi_k}{2\sqrt{\Delta^2 + \xi_k^2}} - \theta(-\xi_k) \right] - \frac{\Delta^2}{2\sqrt{\Delta^2 + \xi_k^2}} \right) \tag{237}$$

$$\begin{aligned}
\Delta E &= 2V \int_0^{\hbar\omega_D} \nu_0 d\xi \left(\xi \left[\frac{1}{2} - \frac{\xi}{2\sqrt{\Delta^2 + \xi^2}} - \theta(-\xi) \right] - \frac{\Delta^2}{2\sqrt{\Delta^2 + \xi^2}} \right) \\
&= 2V \int_0^{\hbar\omega_D} \nu_0 d\xi \left[\xi - \frac{\xi^2}{\sqrt{\Delta^2 + \xi^2}} - \frac{\Delta^2}{2\sqrt{\Delta^2 + \xi^2}} \right] \\
&= 2V \nu_0 \Delta^2 \int_0^{\hbar\omega_D/\Delta} dx \left(x - \sqrt{1+x^2} + \frac{1}{2\sqrt{1+x^2}} \right)
\end{aligned} \tag{238}$$

The last integral is convergent and for $\hbar\omega_D \gg \Delta$ can be taken to ∞ . The integral gives $-1/4$. Thus

$$\Delta E = -V \frac{\nu_0 \Delta^2}{2} . \quad (239)$$

Roughly energy Δ per electron in window of energies of order Δ .

3. Excitations

We want to consider the BCS ground state as vacuum and find the quasiparticle excitations above it. Let us start with the normal state, i.e., $v_k = \theta(-\xi_k)$ and $u_k = \theta(\xi_k)$. For $\xi_k > 0$ we have

$$c_{k,\sigma} |Norm\rangle = 0 \quad (240)$$

while for $\xi_k < 0$

$$c_{k,\sigma}^\dagger |Norm\rangle = 0 \quad (241)$$

we introduce

$$\alpha_{k,\sigma} \equiv \begin{cases} c_{k,\sigma} & \text{if } \xi_k < 0 \\ \pm c_{-k,-\sigma}^\dagger & \text{if } \xi_k > 0 \end{cases} \quad (242)$$

or equivalently

$$\alpha_{k,\sigma} = u_k c_{k,\sigma} \pm v_k c_{-k,-\sigma}^\dagger \quad (243)$$

(the sign to be chosen). We see, thus, that $\alpha_{k,\sigma} |Norm\rangle = 0$, whereas

$$\alpha_{k,\sigma}^\dagger = u_k c_{k,\sigma}^\dagger \pm v_k c_{-k,-\sigma} \quad (244)$$

creates an excitation of energy $|\xi_k|$. For the BCS state we obtain

$$\alpha_{k,\sigma} |BCS\rangle = (u_k c_{k,\sigma} \pm v_k c_{-k,-\sigma}^\dagger) \prod_q (u_q + v_q c_{q,\uparrow}^\dagger c_{-q,\downarrow}^\dagger) |0\rangle \quad (245)$$

We see that the proper choice of sign is

$$\alpha_{k,\sigma} = u_k c_{k,\sigma} - \sigma v_k c_{-k,-\sigma}^\dagger \quad (246)$$

and

$$\alpha_{k,\sigma} |BCS\rangle = 0 . \quad (247)$$

The conjugated (creation) operator reads

$$\alpha_{k,\sigma}^\dagger = u_k c_{k,\sigma}^\dagger - \sigma v_k c_{-k,-\sigma} \quad (248)$$

One can check the commutation relations

$$\{\alpha_{k,\sigma}, \alpha_{k',\sigma'}^\dagger\}_+ = \delta_{k,k'} \delta_{\sigma,\sigma'} \quad (249)$$

$$\{\alpha_{k,\sigma}, \alpha_{k',\sigma'}\}_+ = 0 \quad \{\alpha_{k,\sigma}^\dagger, \alpha_{k',\sigma'}^\dagger\}_+ = 0 \quad (250)$$

The inverse relations read:

$$c_{k,\sigma} = u_k \alpha_{k,\sigma} + \sigma v_k \alpha_{-k,-\sigma}^\dagger, \quad c_{k,\sigma}^\dagger = u_k \alpha_{k,\sigma}^\dagger + \sigma v_k \alpha_{-k,-\sigma} \quad (251)$$

4. Mean field

We adopt the mean field approximation for the BCS Hamiltonian.

$$H_{\text{BCS}} = \sum_{k,\sigma} (\epsilon_k - \mu) c_{k,\sigma}^\dagger c_{k,\sigma} - \frac{g}{V} \sum_{k,k'} c_{k',\uparrow}^\dagger c_{-k',\downarrow}^\dagger c_{-k,\downarrow} c_{k,\uparrow}. \quad (252)$$

Note that in the interaction the terms with $k = k'$ are absent, since the matrix element of the electron-phonon interaction is proportional to the momentum transfer $q = k - k'$. Thus the only averages we can extract in the interaction term are $\langle c_{-k,\downarrow} c_{k,\uparrow} \rangle$ and $\langle c_{k,\uparrow}^\dagger c_{-k,\downarrow}^\dagger \rangle$. We use

$$\begin{aligned} c_{k,\uparrow}^\dagger c_{-k,\downarrow}^\dagger &= (u_k \alpha_{k,\uparrow}^\dagger + v_k \alpha_{-k,\downarrow}^\dagger)(u_k \alpha_{-k,\downarrow}^\dagger - v_k \alpha_{k,\uparrow}^\dagger) \\ &= u_k^2 \alpha_{k,\uparrow}^\dagger \alpha_{-k,\downarrow}^\dagger - v_k^2 \alpha_{-k,\downarrow}^\dagger \alpha_{k,\uparrow}^\dagger + u_k v_k (1 - \alpha_{k,\uparrow}^\dagger \alpha_{k,\uparrow} - \alpha_{-k,\downarrow}^\dagger \alpha_{-k,\downarrow}). \end{aligned} \quad (253)$$

and

$$c_{-k,\downarrow} c_{k,\uparrow} = u_k^2 \alpha_{-k,\downarrow} \alpha_{k,\uparrow} - v_k^2 \alpha_{k,\uparrow}^\dagger \alpha_{-k,\downarrow}^\dagger + u_k v_k (1 - \alpha_{k,\uparrow}^\dagger \alpha_{k,\uparrow} - \alpha_{-k,\downarrow}^\dagger \alpha_{-k,\downarrow}). \quad (254)$$

In the BCS ground state we obtain $\langle c_{-k,\downarrow} c_{k,\uparrow} \rangle = v_k u_k$ and $\langle c_{k,\uparrow}^\dagger c_{-k,\downarrow}^\dagger \rangle = v_k u_k$. We use

$$AB = \langle A \rangle \langle B \rangle + \langle A \rangle (B - \langle B \rangle) + (A - \langle A \rangle) \langle B \rangle + (A - \langle A \rangle)(B - \langle B \rangle)$$

and neglect the last term. The mean field Hamiltonian reads

$$\begin{aligned} H_{\text{BCS}}^{\text{MF}} &= \sum_{k,\sigma} (\epsilon_k - \mu) c_{k,\sigma}^\dagger c_{k,\sigma} + \frac{g}{V} \sum_{k,k'} \langle c_{k',\uparrow}^\dagger c_{-k',\downarrow}^\dagger \rangle \langle c_{-k,\downarrow} c_{k,\uparrow} \rangle \\ &\quad - \frac{g}{V} \sum_{k,k'} \langle c_{k',\uparrow}^\dagger c_{-k',\downarrow}^\dagger \rangle c_{-k,\downarrow} c_{k,\uparrow} - \frac{g}{V} \sum_{k,k'} c_{k',\uparrow}^\dagger c_{-k',\downarrow}^\dagger \langle c_{-k,\downarrow} c_{k,\uparrow} \rangle \\ &= \sum_{k,\sigma} \xi_k c_{k,\sigma}^\dagger c_{k,\sigma} - \sum_k \Delta c_{-k,\downarrow} c_{k,\uparrow} - \sum_k \Delta c_{k,\uparrow}^\dagger c_{-k,\downarrow}^\dagger + V \frac{\Delta^2}{g} \end{aligned} \quad (255)$$

Substituting the expressions for c operators in terms of α operators we obtain a diagonal Hamiltonian (exercise)

$$H = \sum_{k,\sigma} E_k \alpha_{k,\sigma}^\dagger \alpha_{k,\sigma} + \text{const.} , \quad (256)$$

where $E_k = \sqrt{\Delta^2 + \xi_k^2}$. For proof one needs

$$\begin{aligned} c_{k,\uparrow}^\dagger c_{k,\uparrow} + c_{-k,\downarrow}^\dagger c_{-k,\downarrow} &= (u_k \alpha_{k,\uparrow}^\dagger + v_k \alpha_{-k,\downarrow})(u_k \alpha_{k,\uparrow} + v_k \alpha_{-k,\downarrow}^\dagger) \\ &+ (u_k \alpha_{-k,\downarrow}^\dagger - v_k \alpha_{k,\uparrow})(u_k \alpha_{-k,\downarrow} - v_k \alpha_{k,\uparrow}^\dagger) \\ &= (u_k^2 - v_k^2)(\alpha_{k,\uparrow}^\dagger \alpha_{k,\uparrow} + \alpha_{-k,\downarrow}^\dagger \alpha_{-k,\downarrow}) + 2v_k^2 + 2u_k v_k (\alpha_{k,\uparrow}^\dagger \alpha_{-k,\downarrow}^\dagger + \alpha_{-k,\downarrow} \alpha_{k,\uparrow}) \end{aligned} \quad (257)$$

5. Order parameter, phase

Thus far Δ was real. We could however introduce a different BCS groundstate:

$$|BCS(\phi)\rangle = \prod_k (u_k + e^{i\phi} v_k c_{k,\uparrow}^\dagger c_{-k,\downarrow}^\dagger) |0\rangle . \quad (258)$$

Exercise: check that

$$|BCS(N)\rangle = \int_0^{2\pi} \frac{d\phi}{2\pi} |BCS(\phi)\rangle e^{-iN\phi} \quad (259)$$

gives a state with a fixed number of electrons N . We obtain for Δ

$$\Delta = \frac{g}{V} \sum_k \langle c_{-k,\downarrow} c_{k,\uparrow} \rangle = \frac{g}{V} \sum_k u_k v_k e^{i\phi} = |\Delta| e^{i\phi} \quad (260)$$

It is easy to see that the operator $A^\dagger = e^{-i\phi}$ increases the number of Cooper pairs by one

$$A^\dagger |BCS(N)\rangle = \int_0^{2\pi} \frac{d\phi}{2\pi} |BCS(\phi)\rangle e^{-i(N+1)\phi} = |BCS(N+1)\rangle . \quad (261)$$

We have seen that the excitations above the BCS ground state have an energy gap Δ . Thus, if $T \ll \Delta$ no excitations are possible. The only degree of freedom left is the pair of conjugate variables N, ϕ with commutation relations $[N, e^{-i\phi}] = e^{-i\phi}$. Indeed the ground state energy is independent of ϕ . This degree of freedom is, of course, non-existent if the number of particles is fixed. Thus a phase of an isolated piece of a superconductor is quantum mechanically smeared between 0 and 2π and no dynamics of the degree of freedom N, ϕ is possible. However in a bulk superconductor the phase can be space dependent $\phi(\vec{r})$. One can still add a constant phase to $\phi(\vec{r}) + \phi_0$ without changing the state. More precisely the phase

ϕ_0 is smeared if the total number of particles is fixed. However the difference of phases, i.e., the phase gradient can be well defined and corresponds to a super-current.

We have to consider the gauge invariance. The usual gauge transformation reads

$$\vec{A} \rightarrow \vec{A} + \vec{\nabla}\chi, \quad (262)$$

$$\Psi \rightarrow \Psi e^{\frac{ie}{\hbar c}\chi}, \quad (263)$$

where Ψ is the electron wave function (field). Comparing with (258) we see that adding phase ϕ corresponds to a transformation $c_{k,\sigma}^\dagger \rightarrow e^{i\phi/2} c_{k,\sigma}^\dagger$. This we identify

$$\frac{\phi}{2} = -\frac{e}{\hbar c}\chi. \quad (264)$$

Thus

$$\vec{A} \rightarrow \vec{A} - \frac{\hbar c}{2e} \vec{\nabla}\phi \quad (265)$$

We postulate here the gauge invariant form of the London equation

$$\vec{j}_s = -\frac{e^2 n_s}{mc} \left(\vec{A} - \frac{\hbar c}{2e} \vec{\nabla}\phi \right), \quad (266)$$

where n_s is the density of superconducting electrons. At $T = 0$ all electrons are superconducting, thus $n_s = n$. We do not derive this relation here, but we do so later for the tunneling current between two superconductors with a phase difference between them.

6. Flux quantization

In the bulk of a superconductor, where $\vec{j}_s = 0$, we obtain

$$\vec{A} - \frac{\hbar c}{2e} \vec{\nabla}\phi = 0 \quad (267)$$

$$\oint \vec{A} d\vec{l} = \frac{\hbar c}{2e} \oint \vec{\nabla}\phi d\vec{l} = \frac{\hbar c}{2e} 2\pi n = \frac{\hbar c}{2e} n = n\Phi_0 \quad (268)$$

This quantization is very important for, e.g., a ring geometry. If the ring is thick enough (thicker than λ_L) the total magnetic flux threading the ring is quantized.

B. Josephson effect

We consider now a tunnel junction between two superconductors with different phases ϕ_L and ϕ_R . The Hamiltonian reads

$$H = H_{BCS,L} + H_{BCS,R} + H_T , \quad (269)$$

where analogously to (194) we write

$$H_T = \sum_{k_1, k_2, \sigma} T \left[R_{k_1, \sigma}^\dagger L_{k_2, \sigma} + L_{k_2, \sigma}^\dagger R_{k_1, \sigma} \right] . \quad (270)$$

Here $R_{k, \sigma} \equiv c_{k, \sigma}^{(R)}$ is the annihilation operator of an electron in the left superconductor. Two important things: 1) microscopically the electrons and not the quasiparticles tunnel; 2) tunneling conserves spin.

A gauge transformation $L_{k, \sigma} \rightarrow e^{i\phi_L/2} L_{k, \sigma}$ and $R_{k, \sigma} \rightarrow e^{i\phi_R/2} R_{k, \sigma}$ "removes" the phases from the respective BCS wave functions (making v_k , u_k , and Δ real) and renders the tunneling Hamiltonian

$$H_T = \sum_{k_1, k_2, \sigma} T \left[R_{k_1, \sigma}^\dagger L_{k_2, \sigma} e^{-i\phi/2} + L_{k_2, \sigma}^\dagger R_{k_1, \sigma} e^{i\phi/2} \right] , \quad (271)$$

where $\phi \equiv \phi_R - \phi_L$. Note the similarity with the Full Counting Statistics.

Josephson [5] used (271) and calculated the tunneling current. We do so here for a time-independent phase difference ϕ . The current operator is given by time derivative of the number of particles in the right lead $N_R = \sum_{k, \sigma} R_{k, \sigma}^\dagger R_{k, \sigma}$

$$I = -e\dot{N}_R = -\frac{ie}{\hbar} [H_T, N_R] = \frac{ie}{\hbar} \sum_{k_1, k_2, \sigma} T \left[R_{k_1, \sigma}^\dagger L_{k_2, \sigma} e^{-i\phi/2} - L_{k_2, \sigma}^\dagger R_{k_1, \sigma} e^{i\phi/2} \right] . \quad (272)$$

The first order time-dependent perturbation theory gives for the density matrix of the system in the interaction representation

$$\rho(t) = T e^{-i \int_{-\infty}^t dt' H_T(t')} \rho_0 \tilde{T} e^{i \int_{-\infty}^t dt' H_T(t')} \approx -i \int_{-\infty}^t dt' [H_T(t'), \rho_0] . \quad (273)$$

For the expectation value of the current this gives

$$\langle I(t) \rangle = \text{Tr} \{ \rho(t) I(t) \} = -i \int_{-\infty}^t dt' \text{Tr} \{ [H_T(t'), \rho_0] I(t) \} = -i \int_{-\infty}^t dt' \text{Tr} \{ [I(t), H_T(t')] \rho_0 \} . \quad (274)$$

We use

$$\begin{aligned}
& \langle BCS | c_{k,\uparrow}^\dagger(t_1) c_{-k,\downarrow}^\dagger(t_2) | BCS \rangle \\
&= \langle BCS | \left(u_k \alpha_{k,\uparrow}^\dagger(t_1) + v_k \alpha_{-k,\downarrow}(t_1) \right) \left(u_k \alpha_{-k,\downarrow}^\dagger(t_2) - v_k \alpha_{k,\uparrow}(t_2) \right) | BCS \rangle \\
&= v_k u_k e^{-iE_k(t_1-t_2)} ,
\end{aligned} \tag{275}$$

and

$$\begin{aligned}
& \langle BCS | c_{k,\uparrow}(t_1) c_{-k,\downarrow}(t_2) | BCS \rangle \\
&= \langle BCS | \left(u_k \alpha_{k,\uparrow}(t_1) + v_k \alpha_{-k,\downarrow}^\dagger(t_1) \right) \left(u_k \alpha_{-k,\downarrow}(t_2) - v_k \alpha_{k,\uparrow}^\dagger(t_2) \right) | BCS \rangle \\
&= -v_k u_k e^{-iE_k(t_1-t_2)} ,
\end{aligned} \tag{276}$$

After some algebra we obtain (from the anomalous correlators, the rest gives zero)

$$\begin{aligned}
\langle I(t) \rangle &= - 2eT^2 e^{-i\phi} \int_{-\infty}^t dt' \sum_{k_1, k_2} v_{k_1} u_{k_1} v_{k_2} u_{k_2} \left[e^{-i(E_{k_1}+E_{k_2})(t-t')} - e^{i(E_{k_1}+E_{k_2})(t-t')} \right] \\
&\quad + 2eT^2 e^{i\phi} \int_{-\infty}^t dt' \sum_{k_1, k_2} v_{k_1} u_{k_1} v_{k_2} u_{k_2} \left[e^{-i(E_{k_1}+E_{k_2})(t-t')} - e^{i(E_{k_1}+E_{k_2})(t-t')} \right] \\
&= 8eT^2 \sin(\phi) \sum_{k_1, k_2} \frac{v_{k_1} u_{k_1} v_{k_2} u_{k_2}}{E_{k_1} + E_{k_2}} = 2eT^2 \sin(\phi) \sum_{k_1, k_2} \frac{\Delta^2}{E_{k_1} E_{k_2} (E_{k_1} + E_{k_2})} \\
&= 2\pi^2 T^2 \nu^2 e \Delta \hbar^{-1} \sin(\phi) = I_c \sin(\phi) ,
\end{aligned} \tag{277}$$

where the Josephson critical current is given by

$$I_c = \frac{g_T e \Delta}{4\hbar} = \frac{\pi \Delta}{2e R_T} , \tag{278}$$

where $g_T = 2 \times 4\pi^2 T^2 \nu^2$ is the dimensionless conductance of the tunnel junction (factor 2 accounts for spin), while the tunnel resistance is given by $R_T = \frac{\hbar}{e^2} \frac{1}{g_T}$. This is the famous Ambegaokar-Baratoff relation [6] (see also erratum [7]).

Thus we have obtained the first Josephson relation $I = I_c \sin \phi$. We have introduced the variable ϕ as the difference of two phases $\phi = \phi_R - \phi_L$. The gauge invariant definition reads

$$\phi = \phi_R - \phi_L - \frac{2e}{\hbar c} \int_L^R \vec{A} d\vec{l} . \tag{279}$$

As a shortest way to the second Josephson relation we assume that an electric field exists in the junction and that it is only due to the time-dependence of \vec{A} . Then we obtain

$$\dot{\phi} = -\frac{2e}{\hbar c} \int_L^R \left[\frac{\partial}{\partial t} \vec{A} \right] d\vec{l} = \frac{2e}{\hbar} \int_L^R \vec{E} d\vec{l} = -\frac{2e}{\hbar} V , \tag{280}$$

where V is the voltage. Here we all the time treated e as the charge of the electron, i.e., $e < 0$. Usually one uses e as a positive quantity. Then

$$\dot{\phi} = \frac{2eV}{\hbar} . \quad (281)$$

An alternative way to derive this is to start with a difference of (time-dependent) chemical potentials

$$H = H_L + H_R - eV_L(t) \sum_{k,\sigma} L_{k,\sigma}^\dagger L_{k,\sigma} - eV_R(t) \sum_{k,\sigma} R_{k,\sigma}^\dagger R_{k,\sigma} + H_T , \quad (282)$$

where $V_{L/R}$ are the applied electro-chemical potentials (in addition to the constant chemical potential μ , which is included in H_L and H_R). A transformation with

$$U = e^{\frac{e}{\hbar} \hat{N}_L \int^t V_L(t') dt'} e^{\frac{e}{\hbar} \hat{N}_R \int^t V_R(t') dt'} \quad (283)$$

In the new Hamiltonian

$$\tilde{H} = i\dot{U}U^{-1} + UHU^{-1} . \quad (284)$$

the terms with V_L and V_R are cancelled and instead the electronic operators are replaced by, e.g,

$$L \rightarrow ULU^{-1} = Le^{i\phi_L/2} , \quad (285)$$

where $\phi_L = \text{const.} - \frac{2e}{\hbar} \int^t V_L(t') dt'$ and, thus, $\dot{\phi} = \dot{\phi}_R - \dot{\phi}_L = -\frac{2e}{\hbar} V$.

C. Macroscopic quantum phenomena

1. Resistively shunted Josephson junction (RSJ) circuit

Consider a circuit of parallelly connected Josephson junction and a shunt resistor R . A Josephson junction is simultaneously a capacitor. An external current I_{ex} is applied. The Kirchhoff rules lead to the equation

$$I_c \sin \phi + \frac{V}{R} + \dot{Q} = I_{ex} . \quad (286)$$

As $Q = CV$ and $V = \frac{\hbar}{2e} \dot{\phi}$. Thus we obtain

$$I_c \sin \phi + \frac{\hbar}{2eR} \dot{\phi} + \frac{\hbar C}{2e} \ddot{\phi} = I_{ex} . \quad (287)$$

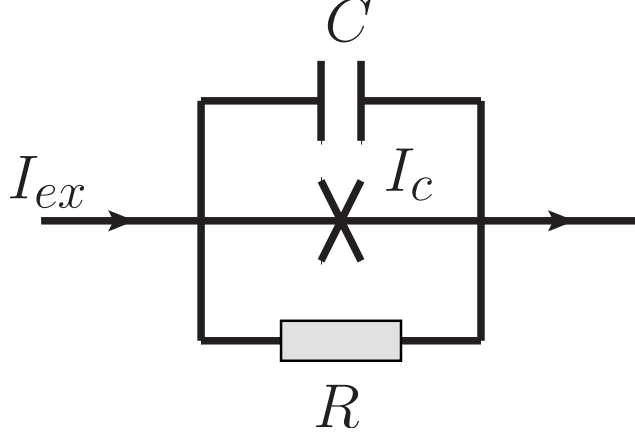


FIG. 22: RSJ Circuit.

It is very convenient to measure the phase in units of magnetic flux, so that $V = \frac{1}{c} \dot{\Phi}$ (in SI units $V = \dot{\Phi}$):

$$\Phi = \frac{c\hbar}{2e} \phi = \frac{\Phi_0}{2\pi} \phi \quad , \quad \phi = 2\pi \frac{\Phi}{\Phi_0} . \quad (288)$$

Then the Kirchhoff equation reads

$$I_c \sin \left(2\pi \frac{\Phi}{\Phi_0} \right) + \frac{\dot{\Phi}}{cR} + \frac{C\ddot{\Phi}}{c} = I_{ex} , \quad (289)$$

or in SI units

$$I_c \sin \left(2\pi \frac{\Phi}{\Phi_0} \right) + \frac{\dot{\Phi}}{R} + C\ddot{\Phi} = I_{ex} . \quad (290)$$

There are two regimes. In case $I_{ex} < I_c$ there exists a stationary solution $\phi = \arcsin(I_{ex}/I_c)$. All the current flows through the Josephson contact as a super-current. Indeed $V \propto \dot{\phi} = 0$. At $I_{ex} > I_c$ at least part of the current must flow through the resistor. Thus a voltage develops and the phase starts to "run".

2. Particle in a washboard potential

The equation of motion (290) can be considered as an equation of motion of a particle with the coordinate $x = \Phi$. We must identify the capacitance with the mass, $m = C$, the inverse resistance with the friction coefficient $\gamma = R^{-1}$. Then we have

$$m\ddot{x} = -\gamma\dot{x} - \frac{\partial U}{\partial x} , \quad (291)$$

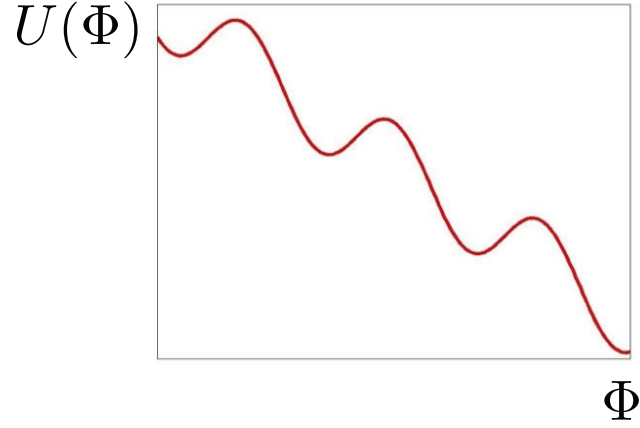


FIG. 23: Washboard potential.

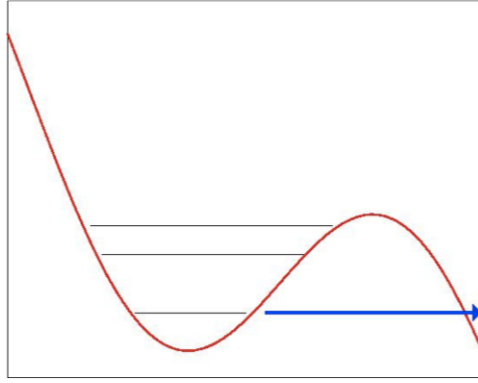


FIG. 24: Macroscopic Quantum Tunneling (MQT).

where for the potential we obtain

$$U(\Phi) = -E_J \cos\left(2\pi \frac{\Phi}{\Phi_0}\right) - I_{ex} \Phi, \quad (292)$$

where

$$E_J \equiv \frac{I_c \Phi_0}{2\pi} = \frac{\hbar I_c}{2e} \quad (293)$$

is called the Josephson energy. The potential energy $U(\Phi)$ has a form of a washboard and is called a washboard potential. In Fig. 23 the case $I_{ex} < I_c$ is shown. In this case the potential has minima and, thus, classically stationary solutions are possible.

When the external current is close to the critical value a situation shown in Fig. 24 emerges. If we allow ourselves to think of this situation quantum mechanically, then we would conclude that only a few quantum levels should remain in the potential well. Moreover a tunneling process out of the well should become possible. This tunneling process was named

Macroscopic Quantum Tunneling because in the 80-s and the 90-s many researchers doubted the fact one can apply quantum mechanics to the dynamics of the "macroscopic" variable Φ . It was also argued that a macroscopic variable is necessarily coupled to a dissipative bath which would hinder the tunneling. Out these discussions the famous Caldeira-Leggett model emerged [8, 9].

3. Quantization

We write down the Lagrangian that would give the equation of motion (291 or 290). Clearly we cannot include the dissipative part in the Lagrange formalism. Thus we start from the limit $R \rightarrow \infty$. The Lagrangian reads

$$L = \frac{C\dot{\Phi}^2}{2} - U(\Phi) = \frac{C\dot{\Phi}^2}{2} + E_J \cos\left(2\pi\frac{\Phi}{\Phi_0}\right) + I_{ex}\Phi . \quad (294)$$

We transform to the Hamiltonian formalism and introduce the canonical momentum

$$Q \equiv \frac{\partial L}{\partial \dot{\Phi}} = C\dot{\Phi} . \quad (295)$$

The Hamiltonian reads

$$H = \frac{Q^2}{2C} + U(\Phi) = \frac{Q^2}{2C} - E_J \cos\left(2\pi\frac{\Phi}{\Phi_0}\right) - I_{ex}\Phi . \quad (296)$$

The canonical momentum corresponds to the charge on the capacitor (junction). The usual commutation relations should be applied

$$[\Phi, Q] = i\hbar . \quad (297)$$

In the Hamilton formalism it is inconvenient to have an unbounded from below potential. Thus we try to transform the term $-I_{ex}\Phi$ away. This can be achieved by the following canonical transformation

$$R = \exp\left[-\frac{i}{\hbar}Q_{ex}(t)\Phi\right] , \quad (298)$$

where $Q_{ex}(t) \equiv \int^t I_{ex}(t')dt'$. Indeed the new Hamiltonian reads

$$\tilde{H} = RHR^{-1} + i\hbar\dot{R}R^{-1} = \frac{(Q - Q_{ex}(t))^2}{2C} - E_J \cos\left(2\pi\frac{\Phi}{\Phi_0}\right) . \quad (299)$$

The price we pay is that the new Hamiltonian is time-dependent. The Hamiltonian (299) is very interesting. Let us investigate the operator

$$\cos\left(2\pi\frac{\Phi}{\Phi_0}\right) = \cos\left(\frac{2e}{\hbar}\Phi\right) = \frac{1}{2} \exp\left[\frac{i}{\hbar}2e\Phi\right] + h.c. \quad (300)$$

We have

$$\exp\left[\frac{i}{\hbar}2e\Phi\right] |Q\rangle = |Q+2e\rangle \quad , \quad \exp\left[-\frac{i}{\hbar}2e\Phi\right] |Q\rangle = |Q-2e\rangle \quad . \quad (301)$$

Thus in this Hamiltonian only the states differing by an integer number of Cooper pairs get connected. The constant offset charge remains undetermined. This, however, can be absorbed into the bias charge Q_{ex} . Thus, we can restrict ourselves to the Hilbert space $|Q = 2em\rangle$.

4. Josephson energy dominated regime

In this regime $E_J \gg E_C$, where $E_C = \frac{(2e)^2}{2C}$ is the Cooper pair charging energy. Let us first neglect E_C completely, i.e., put $C = \infty$. Recall that C plays the role of the mass. Then the Hamiltonian reads $H = -E_J \cos\left(2\pi\frac{\Phi}{\Phi_0}\right)$. On one hand it is clear that the relevant state are those with a given phase, i.e., $|\Phi\rangle$. On the other hand, in the discrete charge representation the Hamiltonian reads

$$H = -\frac{E_J}{2} \sum_m (|m+1\rangle \langle m| + |m\rangle \langle m+1|) \quad . \quad (302)$$

The eigenstates of this tight-binding Hamiltonian are the Bloch waves $|k\rangle = \sum_m e^{ikm} |m\rangle$ with the wave vector k belonging to the first Brillouin zone $-\pi \leq k \leq \pi$. The eigenenergy reads $E_k = -E_J \cos(k)$. Thus we identify $k = \phi = \frac{2\pi\Phi}{\Phi_0}$.

5. Charging energy dominated regime

In this regime $E_J \ll E_C$. The main term in the Hamiltonian is the charging energy term

$$H_C = \frac{(Q - Q_{ex}(t))^2}{2C} = \frac{(2em - Q_{ex})^2}{2C} \quad . \quad (303)$$

The eigenenergies corresponding to different values of m form parabolas as functions of Q_{ex} (see Fig. 25). The minima of the parabolas are at $Q_{ex} = 0, 2e, 4e, \dots$. The Josephson

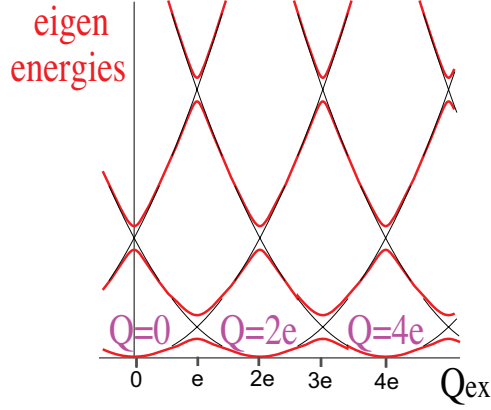


FIG. 25: Eigen levels in the coulomb blockade regime. Different parabolas correspond to different values of $Q = 2em$. The red lines represent the eigenlevels with the Josephson energy taken into account. The Josephson tunneling lifts the degeneracy between the charge states.

tunneling term serves now as a perturbation $H_J = -E_J \cos\left(2\pi\frac{\Phi}{\Phi_0}\right)$. It lifts the degeneracies, e.g., at $Q_{ex} = e, 3e, 5e, \dots$

If a small enough external current is applied, $Q_{ex} = I_{ex}t$ the adiabatic theorem holds and the system remains in the ground state. Yet, one can see that between the degeneracies at $Q_{ex} = e, 3e, 5e, \dots$ the capacitance is charged and discharged and oscillating voltage $V = \partial E_0 / \partial Q_{ex}$ appears. Here $E_0(Q_{ex})$ is the energy of the ground state. The Cooper pairs tunnel only at the degeneracy points. In between the Coulomb blockade prevents the Cooper pairs from tunneling because this would cost energy.

6. Caldeira-Leggett model

In order to describe the dissipation due to the shunt resistor a bath of linear oscillators is added. The Hamiltonian now reads

$$H = \frac{Q^2}{2C} + U(\Phi) + \sum_n \left[\frac{p_n^2}{2m_n} + \frac{m_n \omega_n^2 \left(x_n - \frac{\lambda_n}{m_n \omega_n^2} \Phi \right)^2}{2} \right]. \quad (304)$$

Equations of motion:

$$\begin{aligned} \dot{\Phi} &= \frac{\partial H}{\partial Q} = \frac{Q}{C}, \\ \dot{Q} &= -\frac{\partial H}{\partial \Phi} = -\frac{\partial U}{\partial \Phi} + \sum_n \lambda_n \left(x_n - \frac{\lambda_n}{m_n \omega_n^2} \Phi \right), \end{aligned}$$

$$\begin{aligned}\dot{x}_n &= \frac{\partial H}{\partial p_n} = \frac{p_n}{m_n} , \\ \dot{p}_n &= -\frac{\partial H}{\partial x_n} = -m_n \omega_n^2 \left(x_n - \frac{\lambda_n}{m_n \omega_n^2} \Phi \right) .\end{aligned}\tag{305}$$

This gives

$$\begin{aligned}C\ddot{\Phi} &= -\frac{\partial U}{\partial \Phi} + \sum_n \lambda_n x_n - \Phi \sum_n \frac{\lambda_n^2}{m_n \omega_n^2} , \\ m_n \ddot{x}_n + m_n \omega_n^2 x_n &= \lambda_n \Phi .\end{aligned}\tag{306}$$

The second equation is solved by the Fourier transform. We obtain

$$x_n(t) = \int dt' \alpha_n(t-t') \Phi(t') + x_n^{(\text{free})}(t),\tag{307}$$

where

$$\alpha_n(\omega) = \frac{\lambda_n}{m_n(\omega_n^2 - (\omega + i\delta)^2)} .\tag{308}$$

The sign of the $i\delta$ term is chosen to make α_n retarded, i.e., $\alpha_n(\tau < 0) = 0$. We obtain

$$\sum_n \lambda_n x_n(t) = \int dt' \alpha(t-t') \Phi(t') + \xi(t) ,\tag{309}$$

where

$$\alpha(\omega) = \sum_n \frac{\lambda_n^2}{m_n(\omega_n^2 - (\omega + i\delta)^2)}\tag{310}$$

and

$$\xi(t) = \sum_n \lambda_n x_n^{(\text{free})}(t) .\tag{311}$$

We introduce the spectral density

$$J(\nu) \equiv \frac{\pi}{2} \sum_n \frac{\lambda_n^2}{m_n \omega_n} \delta(\nu - \omega_n) .\tag{312}$$

This gives

$$\alpha(\omega) = \frac{2}{\pi} \int d\nu \frac{\nu J(\nu)}{\nu^2 - (\omega + i\delta)^2}\tag{313}$$

and, finally,

$$\text{Im } \alpha(\omega) = \alpha''(\omega) = \begin{cases} J(\omega) & \text{for } \omega > 0 \\ -J(-\omega) & \text{for } \omega < 0 \end{cases} .\tag{314}$$

An Ohmic bath is defined by

$$J(\omega) = R^{-1} \omega ,\tag{315}$$

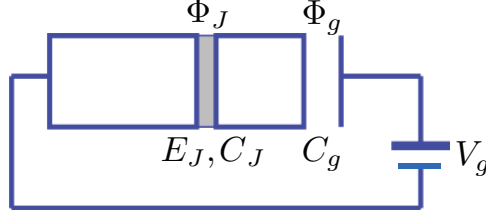


FIG. 26: Cooper Pair Box. The Josephson tunnel junction is characterized by the Josephson energy E_J and by the capacitance C_J . The superconducting island is controlled by the gate voltage V_g via the gate capacitance C_g . To derive the system's Lagrangian and Hamiltonian we introduce the phase drop on the Josephson junction Φ_J and the phase drop on the gate capacitor Φ_g .

up to some cutoff frequency ω_c . We disregard, first, $\text{Re } \alpha(\omega) = \alpha'(\omega)$ and obtain

$$\alpha''(t - t') = \int \frac{d\omega}{2\pi} e^{-i\omega(t-t')} iR^{-1}\omega = R^{-1} \frac{\partial}{\partial t'} \delta(t - t') \quad (316)$$

Thus

$$\int dt' \alpha''(t - t') \Phi(t') = -R^{-1} \dot{\Phi}(t) . \quad (317)$$

The equation of motion now reads

$$C\ddot{\Phi} = -\frac{\partial U}{\partial \Phi} - \frac{\dot{\Phi}}{R} - \Phi \sum_n \frac{\lambda_n^2}{m_n \omega_n^2} + \int dt' \alpha'(t - t') \Phi(t') + \xi(t) \quad (318)$$

The second term of the RHS is the friction force due to the oscillators (resistor). The third and the fourth terms represent the renormalization of $U(\Phi)$. Our choice of coupling to the oscillators was such that these two terms mostly cancel each other. Finally, the last term of the RHS is the Langevin random force. We see that this is due to the free motion of the oscillators.

D. Various qubits

1. Charge qubit

We start by considering the so called Cooper pair box shown in Fig. 26. We derive the Hamiltonian starting from the Lagrangian

$$L = \frac{C_J \dot{\Phi}_J^2}{2} + \frac{C_g \dot{\Phi}_g^2}{2} - U_J(\Phi_J) , \quad (319)$$

where $U_J = -E_J \cos\left(2\pi \frac{\Phi_J}{\Phi_0}\right)$. The sum of all the phases along the loop must vanish and the phase on the voltage source is given by $const. + V_g t$. Thus we obtain

$$\dot{\Phi}_g = -\dot{\Phi}_J - V_g \quad (320)$$

and the Lagrangian in terms of the only generalized coordinate Φ_J reads

$$\begin{aligned} L &= \frac{C_J \dot{\Phi}_J^2}{2} + \frac{C_g (\dot{\Phi}_J + V_g)^2}{2} - U_J(\Phi_J) \\ &= \frac{(C_J + C_g) \dot{\Phi}_J^2}{2} + C_g \dot{\Phi}_J V_g - U_J(\Phi_J) + const. . \end{aligned} \quad (321)$$

The conjugated momentum (charge) reads

$$Q = \frac{\partial L}{\partial \dot{\Phi}_J} = (C_J + C_g) \dot{\Phi}_J + C_g V_g . \quad (322)$$

Since $C_J \dot{\Phi}_J$ is the charge on the Josephson junction capacitance while $C_g \dot{\Phi}_J + C_g V_g = -C_g \dot{\Phi}_g$ is minus the charge on the gate capacitance we conclude that $Q = 2em$ is the charge on the island (we disregard here the possibility to have an odd number of electrons on the island). We obtain

$$\dot{\Phi}_J = \frac{Q - C_g V_g}{C_J + C_g} . \quad (323)$$

The Hamiltonian reads

$$\begin{aligned} H = Q \dot{\Phi}_J - L &= \frac{(Q - C_g V_g)^2}{2(C_J + C_g)} + U_J(\Phi_J) \\ &= \frac{(Q - C_g V_g)^2}{2(C_J + C_g)} - E_J \cos\left(2\pi \frac{\Phi_J}{\Phi_0}\right) . \end{aligned} \quad (324)$$

This is exactly the Hamiltonian (299) with $Q_{ex} = C_g V_g$. The two level system is formed by the two lowest levels around $C_g V_g = e + 2eN$.

In Hamiltonian (324) the interplay of two energy scales determines the physical regime. These are 1) Josephson energy E_J ; 2) Charging energy $E_C \equiv \frac{(2e)^2}{2(C_J + C_g)}$. In the simplest regime $E_J \ll E_C$ and for $Q_{ex} \sim e$ one can restrict the Hilbert space to two charge states with lowest charging energies $|\uparrow\rangle = |Q = 0\rangle$ and $|\downarrow\rangle = |Q = 2e\rangle$. In this Hilbert space we have

$$\cos\left(2\pi \frac{\Phi_J}{\Phi_0}\right) = \frac{1}{2} \sigma_x , \quad (325)$$

and

$$Q = e(1 - \sigma_z) . \quad (326)$$

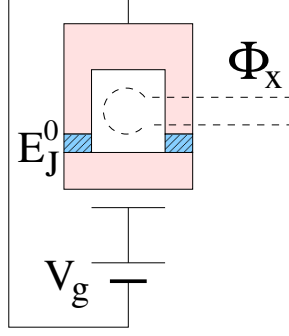


FIG. 27: Charge qubit with controllable Josephson energy.

Substituting these to (324) and disregarding constant energy shifts we obtain

$$H = -\frac{1}{2} \left(1 - \frac{Q_{ex}}{e} \right) E_C \sigma_z - \frac{1}{2} E_J \sigma_x . \quad (327)$$

Thus we obtain an effective spin-1/2 in a magnetic field whose z -component can be controlled by the gate voltage.

In Fig. 27 a charge qubit is shown in which the Josephson junction was replaced by a dc-SQUID. A straightforward derivation (assuming the geometrical inductance of the SQUID loop being vanishingly small) gives again the Hamiltonian (324) with $C_J \rightarrow 2C_J$ (just because there are two junctions instead of one) and

$$E_J \rightarrow 2E_J^{(0)} \cos \left(\frac{\pi \Phi_x}{\Phi_0} \right) . \quad (328)$$

Here $E_J^{(0)}$ is the Josephson energy of a single junction. We assume the two junctions of the SQUID to be identical. Now we can control also the x -component of the effective magnetic field.

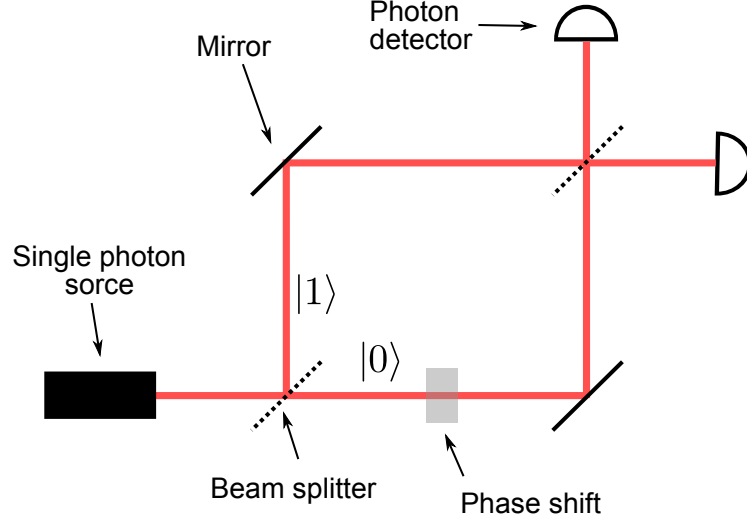


FIG. 28: The qubit is encoded into the path of a single photon. A 50 % beam splitter represents a Hadamard gate, while a phase gate is a simple phase shift in one arm of the interferometer.

2. Flux qubit

3. Phase qubit

XI. OPTICAL QUBITS AND CAVITY QED

A. Photons as Qubits

In many ways photons are the perfect qubits. Their polarization is a natural two level system and one has not to worry about populating higher levels. Alternatively, photons can travel through a Mach-Zehnder interferometer with two paths and the qubit is encoded in the “which path” degree of freedom, as depicted in fig. 28. All single qubit transformations can be easily achieved with mirrors, beam splitters, phase shifts. On demand single photon generators improve rapidly and single photon detectors for the readout are available (although so far only with about 60 % efficiency). Photons interact very little with the

environment and many single qubit operations can be achieved without loss or decoherence of the photon. Furthermore, in a computing device, information needs to be transported. This is a difficult task for many qubit realizations, but not an issue for photons because they naturally travel with the speed of light (but the storage of information encoded in photons is not straight forward).

To all these advantages there is one major downside to optical photons: they do not interact with each other. This is a problem for two-qubit gates. An interaction of the light beams can be achieved via a non-linear medium, such as a Kerr medium where the refractive index depends on the intensity of the light beam

$$n(I) = n + n_2 I. \quad (329)$$

Therefore, the phase shift of a photon depends on the state of a second photon \Rightarrow C-phase gate. Because the intensity of a single photon is very weak, a very strong non-linearity is needed and such materials do not exist. Furthermore, good Kerr media are highly absorptive.

For this reason there is little hope for a purely optical QC. However, because information between photons and other qubits can be exchanged (SWAP-gate), many QC-proposals use photons for information transport.

B. Quantum Cryptography

A well suited application for photons is quantum key distribution (QKD). Once when quantum computers exist to break the known classical cryptography, information can still be distributed safely with quantum key distribution. Furthermore, as classical cryptography is not yet proven to be safe, there is already now a small market for QKD. QKD is not as hard as quantum computing, and indeed, in 2004 *id Quantique* were the first to bring a working quantum key distributor on the market.

We first explain the classical secret key cryptography. If Alice (A) wants to send Bob (B) a message of n bits, they need to share a key of the same length. A adds the key to the message modulo 2, and sends the resulting encrypted message. B adds the key to the encrypted message to find the original message. See the table below.

message	0 1 0 0 1 1 0
key	1 1 0 1 0 1 0
encrypted message	1 0 0 1 1 0 0
decrypted message	0 1 0 0 1 1 0

This protocol is perfectly safe given that no one else knows the key. Therefore, the problem of cryptography is reduced to transmitting or sharing a key. Classically, whenever a key is transmitted, someone else (often called Eve (E)) can intercept the transmission to gain the key. If the key is encoded into a qubit, then, whenever Eve measures the qubit to gain the key, she will also change the state of the qubit. Therefore, Alice and Bob can detect that Eve intercepted the line and not send the message in this case.

There are several protocols for QKD, here we present the simplest BB84 QKD protocol. For A to transfer a key on length n , she needs $4n$ qubits which she can prepare in the states $|0\rangle, |1\rangle, |+\rangle = (|0\rangle + |1\rangle)/\sqrt{2}$, and $|-\rangle = (|0\rangle - |1\rangle)/\sqrt{2}$. The states $|0\rangle$ and $|+\rangle$ are both used to encode a 0, while $|1\rangle$ and $|-\rangle$ encode a 1. Then she generates $4n$ random numbers b . Whenever $b = 0$, then she uses the $(0,1)$ basis to encode bits, while when $b = 1$ she uses the $(+, -)$ basis. Next she generates another $4n$ random numbers a which represent the key and which she will encode in the basis determined by b .

She now sends the qubits to Bob, who will generate $4n$ random numbers b' to determine in which basis he will measure the qubit. If he measures the states $|0\rangle$ or $|+\rangle$ he will note a 0, and if he measures $|1\rangle$ or $|-\rangle$, he will note a 1.

qubit number	b	a	state of qubit	b'	a'
1	0	1	$ 1\rangle$	0	1
2	0	0	$ 0\rangle$	1	0 or 1
3	1	1	$ -\rangle$	0	0 or 1
4	1	1	$ -\rangle$	1	1
5	0	1	$ 1\rangle$	1	0 or 1
6	1	0	$ +\rangle$	1	0
\vdots	\vdots	\vdots	\vdots	\vdots	\vdots
$4n$	0	0	$ 0\rangle$	1	0 or 1

Once Bob has measured all qubits, he tells Alice in which basis b' he measured and Alice tells Bob in which basis b she prepared. This is done using a public line, so Eve is allowed to get this information. Now they discard all bits where they used different bases, i.e. they only keep bits with $b = b'$. For these they know that $a = a'$ and they now share a key of length $2n$.

Now we assume Eve intercepts the line. Assume A sends $|1\rangle$ as in qubit number one. At this time it is not yet public which basis A used. Therefore E can only choose randomly, and with probability $p_1 = 0.5$ she chooses the $(+-)$ basis. Now she would ideally send $|1\rangle$ to B and no one could realize that she intercepted the transmission. However, she does not know that A sent out $|1\rangle$. The best she can do is to send out what she measured. If B measures in the basis $(0,1)$, with probability $p_2 = 0.5$, he will measure 0. Therefore, if E intercepts, then A and B will have different bits $a \neq a'$ with probability $p = p_1 p_2 = 0.25$.

A will now randomly choose n bits which they public compare on a public line. If all n bits are the same, they can use the other n bits as secret key. If about a quarter of the n bits are different, then they know that someone intercepted and do not use the key. Note that E can still prevent A from sending a message to B, but she can do that anyway by cutting the line. But she can not get the message!

One seemingly obvious way for Eve to stay undetected is to copy the state sent by A, then forward one copy to B and use the other for her measurements. However, the *no cloning theorem* forbids copying of an unknown quantum state. The theorem is easy to prove by contradiction. To copy a state from system 1 to system 2 means to perform the transformation $|\psi\rangle_1 \otimes |0\rangle_2 \rightarrow |\psi\rangle_1 \otimes |\psi\rangle_2$. This should be valid for all input states, therefore $|\phi\rangle_1 \otimes |0\rangle_2 \rightarrow |\phi\rangle_1 \otimes |\phi\rangle_2$. Every unitary transformation preserves the scalar product, which leads to $\langle\phi|\psi\rangle = \langle\phi|\psi\rangle^2$. This is clearly not true for general states. This can easily be generalized to trace-preserving and completely positive quantum operations.

This protocol is easily performed using the polarization of a photon as qubit. However, photon detectors are not perfect and Bob will sometimes find the wrong result. Therefore, if A wants to transmit a 0, she tells Bob a number of qubits which he should have detected in the state 0. Given that Bob only rarely finds a wrong measurement result, he can use a majority vote to decide what the bit should be. This is shown below where they use five

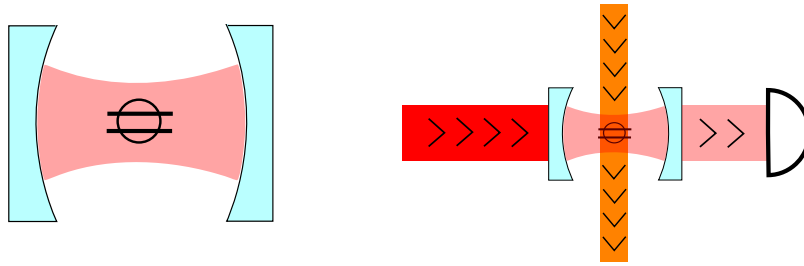


FIG. 29: Left: Schematic of a cavity and a two level atom. Right: Possible experimental setup with a laser (orange) to perform arbitrary transformations of the atom, and another laser (red) to drive the cavity for a dispersive readout of the atom.

bits to encode one key bit.

qubit number	1	4	6	11	17	key bit
a	0	0	0	0	0	$\Rightarrow 0$
a'	0	0	0	1	0	$\Rightarrow 0$

Of course, the more qubits A has to send to transfer a single key bit, the easier it is for E to intercept the line staying undetected, because with a good measurement apparatus she can get enough information by only intercepting some of the qubits. Also, $a \neq a'$ not necessarily proves an interceptor because it might be due to a bad measurement. Therefore, good QKD requires many qubits for good statistics as well as good detectors.

C. Cavity QED

Cavity quantum electrodynamics is about the interaction of a single atom with a single photon. The basic idea to increase the interaction is to put the photon into a cavity such that it can interact many times with the atom. A review of Cavity QED is found in [10].

The system is described by the Jaynes–Cummings Hamiltonian

$$H = \hbar\omega_r \left(a^\dagger a + \frac{1}{2} \right) + \frac{\hbar\omega_a}{2} \sigma_z + \hbar g \left(a^\dagger \sigma_- + a \sigma_+ \right). \quad (330)$$

The first term describes one mode of the cavity, the second the two level system, and the third the coupling. The coupling of an atom to an electric field is given by $\vec{E} \otimes \vec{D}$.

While \vec{E} is proportional to $(a^\dagger + a)$, the dipole moment of the atom is proportional to $\sigma_x = (\sigma_+ + \sigma_-)$. The two terms which do not conserve the number of excitations can be neglected in the rotating wave approximation. That can be seen by transforming into the interaction picture with $U = e^{i\hbar\omega_r a^\dagger a} \otimes e^{i\hbar\omega_a \sigma_z/2}$. The terms which approximately preserve the energy of the system without interaction oscillate slowly, while the others oscillate fast and can be neglected. For the same reason other modes of the cavity and other levels of the atom do not have to be considered.

The regime most interesting is the strong coupling regime $g \gg \gamma, \kappa$, where γ is the rate of spontaneous emission of the atom, and κ is the loss rate of the cavity. To reach this regime (which is very difficult) the following things can be done

- **Small mode volume:** The smaller the cavity, the stronger the electric field of a single photon. The size of the cavity is limited by the wavelength. Also, κ increases with the inverse length of the cavity because the photon has to be reflected more often in the same time interval.
- **Rydberg atoms:** These are highly excited atoms with the principal quantum number n of the order of one hundred. They also have a low decay rate, but they are not easy to prepare with good fidelity.
- **Highly reflective mirrors:** The best mirrors are superconducting mirrors, but they can only be used for microwave cavities because shorter wavelength can excite quasi particles. Also optical mirrors are better for infra red light than for visible or UV light. Therefore, there is a trade-off with the first item.

We introduce $N = a^\dagger a + \sigma_z$ to count the number of excitations. Because $[H, N] = 0$, the number of excitations is preserved. Using the detuning $\Delta = \omega_a - \omega_r$ we write

$$H = \omega_r N + \Delta \sigma_z/2 + g (a^\dagger \sigma_- + a \sigma_+). \quad (331)$$

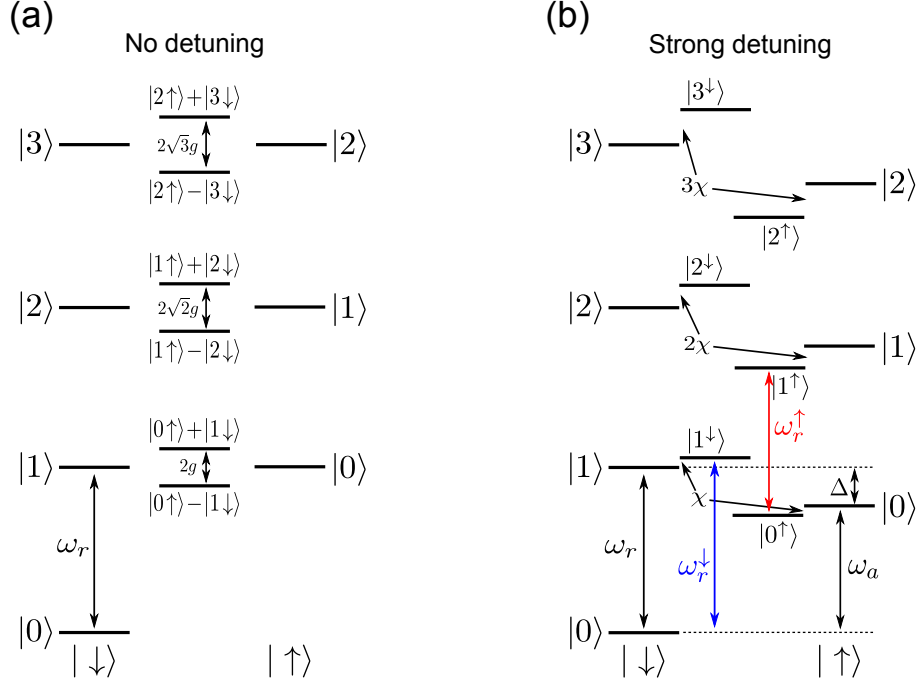


FIG. 30: Left: Experimental setup to measure Rabi oscillations between a two-level atom and an empty cavity. The atoms are generated in the oven O and excited by a laser in B , before they enter the cavity C and the measurement apparatus D . Right: The measured probability to find the atom in the excited state plotted over the time the atom lingers in the cavity.

The Hamiltonian can be written in a block diagonal matrix form

$$H = \begin{pmatrix} -\Delta/2 & 0 & 0 & 0 & 0 & \cdots \\ 0 & -\Delta/2 & g & 0 & 0 & \cdots \\ 0 & g & \Delta/2 & 0 & 0 & \cdots \\ 0 & 0 & 0 & -\Delta/2 & \sqrt{2}g & \cdots \\ 0 & 0 & 0 & \sqrt{2}g & \Delta/2 & \cdots \\ \vdots & \vdots & \vdots & \vdots & \vdots & \ddots \end{pmatrix}; \quad \begin{pmatrix} |0 \downarrow\rangle \\ |1 \downarrow\rangle \\ |0 \uparrow\rangle \\ |2 \downarrow\rangle \\ |1 \uparrow\rangle \\ \vdots \end{pmatrix} \quad (332)$$

where each block accounts for a certain number of excitations. The number in the ket labels the number of photons in the cavity, while \downarrow / \uparrow label the ground state and excited state of the atom, respectively. For shorter notation we removed $\omega_r N$ because within each block it is a constant energy. The energy levels of the system can be visualized with the Jaynes–Cummings ladder as in figure 30. The left and right columns are the levels without cavity–atom coupling, while the center column are the energy levels of the coupled system.

For $\Delta = 0$ [see figure 30 (a)] the cavity and atom will exchange a single excitation with the

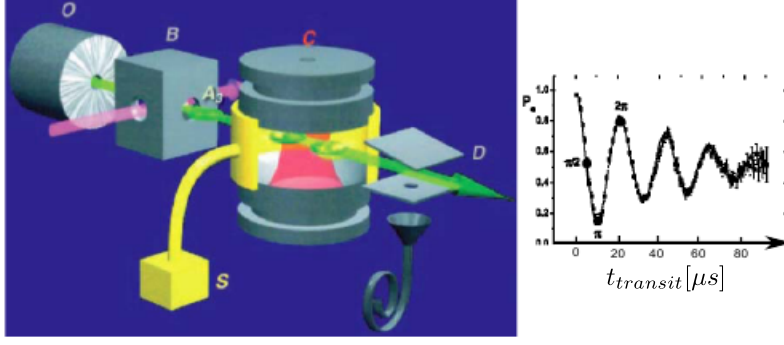


FIG. 31: Left: Experimental setup to measure Rabi oscillations between a two-level atom and an empty cavity. Right: The measured probability to find the atom in the excited state plotted over the time the atom needs to transit the cavity.

frequency $2\sqrt{n}/2\pi$, where n is the number of excitations of the total system. For example, if we insert an excited atom into an empty cavity, the state evolves into

$$\begin{aligned}
 |\psi(t)\rangle &= U(t) |0 \uparrow\rangle \\
 &= \frac{1}{2} U(t) [(|0 \uparrow\rangle + |1 \downarrow\rangle) + (|0 \uparrow\rangle - |1 \downarrow\rangle)] \\
 &= \frac{1}{2} [e^{-igt}(|0 \uparrow\rangle + |1 \downarrow\rangle) + e^{igt}(|0 \uparrow\rangle - |1 \downarrow\rangle)] \\
 &= \cos(gt) |0 \uparrow\rangle - i \sin(gt) |1 \downarrow\rangle.
 \end{aligned} \tag{333}$$

Figure 31 displays an experiment which measures the population of the excited state as a function of time. The oscillations decay due to decoherence, mainly spontaneous emission and loss of photons. The coupling of a single photon and a single atom can also be detected by spectroscopic experiments as shown in figure 32. The probe laser can be slightly transmitted through the cavity if it matches the frequency of the cavity–atom system (note that the reflectivity of the mirrors is slightly smaller than one). The laser intensity has to be small enough such that the system is mostly in the state $|0 \downarrow\rangle$. One will then find transmission at frequencies $\omega_r \pm g$. The splitting by $2g$ can only be seen if the natural line width of the cavity is smaller than g , which is exactly the strong–coupling limit.

In the strong detuning regime [see figure 30 (b)], the energy eigenstates are approximately

$$\begin{aligned}
 |1^\downarrow\rangle &\approx |1 \downarrow\rangle - \frac{g}{\Delta} |0 \uparrow\rangle \\
 |0^\uparrow\rangle &\approx |0 \uparrow\rangle + \frac{g}{\Delta} |1 \downarrow\rangle
 \end{aligned} \tag{334}$$

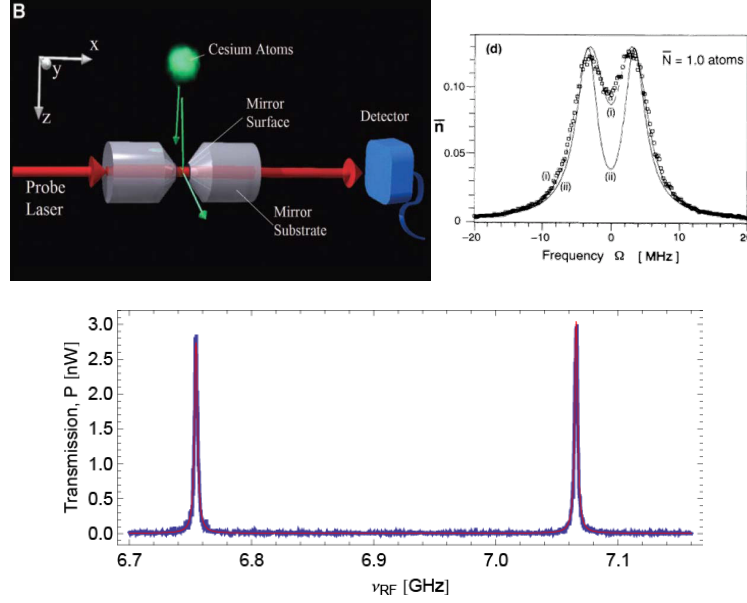


FIG. 32: The top left figure displays an optical experiment to determine the coupling g via spectroscopy. A typical result is shown on the top left. The two Lorentzian peaks are separated by $2g$ which in this plot is of the same order as the natural line width. Therefore, the strong coupling limit is not fully achieved. Although recent optics experiments have improved, the most impressive data from the strong coupling limit comes from circuit cavity QED as shown in the lower figure.

which are almost the product states $|1 \downarrow\rangle$ and $|0 \uparrow\rangle$. The situation is similar for higher levels. The energy levels are

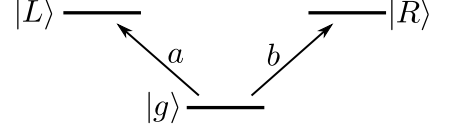
$$\begin{aligned} E_{|n\downarrow\rangle} &\approx n(\omega_r + \chi) \\ E_{|n\uparrow\rangle} &\approx n(\omega_r - \chi) + (\omega_a - \chi), \end{aligned} \quad (335)$$

with $n = 0, 1, 2, \dots$ and $\chi = g^2/\Delta$. In effect, the interaction with the atom barely changes the eigenstates of the system, but depending on the state of the atom, the cavity frequency gets shifted by $\pm\chi$. Although χ is small in the strong coupling regime, in some instances the frequency of the cavity can be measured to great precision. Therefore, this regime can be used to readout the state of the atom. This is the most common principle behind the readout of superconducting qubits.

1. Coupling of photons with Cavity QED

Here we show how a three level atom can be used to couple two photons of different modes

a and b . The modes have the same frequency ω_r and opposite polarization. The mode a couples to the atomic transition $|g\rangle \rightarrow |L\rangle$, and the mode b couples to $|g\rangle \rightarrow |R\rangle$, as shown to the right. The states $|L\rangle$ and $|R\rangle$ are



degenerate and have a different magnetic quantum number such that they can be selectively addressed by photons of different polarization. The Jaynes-Cummings Hamiltonian is

$$H = \omega_r N + \frac{\Delta}{2} \begin{pmatrix} -1 & 0 & 0 \\ 0 & 1 & 0 \\ 0 & 0 & 1 \end{pmatrix} + g \left[a \begin{pmatrix} 0 & 0 & 0 \\ 1 & 0 & 0 \\ 0 & 0 & 0 \end{pmatrix} + a^\dagger \begin{pmatrix} 0 & 1 & 0 \\ 0 & 0 & 0 \\ 0 & 0 & 0 \end{pmatrix} + b \begin{pmatrix} 0 & 0 & 0 \\ 0 & 0 & 0 \\ 1 & 0 & 0 \end{pmatrix} + b^\dagger \begin{pmatrix} 0 & 0 & 1 \\ 0 & 0 & 0 \\ 0 & 0 & 0 \end{pmatrix} \right], \quad (336)$$

where N is again the total number of excitations. The Hamiltonian can be written in a block diagonal form

$$H = \begin{pmatrix} H_0 & 0 & 0 & 0 & \cdots \\ 0 & H_a & 0 & 0 & \cdots \\ 0 & 0 & H_b & 0 & \cdots \\ 0 & 0 & 0 & H_{ab} & \cdots \\ \vdots & \vdots & \vdots & \vdots & \ddots \end{pmatrix}. \quad (337)$$

$H_0 = -\Delta/2$ is the Hamiltonian acting on the zero-excitation subspace $|0_a 1_b g\rangle$,

$$H_a, H_b = \begin{pmatrix} -\Delta/2 & g \\ g & \Delta/2 \end{pmatrix}. \quad (338)$$

are acting on the subspaces $\{|1_a 0_b g\rangle, |0_a 0_b L\rangle\}$ and $\{|0_a 1_b g\rangle, |0_a 0_b R\rangle\}$, respectively, and

$$H_{ab} = \begin{pmatrix} -\Delta/2 & g & g \\ g & \Delta/2 & 0 \\ g & 0 & \Delta/2 \end{pmatrix}. \quad (339)$$

is acting on $\{|1_a 1_b g\rangle, |0_a 1_b L\rangle, |1_a 0_b R\rangle\}$. In the dispersive regime $\Delta \gg g$ and for positive detuning Δ , the ground state within each subspace

$$|g_0\rangle \approx |0_a 0_b g\rangle, \quad |g_a\rangle \approx |1_a 0_b g\rangle, \quad |g_b\rangle \approx |0_a 1_b g\rangle, \quad |g_{ab}\rangle \approx |1_a 1_b g\rangle, \quad (340)$$

have almost no population of the atomic excited states. After a constant energy shift of $\Delta/2$, the corresponding energies are

$$E_0 \approx 0, \quad E_a = E_b \approx -\frac{g^2}{\Delta} + \frac{2g^4}{\Delta^3}, \quad E_{ab} \approx -\frac{2g^2}{\Delta} + \frac{8g^4}{\Delta^3}. \quad (341)$$

That is, the energy of one photon in each cavity $E_{ab} = E_a + E_b + \chi_3$ is by the nonlinearity factor $\chi_3 = 4g^4/\Delta^3$ increased compared to the sum of the single photon energies. In other words, the energy of a photon in mode a depends on the state of mode b . The two qubit Hamiltonian reads

$$H = \begin{pmatrix} 0 & 0 & 0 & 0 \\ 0 & \omega_r + E_a & 0 & 0 \\ 0 & 0 & \omega_r + E_a & 0 \\ 0 & 0 & 0 & 2(\omega_r + E_a) + \chi_3 \end{pmatrix}. \quad (342)$$

and a C-Phase gate $\text{diag}\{1, 1, 1, e^{i\varphi}\}$ can be achieved by time evolution for $t = 2\pi/(\omega_r + E_a)$. The phase φ can be adjusted by the detuning Δ .

XII. ION TRAPS QC

It is fair to say that ion trap QC is the most advanced concept up to date (with the exception of NMR QC which can not be scaled). Two qubit gates between distant qubits have been performed with high accuracy. The main difficulty remains the scaling up because the number of ions in an ion trap is limited.

A. System

The qubit in ion trap QC is a nuclear spin of a single ion. The nuclear spin makes an vary good qubit because it has decoherence times of up to several hours. Ions are used because they can be trapped easily. It is not possible to trap an ion by static fields. A typical ion-trap is shown in Fig. 33. It uses a static field to get an approximately harmonic potential along the z -axis, and an oscillatory field which on average results in an approximately harmonic potential in the x and y direction.

The Hamiltonian of the motional degrees of freedom of N trapped ions is

$$H_m = \sum_{i=1}^N N \frac{M}{2} \left(\omega_x^2 x_i^2 + \omega_y^2 y_i^2 + \omega_z^2 z_i^2 + \frac{|\vec{p}_i|^2}{M^2} \right) + \sum_{i,j=1, i < j}^N \frac{e^2}{4\pi\epsilon_0 |\vec{r}_i - \vec{r}_j|}. \quad (343)$$

Typically one uses $\omega_x, \omega_y \gg \omega_z$ such that the mutual repulsion of the ions leads to a single line of ions in the trap. Oscillations of the ions in the x and y directions as well as the contra directional oscillations in z directions have high frequencies and are not important

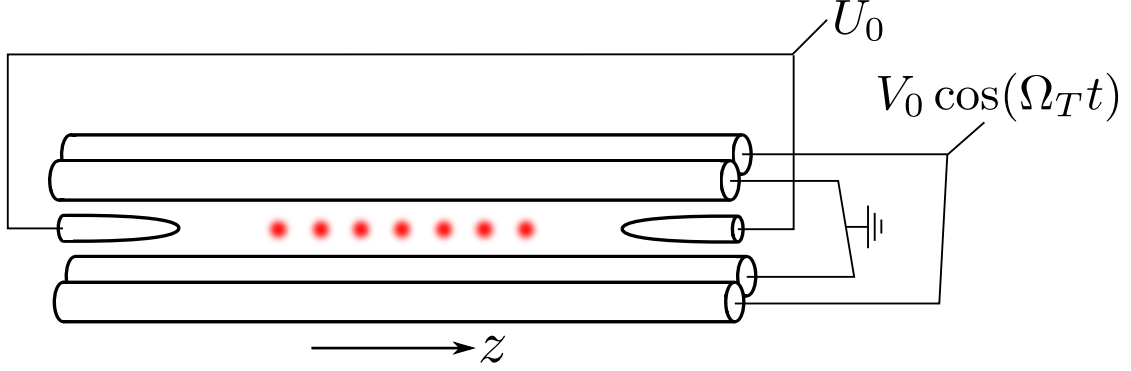


FIG. 33: A typical ion trap with seven ions (red).

in the following. However, the in-phase oscillations in z direction will be used later and we therefore introduce the creation and annihilation operators a^\dagger and a for this phonon mode.

With laser cooling techniques (Doppler cooling up to the Doppler limit, and then with sideband cooling) temperatures with

$$k_B T \ll \hbar \omega_z \quad (344)$$

are achieved, and the ions are let to equilibrate into the motional ground state as well as the electronic hyperfine ground state.

As a toy model we discuss a two-level spin in a harmonic potential with ω_z , but the generalization to higher dimensional spins and N ions is straight forward. The free particle Hamiltonian is

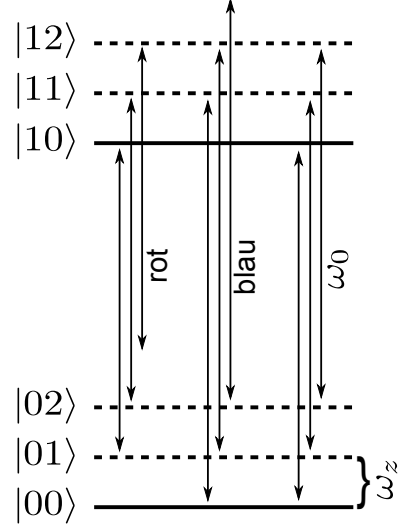
$$H_0 = \hbar \omega_0 \sigma_z + \hbar \omega_z a^\dagger a. \quad (345)$$

The interaction Hamiltonian of the spin with a laser field is $H_I = -\vec{\mu} \cdot \vec{B}$, where $\vec{\mu} = \mu \vec{\sigma}$ is proportional to the spin operator and $\vec{B} = B \vec{e}_x \cos(kz - \omega t + \varphi)$ is the magnetic field of the laser. Defining the Rabi-frequency $\Omega = \mu B / 2\hbar$ and the Lamb-Dicke parameter $\eta = 2\pi \sqrt{\hbar / 2M\omega_z} / \lambda$ (the ratio of the motional movement of the ion over the wave length of the laser), the Hamiltonian is approximately

$$\begin{aligned} H_I = & \frac{\hbar \Omega}{2} \left(\sigma_+ e^{i(\varphi - \omega t)} + \sigma_- e^{-i(\varphi - \omega t)} \right) \\ & + i \frac{\eta \hbar \Omega}{2} \left(\sigma_+ a + \sigma_- a^\dagger + \sigma_- a + \sigma_+ a^\dagger \right) \left(e^{i(\varphi - \omega t)} - e^{-i(\varphi - \omega t)} \right) \\ & + \mathcal{O}(\eta^2). \end{aligned} \quad (346)$$

The first term is the coupling of a spatially uniform magnetic field. The second term is due to the spatial variation of the magnetic field around the center of the potential well. It excites and relaxes the ions state and simultaneously creates and annihilates phonons. Using the bases $\{|0\rangle, |1\rangle\}$ for the spin and $\{|n\rangle\}$ for the oscillation, H_I couples the eigenstates of H_0 as shown below.

The main transitions at ω_0 and the blue and red sideband transitions. Depending on the laser frequency one can selectively drive one of these three transitions.

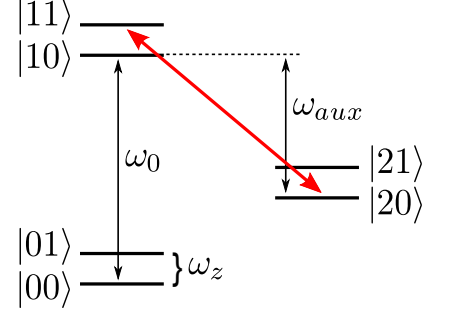


The extension to N spins is done by $\eta \rightarrow \eta/\sqrt{N}$ because all spins move together. If the laser points to one ion, only this ions electronic state is modified but all ions oscillate together in phase (\rightarrow Mössbauer effect).

B. Quantum computation

An arbitrary single qubit operation is performed by pointing a laser with frequency ω_0 to the respective ion. Two-qubit operations are performed in two steps. First the desired operation is performed between one ion and the two lowest levels of the phonon mode. Then a SWAP operation between the phonon mode and the other ion is used. Because the phonons are shared between all ions, it is called a *phonon bus qubit*. We discuss a C-Phase gate between the ions with numbers i and j .

The C-Phase gate between the ion i and the phonon mode is done with the help of an auxiliary level $|2_i\rangle$ of the ions internal state. Driving a 2π -rotation between $|1_i1\rangle$ and $|2_i0\rangle$ results in $|1_i1\rangle \rightarrow -|1_i1\rangle$ and $|2_i0\rangle \rightarrow -|2_i0\rangle$. Restricted to the subspace $\{|0_i0\rangle, |0_i1\rangle, |1_i0\rangle, |1_i1\rangle\}$ this is exactly the C-Phase gate because the levels $|0_i0\rangle, |0_i1\rangle, |1_i0\rangle$ are not disturbed. A more complicated scheme is possible without using an auxiliary level.



The SWAP operation is simply achieved by pointing a laser on ion j with the frequency $\omega_0 - \omega_z$ to induce a π -rotation between $|1_j0\rangle$ and $|0_j1\rangle$:

$$\text{SWAP}_j = \begin{pmatrix} 1 & 0 & 0 & 0 \\ 0 & 0 & 1 & 0 \\ 0 & -1 & 0 & 0 \\ 0 & 0 & 0 & 1 \end{pmatrix}. \quad (347)$$

A CNOT between i and j is then

$$\text{CNOT}_{ij} = H_j \text{SWAP}_j \text{CNOT}_i \text{SWAP}_j^\dagger H_k, \quad (348)$$

where the Hadamard gates transform the C-Phase $_{ij}$ into a CNOT $_{ij}$

The first CNOT between two ions was achieved with hyperfine states of Beryllium ions $^9\text{Be}^+$. Figure 34 displays the energies of the ion states labeled according to the total spin $\vec{F} = \vec{S} + \vec{I}$ of the nucleon and electron.

The hyperfine states (F, m_F) are splitted by means of a static magnetic field of 0.18 mT. The vibrational modes are denoted by n . The states $^2S_{1/2}(2, 2)$ and $^2S_{1/2}(1, 1)$ are used as qubit states, and the state $^2S_{1/2}(2, 0)$ as auxiliary level.

Instead of direct driving, so-called *Raman transitions* via the $^2P_{1/2}(2, 2)$ level are employed. For that one uses two laser beams with a frequency difference matching the desired transition of 1.25 GHz. The population of the $^2P_{1/2}(2, 2)$ level can be avoided by a strong detuning Δ the lasers from the corresponding transition. That is necessary because this excited level has a large spontaneous decay rate. The advantage of Raman transitions are that lasers with optical frequencies can be focused easily on single ions.

To read out the qubit state, one drives the transition $^2S_{1/2}(2, 2) \rightarrow ^2P_{3/2}(3, 3)$. If the qubit is in the state $^2S_{1/2}(2, 2)$, then the laser will excite the ion. The state $^2P_{3/2}(3, 3)$ then

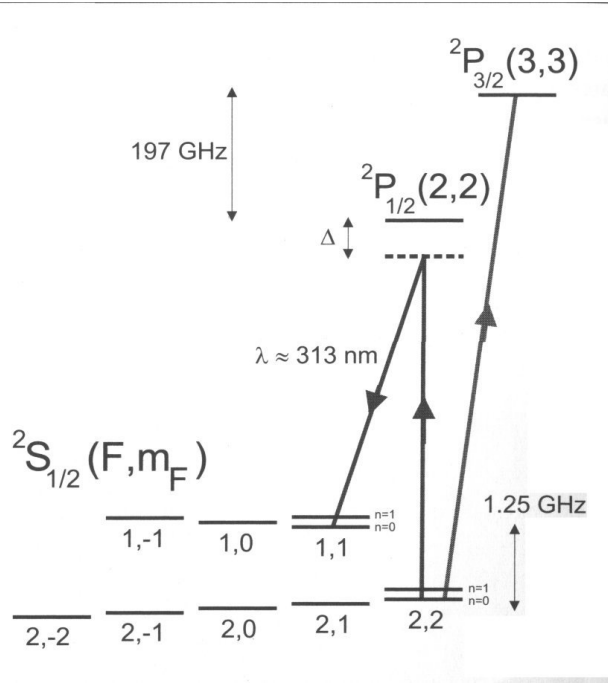


FIG. 34: Some energy levels of ${}^9\text{Be}^+$.

decays by emitting a photon in a random direction. Because of selection rules, the ion can only relax into ${}^2S_{1/2}(2,2)$ and the process starts again. This fluorescence can be measured with photon detectors. If the qubit is in the state ${}^2S_{1/2}(1,1)$, then the laser light does not match any possible transition frequency and no photons are observed.

C. Limitations

The decoherence times of the motional states is much shorter compared to the hyperfine states. Much improvement is possible by exciting them only for a short time.

More than 20 ions per trap are difficult, the limitation is due to non-center-of-mass phonons. For large scale QC it is necessary to couple many ion traps.

XIII. LIQUID STATE NMR QC

The qubit is represented by hyperfine states like in ion trap QC. The main idea of nuclear magnetic resonance QC is to circumvent the shared phonons (weak induced coupling and strong decoherence) by using several nuclear spins of a single molecule as qubits. The spins

are then sufficiently close together to interact via dipole interaction and electron induced interaction. The downside is that the many vibrational degrees of freedom makes it difficult to trap and cool the molecules. Therefore, they are dissolved in a solvent at room temperature.

Because all spins used for qubits have different transition frequencies (to the contrary to ion trap QC), one can selectively address a single qubit without focusing the electromagnetic wave to the respective atom. The manipulation and measurement of nuclear spins with radio waves is very well developed (\rightarrow chemistry), which is a big advantage.

There are two downsides of NMR QC which can be overcome by interesting new concepts. First, the magnetic moment of a single nuclear spin is too small to be detectable. Therefore one uses about 10^8 molecules to enhance the signal. Therefore, we are considering an ensemble of quantum computers! Second, the liquid samples can not be cooled well and $k_B T \gg \hbar \omega_0$ results in an almost random direction of the spins. The initialization into a pure state is far from possible. The solution to that problem will be discussed later.

There is a further conceptional limitation concerning the scaling. The number of atoms with sufficiently distinct transition frequencies is limited. It is clear that large scale liquid state NMR QC is not possible with the methods outlined in this section. Nevertheless, it was possible to perform some small scale quantum computing which served as proof of principle and major milestone in the history of QC. Furthermore, many control techniques were developed and optimized in NMR systems, and later used in other architectures.

A. System

Molecule:

- N protons (or other spin-1/2 nucleons like ^{13}C , ^{15}N , ^{19}F , ^{31}P) with $\omega_0 \approx 500$ MHz in a magnetic field of 10 T.
- Different protons have slightly different ω_0 due to different neighboring atoms shielding the magnetic field: $\Delta\omega_0 \approx 10 - 100$ kHz.
- No inter molecular interaction due to low density of molecules \rightarrow Ensemble of independent quantum computers.

The setup is shown in Fig. 35. The static field B_0 has to be homogeneous up to a relative error of 10^{-9} within a volume of 1 cm^3 . The radio frequency coil is not only used

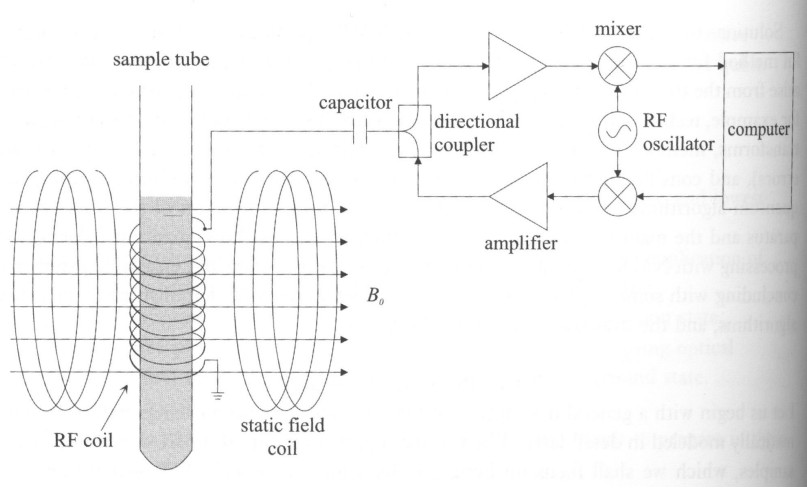


FIG. 35: A typical setup for liquid state NMR.

to manipulate the nuclear spins, but also for their readout. That is because the precessing nuclear spins generate an RF-field, inducing a current in the coil which can be detected.

B. Time evolution

The Hamiltonian of a single nuclear spin j is

$$\begin{aligned}
 H_j &= \frac{\hbar\omega_{0j}}{2}\sigma_{zj} + g_j\hbar(\sigma_{xj}\cos\omega_j t + \sigma_{yj}\sin\omega_j t) \\
 &\stackrel{\text{rot. frame}}{=} \hbar \begin{pmatrix} \Delta_j/2 & g_j \\ g_j & -\Delta_j/2 \end{pmatrix},
 \end{aligned} \tag{349}$$

with $\Delta_j = \omega_{0j} - \omega_j$. The dipole coupling between two spins i and j is

$$H_{ij}^D = \frac{\mu_1\mu_2\hbar}{4|r_{ij}|^3} [\vec{\sigma}_i \cdot \vec{\sigma}_j - 3(\vec{\sigma}_i \cdot \vec{n})(\vec{\sigma}_j \cdot \vec{n})], \tag{350}$$

where $\vec{n} = \vec{r}_{ij}/|r_{ij}|$ and \vec{r}_{ij} is the vector from spin i to spin j . Because the molecules in a liquid are rotating fastly, the system experiences the Hamiltonian averaged over all directions of \vec{n} , which vanishes for H_{ij}^D :

$$\langle H_{ij}^D \rangle_{\vec{n}} = 0. \tag{351}$$

Therefore, one only has to consider the electron mediated coupling

$$\begin{aligned}
 H_{ij}^J &= \frac{\hbar J}{4} \vec{\sigma}_i \cdot \vec{\sigma}_j \\
 &= \frac{\hbar J}{4} \vec{\sigma}_{z,i} \cdot \vec{\sigma}_{z,j} + \frac{\hbar J}{8} (\vec{\sigma}_{+,i} \cdot \vec{\sigma}_{-,j} + \vec{\sigma}_{-,i} \cdot \vec{\sigma}_{+,j})
 \end{aligned}$$

$$\approx \frac{\hbar J}{4} \vec{\sigma}_{z,i} \cdot \vec{\sigma}_{z,j}, \quad (352)$$

where the RWA was used which is valid if the precession frequencies of the two spins are sufficiently different $\omega_{0,i} - \omega_{0,j} \gg J$.

All single qubit operations can be performed with the Hamiltonian Eq. (349). They have to be performed sufficiently fast, such that the relatively weak two qubit coupling (which can not be switched off) can be neglected. For two qubit operations we write the non-driven two qubit Hamiltonian as

$$H_{sys} = a\sigma_{z1} + b\sigma_{z2} + c\sigma_{z1} \otimes \sigma_{z2} \quad (353)$$

Therefore, the free evolution for $T = \pi/4c$ results in a C-phase gate up to one qubit rotations around the z -axis. The latter can be undone by further single qubit rotations. With these techniques (and spin echo) high precision gates are possible.

Decoherence:

- Inhomogeneity of B_0 : Can be mostly corrected by spin echo techniques.
- Dipole spin-spin coupling: Can not be corrected, but is minimized with large(!) temperature because the molecules rotate faster and the interaction averaged to zero.
- T_1 and T_2 can be easily measured. E.g. for T_1 a π -pulse is applied to excite the system. After waiting some time for the system to relax, a $\pi/2$ -pulse leads to a superposition state and its precession strength give the coherence.
- T_1 and T_2 are used in NMR-imaging to distinguish between different molecules.

C. Magnetization Readout

The output of an experiment is the free induction decay signal

$$V(t) = V_0 \left[e^{-iHt/\hbar} \rho e^{iHt/\hbar} \sum_k (i\sigma_{xk} + \sigma_{yk}) \right] \quad (354)$$

The signal oscillates with the eigen frequencies of the system and usually the Fourier transform $\tilde{V}(\omega)$ is measured.

Figure 36 shows the spectrum of ^{13}C labeled trichloroethylene near the typical transition frequency of ^{13}C . Because of the different shielding of the magnetic field the frequency of

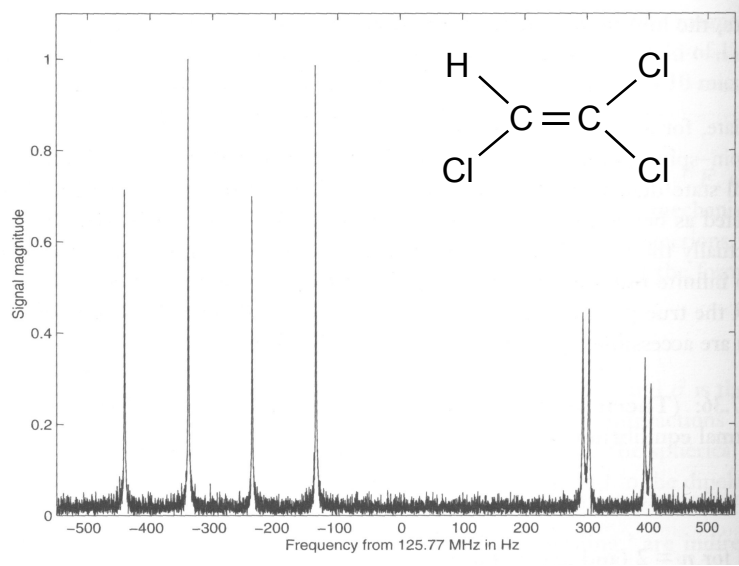


FIG. 36: The carbon spectrum of ^{13}C labeled trichloroethylene. The proton and two carbons give a three qubit system

the left Carbon is about 600 MHz lower. Furthermore, because the left ^{13}C couples to the right ^{13}C and the proton, four lines can be seen; depending on their state, the left ^{13}C has a modified transition frequency. The proton splits the lines by 200 MHz, the right ^{13}C by about 100 MHz. The right ^{13}C transition frequency is also split into four peaks, but the splitting due to the proton is fine because the proton is far away from the right ^{13}C .

D. Initial state and “labeling”

For the initial state the system is let to equilibrate in the static field B_0 , which may take a few minutes. The state of the system of all nuclear spins is then

$$\begin{aligned}\rho &= \frac{e^{-H/k_B T}}{\text{tr}(e^{-H/k_B T})} \\ &\approx 2^{-N}(1 - H/k_B T),\end{aligned}\tag{355}$$

where typically $H/k_B T \approx 10^{-4}$. For small couplings this state is diagonal in the Z -basis $|0, \dots, 0, 0\rangle, |0, \dots, 0, 1\rangle, \dots, |1, \dots, 1, 1\rangle$.

Now we tackle the problem how to use an almost random state for quantum computing. For simplicity we assume computation with two qubits only. Instead of the desired initial

ground state we have

$$\rho_1 = \begin{pmatrix} a & 0 & 0 & 0 \\ 0 & b & 0 & 0 \\ 0 & 0 & c & 0 \\ 0 & 0 & 0 & d \end{pmatrix} \neq \begin{pmatrix} 1 & 0 & 0 & 0 \\ 0 & 0 & 0 & 0 \\ 0 & 0 & 0 & 0 \\ 0 & 0 & 0 & 0 \end{pmatrix} \quad (356)$$

With the help of CNOT one can construct the unitary operator P with

$$\rho_2 = P\rho_1P^\dagger = \begin{pmatrix} a & 0 & 0 & 0 \\ 0 & c & 0 & 0 \\ 0 & 0 & d & 0 \\ 0 & 0 & 0 & b \end{pmatrix}, \quad \rho_3 = P^\dagger\rho_1P = \begin{pmatrix} a & 0 & 0 & 0 \\ 0 & d & 0 & 0 \\ 0 & 0 & b & 0 \\ 0 & 0 & 0 & c \end{pmatrix} \quad (357)$$

Any computation U is now performed with each $\rho(t=0) = \rho_1, \rho_2, \rho_3$ at separate times and the results are averaged to give

$$\sum_k U\rho_kU^\dagger = (4a-1)U \begin{pmatrix} 1 & 0 & 0 & 0 \\ 0 & 0 & 0 & 0 \\ 0 & 0 & 0 & 0 \\ 0 & 0 & 0 & 0 \end{pmatrix} U^\dagger + (1-a) \begin{pmatrix} 1 & 0 & 0 & 0 \\ 0 & 1 & 0 & 0 \\ 0 & 0 & 1 & 0 \\ 0 & 0 & 0 & 1 \end{pmatrix} \quad (358)$$

Because any measurement of spin operators are traceless, the last term does not give a measurement signal. **The sum of all measurements give the same result as if the initial system where in a pure state, but with a signal reduced by the factor $(4a-1)$!** This technique is called *temporal labeling*.

Other similar techniques are *spatial labeling*, where the three computations are performed simultaneously but at either different systems or at different parts of one system. In *logical labeling* one performs only one experiment, but uses three mixed state qubits for a computation involving two pure states.

The problem with labeling is that α is only slightly more than 1/4 if the thermal state is close to a random state. Even worst, this small signal reduces exponentially with the number of qubits because the probability of being in the ground state

$$p_{00\dots 0} = \frac{1}{Z} \langle 0 |^{\otimes N} e^{-H/k_B T} | 0 \rangle^{\otimes N} \propto N 2^{-N} \quad (359)$$

reduces exponentially. Therefore, liquid NMR QC can not be used for large scale QC.

Nevertheless, NMR QC is the most advanced technique and it has been used to perform impressive proof of principle experiments, such as the factorization of $15 = 3 \times 5$, or the implementation of Grover's search algorithm. Also, in trichloroethylene, the protons state got teleported to the right carbon.

XIV. ELEMENTS OF QUANTUM ERROR CORRECTION

Quantum error correction is a very large field by itself. We only discuss the correction of errors during information transfer and say a few words about gate errors at the end of this section. The basic idea is to encode one logical bit into several physical bits. This way, if one physical bit gets corrupted, there is still sufficient information to recover the logical bit.

A. Classical error correction

Some components of classical hardware, such as modems and CD-players, require error correction. Let's assume Alice wants to transfer information to Bob, but each transferred bit can undergo bit flip error with probability p . The simplest code is the repetition code. Before sending the information to Bob, Alice copies each bit twice

$$\begin{aligned} 0 &\rightarrow 000 \\ 1 &\rightarrow 111. \end{aligned} \tag{360}$$

This process is called encoding. If Alice sends a 000, Bob may obtain one of the following states:

$$000 \xrightarrow{\text{transmission}} \begin{cases} 000 & \text{with probability } (1-p)^3 \\ 001 & \text{with probability } (1-p)^2p \\ 010 & \text{with probability } (1-p)^2p \\ 100 & \text{with probability } (1-p)^2p \\ 011 & \text{with probability } (1-p)p^2 \\ 101 & \text{with probability } (1-p)p^2 \\ 110 & \text{with probability } (1-p)p^2 \\ 111 & \text{with probability } p^3 \end{cases}. \tag{361}$$

Bob decodes the message using majority voting, that is

$$\begin{aligned}\{000, 001, 010, 100\} &\rightarrow 0 \\ \{111, 110, 101, 011\} &\rightarrow 1.\end{aligned}\tag{362}$$

To perform the decoding, of course he has to be able to measure every physical bit sent to him. According to Eq. (361), the repetition code reduces the error rate from p to $3p^2 - 2p^3$. Of course one can arbitrarily reduce the error rate if enough recourses are available.

If bob wants to send the information further, he doesn't need to decode and encode again, he may just correct for the error by

$$\begin{aligned}\{000, 001, 010, 100\} &\rightarrow 000 \\ \{111, 110, 101, 011\} &\rightarrow 111.\end{aligned}\tag{363}$$

B. Quantum error correction

Apparent difficulties with quantum error correction include:

- No cloning theorem forbids copying the qubits: $|\psi\rangle \rightarrow |\psi\rangle |\psi\rangle |\psi\rangle$ is not possible.
- Measurement destroys the state: $|\psi\rangle |\psi\rangle |\varphi\rangle \rightarrow |\psi\rangle |\psi\rangle |\psi\rangle$ is not possible.
- Two types of errors: Bit flip and phase flip.
- Errors are continuous.

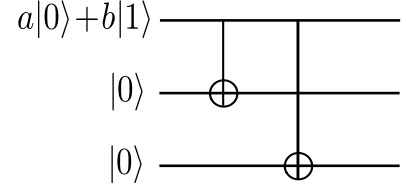
Quite amazingly, quantum error correction is still possible. We first outline the *bit-flip code* which corrects for bit-flips which happen with probability p . We encode

$$\begin{aligned}|0\rangle &\rightarrow |0_L\rangle = |000\rangle \\ |1\rangle &\rightarrow |1_L\rangle = |111\rangle\end{aligned}\tag{364}$$

It is important to realize that this is no copying of a quantum state, because

$$a|0\rangle + b|1\rangle \rightarrow a|000\rangle + b|111\rangle \neq (a|0\rangle + b|1\rangle)^{\otimes 3},\tag{365}$$

where we introduced the notation $|\psi\rangle^{\otimes n} = |\psi\rangle \otimes |\psi\rangle \otimes \dots \otimes |\psi\rangle$. The encoding can be done with simple CNOT-gates as shown to the right.



For the error diagnoses, one could just measure the state of the three physical Qubits. Obtaining e.g. $|010\rangle$ then indicates that the second qubit flipped. However, the measurement destroyed the superpositions of $|0\rangle$ and $|1\rangle$ and it is not possible to recover the desired state $|\psi_L\rangle = a|000\rangle + b|111\rangle$.

The key idea is to only measure if the qubits are in the same state or not, and if not, then which qubit differs from the other two. This can be done without measuring the actual state of each qubit by measuring the four *error syndromes*:

$$\begin{aligned} P_0 &= |000\rangle\langle 000| + |111\rangle\langle 111| \\ P_1 &= |100\rangle\langle 100| + |011\rangle\langle 011| \\ P_2 &= |010\rangle\langle 010| + |101\rangle\langle 101| \\ P_3 &= |001\rangle\langle 001| + |110\rangle\langle 110| \end{aligned} \tag{366}$$

These are all Hermitian operators and can easily be measured (If one is restricted to one qubit measurements, then one needs to transform the three qubit state appropriately before the measurement. Using the same transformation as for the encoding results in $P_0 \rightarrow \mathbb{1} \otimes |00\rangle\langle 00|$, $P_1 \rightarrow \mathbb{1} \otimes |11\rangle\langle 11|$, $P_2 \rightarrow \mathbb{1} \otimes |10\rangle\langle 10|$, and $P_3 \rightarrow \mathbb{1} \otimes |01\rangle\langle 01|$). If the measurement of P_0 gives the result one, then we know that all three qubits are in the same state and assume that no qubit flipped. If P_1 results in one, then the state of the first qubit differs from the state of the other qubits. We then conclude that the first qubit must have flipped, and correct this error by flipping it again. Similar for the other syndromes. As an example we look at the state after each step for a bit-flip error on qubit two. Note that the projective measurement does not alter the state

$$a|000\rangle + b|111\rangle \xrightarrow[\text{error}]{\text{bit-flip}} a|010\rangle + b|101\rangle \xrightarrow[\text{with } P_2]{\text{projection}} a|010\rangle + b|101\rangle \xrightarrow[\text{with } \sigma_x^{(2)}]{\text{correction}} a|000\rangle + b|111\rangle$$

Like in the classical scheme, we can only correct the error if maximally one qubit flipped. The error rate is again reduced from p to $3p^2 - 2p^3$.

Next we discuss the *phase-flip code*. Noting that a phase flip

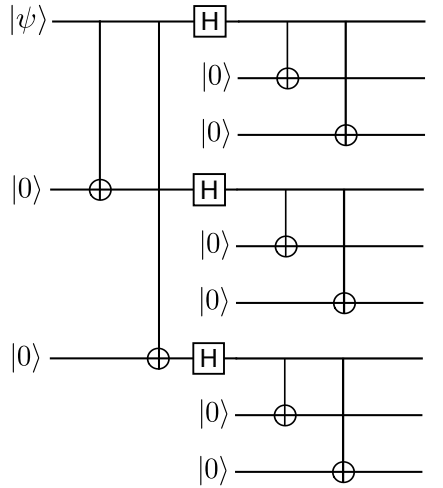
$$\begin{aligned} |0\rangle &\rightarrow |0\rangle \\ |1\rangle &\rightarrow -|1\rangle \end{aligned} \quad (367)$$

is equivalent to a bit-flip in the basis $|\pm\rangle$, we only have to change the basis and we can use the bit-flip code to correct for phase-flip errors. The encoding is according to

$$\begin{aligned} |0\rangle &\rightarrow |0_L\rangle = |+++\rangle \\ |1\rangle &\rightarrow |1_L\rangle = |--\rangle \end{aligned}$$


and the four error syndromes are $\tilde{P}_j = H^{\otimes 3} P_j H^{\otimes 3}$.

The *Shore code* combines the bit-flip and phase-flip codes to correct for both errors:

$$\begin{aligned} |0_L\rangle &= \frac{(|000\rangle + |111\rangle) \otimes (|000\rangle + |111\rangle) \otimes (|000\rangle + |111\rangle)}{\sqrt{8}} \\ |1_L\rangle &= \frac{(|000\rangle - |111\rangle) \otimes (|000\rangle - |111\rangle) \otimes (|000\rangle - |111\rangle)}{\sqrt{8}} \end{aligned}$$


Quite amazingly, the Shore code does not only correct phase-flips and bit-flips, but any error, unitary or not unitary (such as decoherence). We only outline the proof. Every error is a quantum map (completely positive and trace preserving) and can be written in Kraus representation

$$|\psi\rangle\langle\psi| \rightarrow \sum_j K_j |\psi\rangle\langle\psi| K_j^\dagger. \quad (368)$$

The Kraus operators can in turn be decomposed as

$$K_j = k_{j0} \mathbb{1} + k_{j1} \sigma_x + k_{j2} \sigma_z + k_{j3} \sigma_x \sigma_z, \quad (369)$$

that is, $K_j |\psi\rangle$ is a superposition of the states without error, with a bit-flip error, with a phase-flip error and with both errors. Measuring an error syndromes then collapses the

state to be either without error, or with one of the errors, depending on the measurement outcome (but does not collapse $a|0_L\rangle + b|1_L\rangle$). This error is then corrected by the usual error correction. As an example consider an $\begin{pmatrix} 1 & 0 \\ 0 & e^{i\phi} \end{pmatrix}$ -error on the first qubit. The measurement of \tilde{P}_1 gives the result one with probability $\sin^2(\phi/2)$ and in this case the state is projected onto $\sigma_z^{(1)}|\psi_L\rangle$ as if it had undergone a full phase-flip. The error correction protocol then corrects this error by another $\sigma_z^{(1)}$. With probability $\cos^2(\phi/2)$, the measurement of \tilde{P}_0 gives the result one. The state is then projected onto the desired state $a|0_L\rangle + b|1_L\rangle$ and the error correction protocol leaves it like that. It is remarkable that a continuous set of errors can be corrected by a finite number of mechanisms.

The Shore code reduces the error rate from p to $36p^2 + \mathcal{O}(p^3)$. If the error rate $p < p_c$ is smaller than a critical error rate of $p_c \approx 1/36$, then the error can be reduced further by *concatenation*. E.g. encoding a logical qubit into 81 physical qubits according to

$$\begin{aligned} |0_{LL}\rangle &= \frac{(|0_L 0_L 0_L\rangle + |1_L 1_L 1_L\rangle) \otimes (|0_L 0_L 0_L\rangle + |1_L 1_L 1_L\rangle) \otimes (|0_L 0_L 0_L\rangle + |1_L 1_L 1_L\rangle)}{\sqrt{8}} \\ |1_{LL}\rangle &= \frac{(|0_L 0_L 0_L\rangle - |1_L 1_L 1_L\rangle) \otimes (|0_L 0_L 0_L\rangle - |1_L 1_L 1_L\rangle) \otimes (|0_L 0_L 0_L\rangle - |1_L 1_L 1_L\rangle)}{\sqrt{8}} \end{aligned}$$

results in an error rate of $36(36p^2)^2 + \mathcal{O}(p^6)$. This process can be continued to achieve an arbitrarily small error rate as long as the error rate for a physical qubit is below the critical p_c .

The *threshold theorem* is essential to the success of quantum computing. It states that as long as the error rate is below a critical threshold rate and if sufficient resources are available, then arbitrarily complex quantum computing is possible due to concatenation of error correcting codes. The actual threshold is hard to state because one also has to take into account errors in the encoding process and in the syndrome measurements. Furthermore, for a simple single qubit transformation on the logical qubit one needs to perform a nine qubit transformation if one uses the Shore code. Typical values for the threshold found in the literature range between 10^{-2} and 10^{-4} .

XV. TOPOLOGICAL IDEAS

A. Error correction: stabilizers formalism

The error correction codes can be formulated using "code stabilizers" (D. Gottesmann). To motivate, consider once again the simplest 3-bit code:

$$|\tilde{0}\rangle = |000\rangle \quad \text{and} \quad |\tilde{1}\rangle = |111\rangle . \quad (370)$$

Consider operators $S_1 = Z_1 Z_2$ (we introduce a notation $Z_i \equiv \sigma_{zi}$) and $S_2 = Z_2 Z_3$. We have

$$\begin{aligned} S_1 |\tilde{0}\rangle &= |\tilde{0}\rangle \\ S_1 |\tilde{1}\rangle &= |\tilde{1}\rangle \\ S_2 |\tilde{0}\rangle &= |\tilde{0}\rangle \\ S_2 |\tilde{1}\rangle &= |\tilde{1}\rangle . \end{aligned} \quad (371)$$

One says that S_1 and S_2 stabilize the code. Measuring S_1 or S_2 we will not distinguish between the two logical states. Yet measuring S_1 and S_2 we can detect any one-bit X_i error (spin flip). That is if initially we have

$$|\psi\rangle = \alpha |\tilde{0}\rangle + \beta |\tilde{1}\rangle \quad (372)$$

and, then an error happens, i.e., our state is now, e.g., $X_1 |\psi\rangle = \alpha |100\rangle + \beta |011\rangle$. Measuring both S_1 and S_2 we obtain $S_1 X_1 |\psi\rangle = -X_1 |\psi\rangle$ and $Z_2 X_1 |\psi\rangle = X_1 |\psi\rangle$. The state $X_1 |\psi\rangle$ is an eigenstate of both S_1 and S_2 and it remains intact after the measurement. The combination $S_1 = -1$, $S_2 = 1$ uniquely distinguishes the X_1 error from X_2 and X_3 . Thus we can now correct, e.g, by applying X_1 once again.

Instead of specifying the code states it is sufficient to specify the stabilizers. The code subspace is uniquely determined by the conditions $S_1 |\psi\rangle = |\psi\rangle$ and $S_2 |\psi\rangle = |\psi\rangle$.

A detectable error operator anti commutes necessarily with at least one of the stabilizers. In our case $E = X_1$ and $\{X_1, S_1\} = 0$ whereas $[X_1, S_2] = 0$. The anti commuting gives rise to the negative eigenvalues. Indeed if an error operator E anti commutes with the stabilizer S we obtain

$$SE |\psi\rangle = -ES |\psi\rangle = -E |\psi\rangle . \quad (373)$$

1. Stabilizers of the Shor code

The 9-bit code of Shor is given by

$$\begin{aligned} |\tilde{0}\rangle &= \frac{1}{2^3}(|000\rangle + |111\rangle)(|000\rangle + |111\rangle)(|000\rangle + |111\rangle) \\ |\tilde{1}\rangle &= \frac{1}{2^3}(|000\rangle - |111\rangle)(|000\rangle - |111\rangle)(|000\rangle - |111\rangle) . \end{aligned} \quad (374)$$

The 8 stabilizers of this code read

$$\begin{aligned} S_1 &= Z_1 Z_2 \\ S_2 &= Z_2 Z_3 \\ S_3 &= Z_4 Z_5 \\ S_4 &= Z_5 Z_6 \\ S_5 &= Z_7 Z_8 \\ S_6 &= Z_8 Z_9 \\ S_7 &= X_1 X_2 X_3 X_4 X_5 X_6 \\ S_8 &= X_4 X_5 X_6 X_7 X_8 X_9 . \end{aligned} \quad (375)$$

Detectable errors, e.g., $X_1 \dots X_9$, $Z_1 \dots Z_9$, $Y_1 \dots Y_9$ etc. For example X_1 can be distinguished from Y_1 because X_1 anti commutes with S_1 only, while Y_1 anti commutes with S_1 and S_7 .

Z_1 seems to be indistinguishable from Z_2 . Indeed both anti commute with S_7 only. Thus by measuring all 8 stabilizes and getting -1 only for S_7 we can only conclude that one of the three possible errors, i.e. Z_1 , Z_2 , Z_3 happened. These three are all corrected by, e.g., applying Z_1 .

B. Toric code

This code has been proposed by Kitaev.

C. Majorana bound states

We consider another model proposed by Kitaev, a 1-D p-wave superconductor. The Hamiltonian reads

$$H = \sum_{j=1}^{N-1} \left[-t c_j^\dagger c_{j+1} + \Delta c_j c_{j+1} + h.c. \right] . \quad (376)$$

We assume the order parameter Δ to be real. We introduce the Majorana operators (not really related to Majorana particles)

$$\begin{aligned} c_j &= \frac{1}{2}(\gamma_{A,j} + i\gamma_{B,j}) \\ c_j^\dagger &= \frac{1}{2}(\gamma_{A,j} - i\gamma_{B,j}) . \end{aligned} \quad (377)$$

The inverse relations read

$$\begin{aligned} \gamma_{A,j} &= c_j + c_j^\dagger \\ \gamma_{B,j} &= -i(c_j - c_j^\dagger) . \end{aligned} \quad (378)$$

The commutation relations of the Majorana operators read $\{\gamma_{\alpha,j}, \gamma_{\alpha',j'}\}_+ = 2\delta_{\alpha,\alpha'}\delta_{j,j'}$. Here $\alpha, \alpha' = A/B$. In particular $\gamma_{\alpha,j}^2 = 1$. Also these operators are Hermitian, $\gamma_{\alpha,j}^\dagger = \gamma_{\alpha,j}$. Substituting we obtain

$$H = \frac{1}{4} \sum_{j=1}^{N-1} \left[-t(\gamma_{A,j} - i\gamma_{B,j})(\gamma_{A,j+1} + i\gamma_{B,j+1}) + \Delta(\gamma_{A,j} + i\gamma_{B,j})(\gamma_{A,j+1} + i\gamma_{B,j+1}) + h.c. \right] . \quad (379)$$

The AA and BB terms vanish and we are left with

$$H = \frac{i}{2} \sum_{j=1}^{N-1} \left[(-t + \Delta)\gamma_{A,j}\gamma_{B,j+1} + (t + \Delta)\gamma_{B,j}\gamma_{A,j+1} \right] . \quad (380)$$

An interesting situation arises if $\Delta = t$. We obtain

$$H = i \sum_{j=1}^{N-1} t \gamma_{B,j} \gamma_{A,j+1} . \quad (381)$$

Two Majoranas are not involved in this Hamiltonian and, thus, commute with it. These are $\gamma_L \equiv \gamma_{A,1}$ and $\gamma_R \equiv \gamma_{B,N}$. This means that all the eigenstates including the ground state are double degenerate. Indeed from γ_L and γ_R we can form a new pair of Fermi operators

$$d \equiv \frac{1}{2}(\gamma_L + i\gamma_R) \quad \text{and} \quad d^\dagger \equiv \frac{1}{2}(\gamma_L - i\gamma_R) . \quad (382)$$

The operators d and d^\dagger commute with the Hamiltonian. The doubling of the states in according to the occupation number $d^\dagger d$. If there exist a ground state $|g0\rangle$ such that $d|g0\rangle = 0$, then also the state $|g1\rangle = d^\dagger|g0\rangle$ is a ground state, i.e., it has the same energy.

What happens if $\Delta \neq t$ (but they are still close). We start again from (376) and rewrite it as

$$H = \sum_{j=1}^{N-1} \left[t c_j^\dagger c_{j+1} + \Delta c_j c_{j+1} + h.c. \right] . \quad (383)$$

- [1] M. V. Berry, Proc. R. Soc. Lond. A **414**, 31 (1987).
- [2] G. Lindblad, Commun. Math. Phys. **48**, 119 (1976).
- [3] G. S. V. Gorini, A. Kossakowski, J. Math. Phys. **17**, 821 (1976).
- [4] J. von Neumann, *Mathematische Grundlagen der Quantenmechanik* (Springer-Verlag, 1968).
- [5] B. D. Josephson, Physics Letters **1**, 251 (1962).
- [6] V. Ambegaokar and A. Baratoff, Phys. Rev. Lett. **10**, 486 (1963).
- [7] V. Ambegaokar and A. Baratoff, Phys. Rev. Lett. **11**, 104 (1963).
- [8] A. O. Caldeira and A. J. Leggett, Phys. Rev. Lett. **46**, 211 (1981).
- [9] A. O. Caldeira and A. J. Leggett, Annals of Physics **149**, 374 (1983).
- [10] H. Mabuchi and A. C. Doherty, Science **298**, 1372 (2002).
- [11] If the system is initially entangled with the environment, then \mathcal{V}_S is generally not positive.